First Row Transition Metal Complexes of Heptadentate N_7 Donor Ligands

Jiawei Guan

A thesis submitted to
Auckland University of Technology
in requirements for the degree of
Master of Science in Chemistry (Research)

2023

Department of Chemistry
School of Science

ABSTRACT

Three heptadentate N_7 ligands have been studied in this thesis: N, N'-bis(2,2'-bipyridin-6-ylmethyl)pyridine-2,6-dimethylamine (bmpy), N, N'-bis(2,2'-bipyridin-6-ylmethyl)diethylamine-1,2-dimethylamine (bmdet) and N, N'-bis(6-methyl-2,2'-bipyridin-6'-ylmethyl)diethylamine-1,2-dimethylamine (DMbmdet). Bmpy is a new ligand while bmdet and DMbmdet were first prepared by a previous group member and their successful purification by column chromatography from their degraded products was achieved.

The coordination behaviours of these ligands towards first row transition metals (Co, Cu, Fe, Ni, Zn) was studied. Despite many attempts, X-ray quality crystals could not be obtained for any of the complexes studied. Therefore, their solution-phase identities were investigated directly by ESI-MS. The mole ratio between the five metal ions and all three ligands is shown largely not to influence the nature of the complexes formed; in nearly all cases, mononuclear species are predominantly formed regardless of the M:L mole ration. Exceptions are the nickel / DMbmdet system, which exhibited a tendency to form dimeric species as the concentration of Ni^{2+} ions was increased, while the Cu^{2+} / bmpy system gives rise to a dimeric complex as the main product.

TABLE OF CONTENTS

Abstract

Table of Contents

Attestation of Authorship

List of Figures

Acknowledgements

1. Introduction

1.1. Coordination Complexes

1.1.1. Seven-coordinate geometries

1.1.2. Multidentate ligands containing bipyridine units

1.2. Heptadentate ligands

1.3. Potential applications of seven-coordinate complexes

1.4. Project Aim

2. Experimental

2.1. Synthesis of 2,6-dibromomethylpyridine

2.2. Synthesis of Potassium phthalimide

2.3. Synthesis of 2,6-diaminomethylpyridine

2.4. Synthesis of 6-methyl-2,2'-bipyridine

2.4.1. Method A

2.4.2. Method B

2.5. Synthesis of 2,2'-bipyridine-6-carboxaldehyde

2.6. Synthesis of N, N'-bis(2,2'-bipyridin-6-ylmethyl)pyridine-2,6-dimethylamine (bmpy)

2.6.1. Method A

2.6.2. Method B

2.6.3. Purification

2.7. Purification of N, N'-bis(2,2'-bipyridin-6-ylmethyl)diethylamine-1,2-dimethylamine (bmdet)

2.8. Purification of N, N'-bis(6-methyl-2,2'-bipyridin-6'-ylmethyl)diethylamine-1,2-dimethylamine (DMbmdet)

2.9. Studies of bmpy complexes

2.9.1. Preparation of solutions of complexes

2.9.1.1. Attempted synthesis of Cu(II), Fe(II), Co(II), Ni(II), Zn(II), Mn(II), Pd(II) complexes in mixed solutions of MeOH/Acetonitrile or MeOH/Water
2.9.1.2. Attempted synthesis of Cu(II), Fe(II), Co(II), Ni(II) complexes in 1:1, 1:2 and 1:3 ratios in acetonitrile
2.9.1.3. Attempted synthesis of a Co(III) complex of bmpy
2.9.1.3.1. Method A
2.9.1.3.2. Method B
2.9.2. MS studies of bmpy complexes
2.9.2.1. MS studies in a mixed solution of MeOH and acetonitrile with Cu(II), Fe(II), Co(II), Ni(II), Zn(II) in 1:1, 1:2 and 1:3 ratios
2.9.2.2. Attempted synthesis of Co(II) and Fe(II) complexes of bmpy
2.10. MS studies of bmdet cmoplexes
2.11. MS studies of DMbmdet complexes
2.12. Attempted synthesis of a Cu(II) complex of 2, 6-dibromomethylpyridine
2.12.1. Method A
2.12.2. Method B

3. Results and Discussion

3.1. Syntheses of ligand precursors
3.1.1. 2,6-dibromomethylpyridine
3.1.2. 2,6-diaminomethylpyridine
3.1.3. 6-methyl-2, 2'-bipyridine
3.1.4. 2, 2'-bipyridine-6-carboxaldehyde
3.2. Ligand synthesis: N, N'-bis(2,2'-bipyridin-6-ylmethyl)pyridine-2,6-dimethylamine (bmpy)
3.3. Transition metal complexes of bmpy
3.3.1. Bmpy + $Co(ClO_4)_2 \cdot 6H_2O$
3.3.2. Bmpy + $Cu(ClO_4)_2 \cdot 6H_2O$
3.3.3. Bmpy + $Fe(ClO_4)_2 \cdot 6H_2O$
3.3.4. Bmpy + $Ni(ClO_4)_2 \cdot 6H_2O$
3.3.5. Bmpy + $Zn(ClO_4)_2 \cdot 6H_2O$
3.4. Purification of N, N'-bis(2,2'-bipyridin-6-ylmethyl)diethylamine-1,2-dimethylamine (bmdet) and the transition metal complexes of bmdet
3.4.1. Bmdet + $Co(ClO_4)_2 \cdot 6H_2O$

3.4.2. Bmdet + $Cu(ClO_4)_2 \cdot 6H_2O$
3.4.3. Bmdet + $Fe(ClO_4)_2 \cdot 6H_2O$
3.4.4. Bmdet + $Ni(ClO_4)_2 \cdot 6H_2O$
3.4.5. Bmdet + $Zn(ClO_4)_2 \cdot 6H_2O$
3.5. Purification of N, N'-bis(6-methyl-2,2'-bipyridin-6'-ylmethyl)diethylamine-1,2-dimethylamine (DMbmdet) and the complexes of DMbmdet
3.5.1. DMbmdet + $Co(ClO_4)_2 \cdot 6H_2O$
3.5.2. DMbmdet + $Cu(ClO_4)_2 \cdot 6H_2O$
3.5.3. DMbmdet + $Fe(ClO_4)_2 \cdot 6H_2O$
3.5.4. DMbmdet + $Ni(ClO_4)_2 \cdot 6H_2O$
3.5.5. DMbmdet + $Zn(ClO_4)_2 \cdot 6H_2O$
3.6. Discussion
3.6.1. Heptadentate ligands
3.6.2. Transition metal cmoplexes of bmpy
3.6.3. Transition metal complexes of bmdet and DMbmdet
4. Conclusion
References

Attestation of Authorship

“I hereby declare that this submission is my own work and that, to the best of my knowledge and belief, it contains no material previously published or written by another person (except where explicitly defined in the acknowledgements), nor material which to a substantial extent has been submitted for the award of any other degree or diploma of a university or other institution of higher learning.”

18005818

14/02/2023

LIST OF FIGURES

Figure 1: pentagonal bipyramid (left), capped trigonal prism (middle) and capped octahedron (right).

Figure 2: The addition of a vertex (ligand) to an octahedron (six-coordinate complex).

Figure 3: A series of bipyridine-based hexadentate ligands with different lengths of alkyl chain in the aliphatic amine.

Figure 4: (a). bis-bidentate bridging ligands with polyamine bridges (bbN_7, bbN_9 and bbN_{12}). (b). dinuclear polypyridyl complexes with bbN_7 as the flexible bridge.

Figure 5: (a). The structure of N^1,N^2-Bis([2,2′-bipyridin]-6-ylmethylene)-1,2-ethanediamine (L). (b). Crystal structure of $[Eu(L)(NO_3)_2]^+$.

Figure 6: (a). The structure of the N_5 ligand (2,6-bis[2-(2,2′-bipyridin-6′-yl)ethyl]pyridine). (b). Crystal structure of the Ru(II) complex of the N_5 ligand. (c). Crystal structure of the Co complex of the N_5 ligand.

Figure 7: Crystal structures of the seven-coordinate $[Fe(OH_2)Y]^-$ (left) and $[Mn(OH_2)Y]^{2-}$ (right) complex anions.

Figure 8: The heptadentate ligand tren-py, $N(CH_2CH_2N{=}CHC_5H_4N)_3$ (left) and the complex ion $[Ni(tren\text{-}py)]^{2+}$ showing the helical C_3 geometry (right).

Figure 9: (A): The structure of the N7 ligand (L_D) synthesized by Drew et al.; (B): The 3D structure of $[CuL_D]^{2+}$.

Figure 10: (a). The structure of tris-(o-aminobenzyl)aminoethylamine (L^4). (b). The structure of $Ni[L^4]^{2+}$. (c). The structure of $Cu[HL^4]^{3+}$.

Figure 11: Structures of the N_7 heptadentate ligand TPAA and the N_6 hexadentate ligand TPEN.

Figure 12: ^1H NMR spectrum of 2,6-dibromomethylpyridine.

Figure 13: ^{13}C NMR spectrum of 2,6-dibromomethylpyridine.

Figure 14: Procedure of synthesizing 2,6-diaminomethylpyridine.

Figure 15: ^1H NMR spectrum of 2,6-diaminomethylpyridine.

Figure 16: ^{13}C NMR spectrum of 2,6-diaminomethylpyridine.

Figure 17: ^1H NMR spectrum of 6-methyl-2, 2'-bipyridine.

Figure 18: ^{13}C NMR spectrum of 6-methyl-2, 2'-bipyridine.

Figure 19: Structure and atom numbering of 6-methyl-2, 2'-bipyridine.

Figure 20: Proposed mechanism for the SeO_2 oxidation of 6-methyl-2, 2'-bipyridine.

Figure 21: ^{1}H NMR spectrum of 2, 2'-bipyridine-6-carboxaldehyde.

Figure 22: ^{13}C NMR spectrum of 2, 2'-bipyridine-6-carboxaldehyde.

Figure 23: Procedure used to synthesise N, N'-bis(2,2'-bipyridin-6-ylmethyl)pyridine-2,6-dimethylamine (bmpy).

Figure 24: Predicted spectrum (Molecular Formula: $C_{29}H_{28}N_7$, Charge: +1).

Figure 25: HRMS result of the product (impure).

Figure 26: (A): $C_{29}H_{23}N_7$, diimine. (B): $C_{29}H_{25}N_7$, one of the imines being reduced to an amine. (C): $C_{29}H_{27}N_7$, both imines being reduced to amines (desired product).

Figure 27: HRMS spectrum of the first band.

Figure 28: HRMS spectrum of the second band.

Figure 29: MS spectra of bmpy (portion A).

Figure 30: MS spectra of bmpy (portion B).

Figure 31: *m/z* 474.3 and *m/z* 496.3 of MS spectra of bmpy (portionB).

Figure 32: Top: ^{1}H NMR spectrum of N, N'-bis(2,2'-bipyridin-6-ylmethyl)pyridine-2,6-dimethylamine (bmpy). Bottom: Downfield region of the ^{1}HNMR spectrum.

Figure 33: ^{13}C NMR spectrum of N, N'-bis(2,2'-bipyridin-6-ylmethyl)pyridine-2,6-dimethylamine (bmpy).

Figure 34: Mass spectra of solutions containing bmpy and $Co(ClO_4)_2{\cdot}6H_2O$ in differing mole ratios. (A). (1:1), (B). (1:2), (C). (1:3).

Figure 35: Expansion of the peak at *m/z* 631.2 in the mass spectrum of bmpy: $Co(ClO_4)_2{\cdot}6H_2O$ (1:3).

Figure 36: Mass spectra of solutions containing bmpy and $Cu(ClO_4)_2{\cdot}6H_2O$ in differing mole ratios. (A). (1:1), (B). (1:2), (C). (1:3).

Figure 37: Expansion of the base peak *m/z* 298.6 in the mass spectrum of Bmpy:$Cu(ClO_4)_2{\cdot}6H_2O$ (1:1).

Figure 38: Mass spectra of solutions containing bmpy and $Fe(ClO_4)_2{\cdot}6H_2O$ in differing mole ratios. (A). (1:1), (B). (1:2), (C). (1:3).

Figure 39: Mass spectra of solutions containing bmpy and $Ni(ClO_4)_2{\cdot}6H_2O$ in differing mole ratios. (A). (1:1), (B). (1:2), (C). (1:3).

Figure 40: Expansions of the peaks at *m/z* 265.7 and *m/z* 630.2 showing their isotope patterns of bmpy:$Ni(ClO_4)_2{\cdot}6H_2O$ (1:3).

Figure 41: Mass spectra of solutions containing bmpy and $Zn(ClO_4)_2{\cdot}6H_2O$ in differing mole ratios. (A). (1:1), (B). (1:2), (C). (1:3).

Figure 42: Isotope pattern of the base peak in the mass spectrum of bmpy:$Zn(ClO_4)_2 \cdot 6H_2O$ (1:3).

Figure 43: Structure of bmdet.

Figure 44: ^{13}C NMR spectrum of N, N'-bis(2,2'-bipyridin-6-ylmethyl)diethylamine-1,2-dimethylamine (bmdet).

Figure 45: Mass spectrum of N, N'-bis(2,2'-bipyridin-6-ylmethyl)diethylamine-1,2-dimethylamine (bmdet).

Figure 46: MS spectra of Bmdet/$Co(ClO_4)_2 \cdot 6H_2O$ (A). (1/1), (B). (1/2), (C). (1/3).

Figure 47: MS spectra of Bmdet/$Cu(ClO_4)_2 \cdot 6H_2O$ (A). (1/1), (B). (1/2), (C). (1/3).

Figure 48: MS spectra of Bmdet/$Fe(ClO_4)_2 \cdot 6H_2O$ (A). (1/1), (B). (1/2), (C). (1/3).

Figure 49: MS spectra of Bmdet/$Ni(ClO_4)_2 \cdot 6H_2O$ (A). (1/1), (B). (1/2), (C). (1/3).

Figure 50: Expansion of peaks at *m/z* 248.8 and *m/z* 249.5 in the mass spectrum of Bmdet/$Ni(ClO_4)_2 \cdot 6H_2O$ (1/1).

Figure 51: MS spectra of Bmdet/$Zn(ClO_4)_2 \cdot 6H_2O$ (A). (1/1), (B). (1/2), (C). (1/3).

Figure 52: Expansion of the peaks at m/z 251.7, and m/z 252.6 and m/z 253.5 in the mass spectrum of Bmdet/$Zn(ClO_4)_2 \cdot 6H_2O$ (1/1).

Figure 53: Structure of DMbmdet.

Figure 54: ^{1}H NMR spectrum of DMbmdet.

Figure 55: ^{13}C NMR spectrum of DMbmdet.

Figure 56: MS spectrum of DMbmdet.

Figure 57: MS spectra of DMbmdet/$Co(ClO_4)_2 \cdot 6H_2O$ (A). (1/1), (B). (1/2), (C). (1/3).

Figure 58: MS spectra of DMbmdet/$Cu(ClO_4)_2 \cdot 6H_2O$ (A). (1/1), (B). (1/2), (C). (1/3).

Figure 59: MS spectra of DMbmdet/$Fe(ClO_4)_2 \cdot 6H_2O$ (A). (1/1), (B). (1/2), (C). (1/3).

Figure 60: MS spectra of DMbmdet/$Ni(ClO_4)_2 \cdot 6H_2O$ (A). (1/1), (B). (1/2), (C). (1/3).

Figure 61: MS spectra of DMbmdet/$Zn(ClO_4)_2 \cdot 6H_2O$ (A). (1/1), (B). (1/2), (C). (1/3).

ACKNOWLEDGEMENTS

First I would like to show my most sincere gratitude to my supervisor Professor Allan Blackman. I cannot get through these two tough years to complete my MSc in chemistry without his kindness, patience and massive guidance and feedback on my work. I especially would like to show my eternal gratefulness for his additional support when I was facing unexpected challenges from the supervision problem during my thesis writing time and the covid-19 lockdown.

Many thanks to all the academic and administrative staff of the School of Science, Auckland University of Technology, for their support of my study at AUT. To Mark Johnstone and Cassandra Fleming for their help and suggestions on my lab work. To Jack Chen for the drinks on Friday nights. To Marcus Jones for his suggestions on my writing. To Tony Chen, for his support and knowledge on Mass specs. To Yan Wang and Rahul Permal for their assistance with lab equipment and chemical supplement.

I also would like to thank all my friendly lab mates, Anau Lautaha, Bryan Anrango, Cailin Carmichael, Chloe Ren, Congyue Wei, Dora Laczi, Fouad Ismael, Jessica Fredericksen, Marc Malingin, Roisin Mooney and Shaun Souza for making the lab like a big family. I especially would like to thank Bronte Carr, for always being supportive when I need help on lab skills or study.

I would like to thank my best friends, Sherry Wei for her mental support when I feel suffocating due to the stress from writing my thesis, Angela Zhang for complaining about life together and Zhiheng yuan for his company of hanging out.

Finally, I cannot thank enough my parents, not only for their financial support, but also for their understanding, their concern and their love, which warmed my heart when I feel desperate for the view that the existence of creatures is possibly meaningless to the universe.

Chapter 1: Introduction

Coordination chemistry can be described as the chemistry of the transition metals. These 30 elements lie in the centre of the periodic table, and their chemistry is dominated by the presence of partially filled *d* orbitals. These contribute to their spectral and magnetic properties, with compounds containing transition metals often being coloured and paramagnetic. While the first application of coordination chemistry can be traced back to ancient times using mordants to fix dyes to fibres, coordination chemistry is a relatively young science, with the modern theory not established until the early 20th century, based on the work of both Jørgensen and Werner.[1] They developed the concepts of coordination number and oxidation state, both of which play a crucial part in the understanding of the chemistry of coordination complexes. Since this time, coordination chemistry has grown to be a vitally important discipline in chemistry, with numerous Nobel prizes having been awarded to coordination chemists like Werner,[2] Wilkinson,[3] Taube,[4] Grubbs[5] etc. It has also led to the development of organometallic chemistry and supramolecular chemistry as important subdisciplines.

This thesis describes the design, synthesis and characterisation of heptadentate N-donor ligands, and attempts to coordinate these to a number of transition metal ions. With this in mind, it is important that one of the fundamental concepts of coordination chemistry, the idea that a coordination complex is made up of a metal ion and one or more ligands, is discussed.

1.1 Coordination complexes

Coordination complexes are comprised of two components; a transition metal ion and one or more ligands. The metal ion can exist in a variety of oxidation states, owing to the fact that it can formally lose various numbers of *d* electrons. The ligand(s) are bonded to the metal ion through lone pairs on the donor atom. This bonding can be thought of as a Lewis acid/Lewis base interaction, in which the metal ion acts as the Lewis acid. In classical terms, this then requires each ligand donor atom to have a lone pair of electrons, and restricts donors to O, N, S, and P atoms and halide ions. The overall geometry of the coordination complex is determined by the natures of both the metal ion and the ligand(s). Particular d-electron configurations favour certain geometries about the metal ion, while multidentate ligands can

impose particular geometries on the metal ion. The most common coordination number in coordination complexes is 6, followed by 4 and 5, with the corresponding ideal geometries being octahedral, tetrahedral/square planar, and trigonal bipyramidal/square pyramidal, respectively. While coordination numbers up to 16 are known (CoB_{16}^-, for example),[6] coordination numbers greater than 6 are relatively rare, and are usually found in lanthanoid complexes, owing to the relatively large radii of the metal ions. Of particular interest to this thesis are seven-coordinate complexes.

1.1.1 Seven-coordinate geometries

Coordination numbers higher than 6 in transition metal complexes are relatively rare because a very large cation or a very small anion, or a combination of both, are often required to avoid steric repulsion between ligand atoms.[7] Therefore, in situations like this, not only does the metal ion need to be an appropriate size, but the ligand (or ligands) also needs to meet some electronic and steric requirements, especially for multidentate ligands. There are three ideal structures of seven-coordinate complexes in which inter-ligand repulsions are minimised; these are pentagonal bipyramidal (e.g., ZrF_7^{3-}), capped trigonal prismatic (e.g., TaF_7^{2-}) and capped octahedral (e.g., MoF_7^-),[7] with their respective symmetries being D_{5h}, C_{2v}, and C_{3v}.[8]

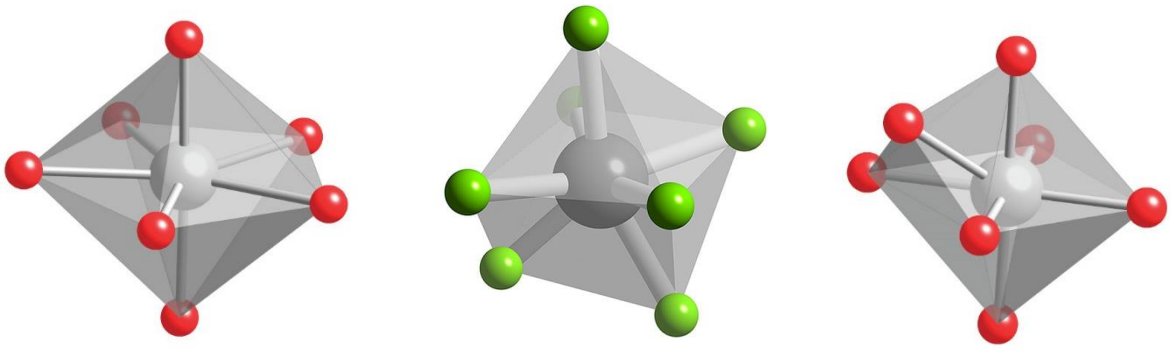

Figure 1. pentagonal bipyramid (left), capped trigonal prism (middle) and capped octahedron (right) geometries (https://www.chemtube3d.com/).

While these three structures look outwardly quite different, they can all be derived from an octahedron by addition of a single ligand. Hoffmann showed that a D_{5h} pentagonal bipyramid can be generated from a vertex addition along an octahedral edge to make five coplanar vertices (1→2, Figure 2), while a C_{3v} capped octahedron (1→3, Figure 2) and a C_{2v} capped

trigonal prism (1→4, Figure 2) can be both obtained by addition of a vertex to a face of an octahedron.

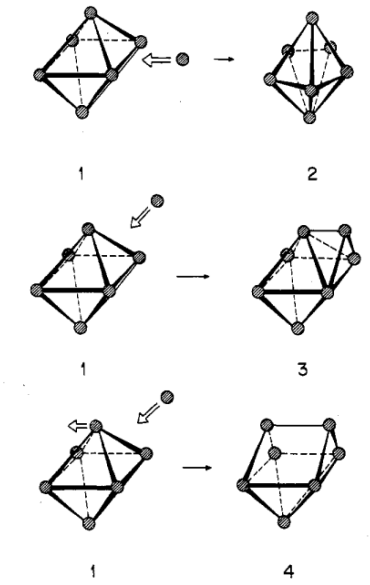

Figure 2. The addition of a vertex (ligand) to an octahedron (six-coordinate complex).[9]

The addition of a vertex to an octahedron can also be considered as an addition of a ligand to a six-coordinate complex, which indicates that seven-coordination can play a significant role when studying the reaction intermediates or transition states in associative substitution reactions of six-coordinate complexes and alternatively, those in oxidative addition reactions of five-coordinate complexes or dissociative reactions of eight-coordinate complexes.

1.1.2 Multidentate ligands containing bipyridine units.

The preparation of seven-coordinate complexes of first row transition metals is of interest given that such complexes may exhibit unusual spectral or electronic properties. Given the small size of such metal ions, it is unlikely that homoleptic complexes will be able to be formed, and multidentate ligands in which all donor atoms can coordinate to a metal ion are likely to be required.

Our group has had experience in the synthesis of multidentate ligands containing 2,2'-bipyridine moieties. We prepared a series of hexadentate ligands containing two bipyridine units that are linked by aliphatic diamine units (Figure 3). These ligands, which were prepared by reaction of 2,2'-bipyridine-6-aldehyde with the appropriate diamine and subsequent reduction of the diimine, differ only in the length of the alkyl chain in the

aliphatic diamine, and this chain length was found to have significant effects on the nature of the complexes formed, especially their nuclearities.[10] The study of this series of ligands was driven by the interest in multidentate ligands which can form multinuclear metal complexes. In reality, multidentate ligands often tend to bind all suitably positioned donor atoms to a single metal ion to give mononuclear complexes, as a result of the chelate effect. The formation of mutinuclear metal complexes containing multidentate ligands usually requires the ligand(s) to have separate binding domains. However, if the ligand is big enough to have multiple binding zones but is too flexible, the formation of multinuclear complexes will be difficult because of the lack of control over the binding of the ligand.

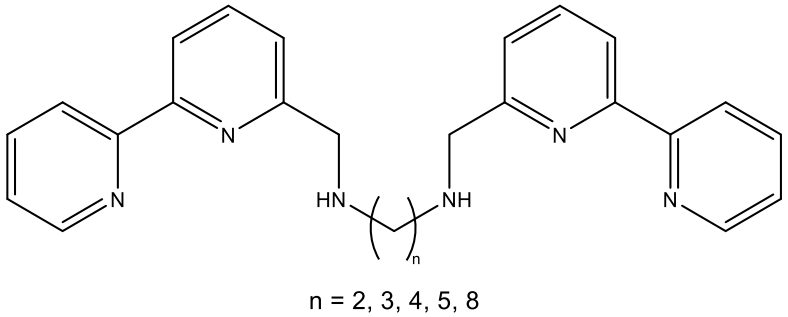

Figure 3. A series of bipyridine-based hexadentate ligands with different lengths of alkyl chain in the aliphatic amine

This series of ligands was therefore designed to discover how the length of the aliphatic segment would affect the formation of metal complexes containing Mn^{2+}, Ni^{2+}, Fe^{2+}, Cu^{2+}, Zn^{2+} and Co^{3+} ions. While mononuclear complexes were formed exclusively for n = 2 and 3, mass spectra showed that dinuclear complexes and even trinuclear complexes in some cases became increasingly favoured as n increased. This was because the increasing size of the aliphatic chelate ring made formation of mononuclear complexes unfavourable.

In the same year (2011) another series of multidentate ligands containing bipyridines was published by Mulyana et al.,[11] including ligands composed of two 4-methyl-2,2'-bipyridine groups linked with a series of linear alkylamine chains with varying lengths (Figure 4, a). These were synthesized by the reaction between 4-methyl-2,2'-bipyridine-4'- carboxaldehyde and the appropriate polyamine compounds followed by reducing the resulting Schiff base products with $NaBH_4$. These ligands were used to synthesize dinuclear polypyridyl complexes with flexible bridges (one example is given in Figure 4, b) which were found to have excellent DNA-binding properties. The different bridge lengths between the two 4-

methyl-2,2'-bipyridine groups were important because DNA affinity was found to be enhanced by a more flexible bridge in these kinds of ligands while the increasing chain length also leads to higher cytotoxicity.

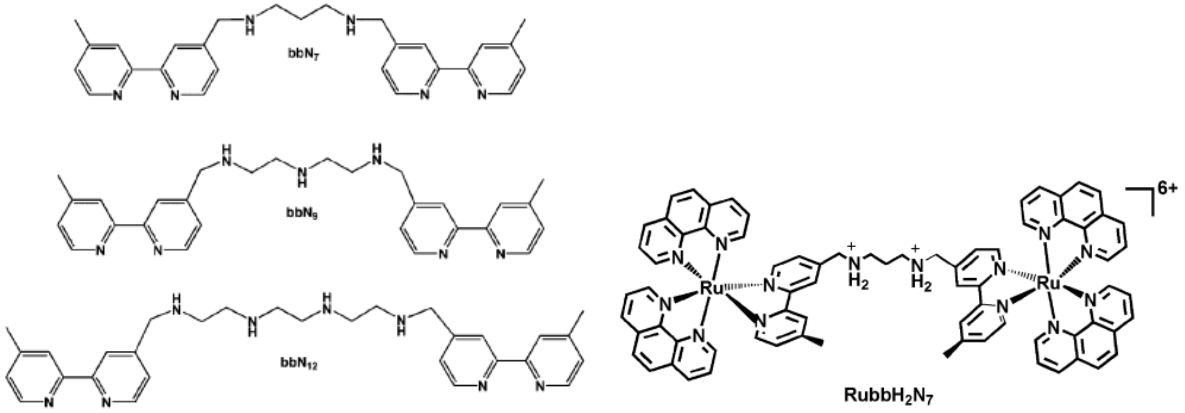

a b

Figure 4. (a). bis-bidentate bridging ligands with polyamine bridges (bbN_7, bbN_9 and bbN_{12}). (b). dinuclear polypyridyl complexes with bbN_7 as the flexible bridge.[11]

In addition to the dinuclear complexes, mononuclear, trinuclear and even tetranuclear species were also successfully synthesized. Compared with the dinuclear complexes, mononuclear ones showed a lower affinity for DNA while the trinuclear and tetranuclear ones were shown to have a higher affinity. The dinuclear complexes containing polyamine bridges exhibited a lower affinity compared to their polymethylene analogues while also having lower cytotoxicity. The complexation behaviour of the bbN_9 ligand with first-row transition metals is studied in this thesis (named DMbmdet), as it was only studied with ruthenium(II) previously.[11,12]

A diimine ligand with a similar structure to a ligand made previously by our group (Figure 3)[10] (Figure 5, a) was made by Hasegawa et al. via a direct reaction between 2,2'-bipyridine-6-aldehyde and ethylenediamine in order to study the luminescence properties of its lanthanide complexes; the crystal structure of one of the complexes synthesized is given in Figure 5, b).[13] Their luminescence spectral features originate from the *ff*-electronic transitions of Ln complexes and this can be induced by the photo-excitation of π-electronic systems from the ligand via an intramolecular energy transfer. This means the π-electronic moieties of the ligands are acting as photo-antennae or energy donors. The two bipyridine moieties were therefore designed in the hexadentate ligand in this study while the ethylenediamine group

was designed to prevent conjugation of two bipyridines in the complexes. Moreover, the multidentate ligand will induce a large chelate effect which brings stability, and can act as a steric shield to the outer-sphere, thus potentially inducing an enhanced *ff*-emission.

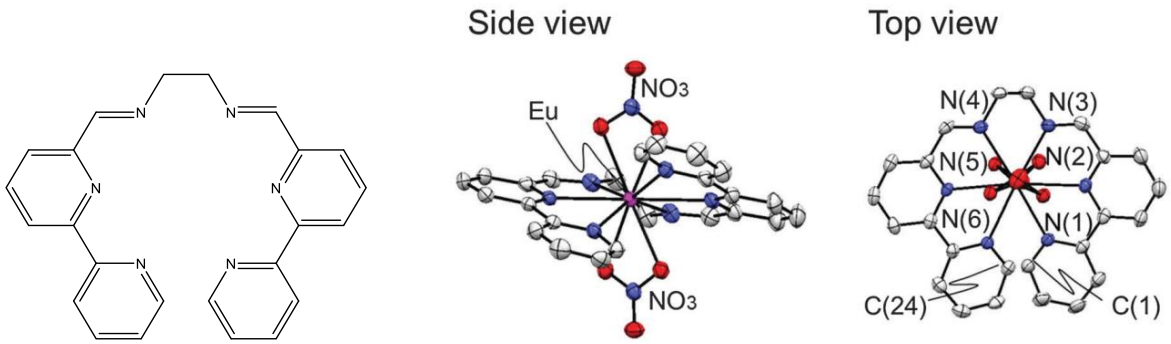

a b

Figure 5. (a). The structure of N^1,N^2-Bis([2,2′-bipyridin]-6-ylmethylene)-1,2-ethanediamine (L). (b). Crystal structure of $[Eu(L)(NO_3)_2]^+$.

The pentadentate N_5 ligand (Figure 6, a) first synthesized by Hamelin et al.[14] in 2008 has a similar structure to the new heptadentate N_7 ligand bmpy synthesized in this thesis. This ligand, synthesized via the reaction between 6-methyl-2,2'-bipyridine and 2,6-bis(chloromethyl)pyridine, was designed to form a novel ruthenium polypyridyl complex, as such complexes are well-known as a class of active catalysts for oxidation reactions including sulfoxidation and epoxidation. An extra pyridine was included in addition to the two bipyridines to evaluate how the chelate effect would affect the catalysis, relative to complexes containing two individual bipyridine ligands. The complex obtained was found to exhibit an octahedral geometry with an acetonitrile molecule coordinated at the sixth position (Figure 6, b). This complex and was shown to have higher efficiency in the catalysis of sulfide oxidation by H_2O_2 and olefin epoxidation by $PhI(OAc)_2$ (OAc = acetate) compared to its analogue with two bipyridines and a pyridine as ligands.

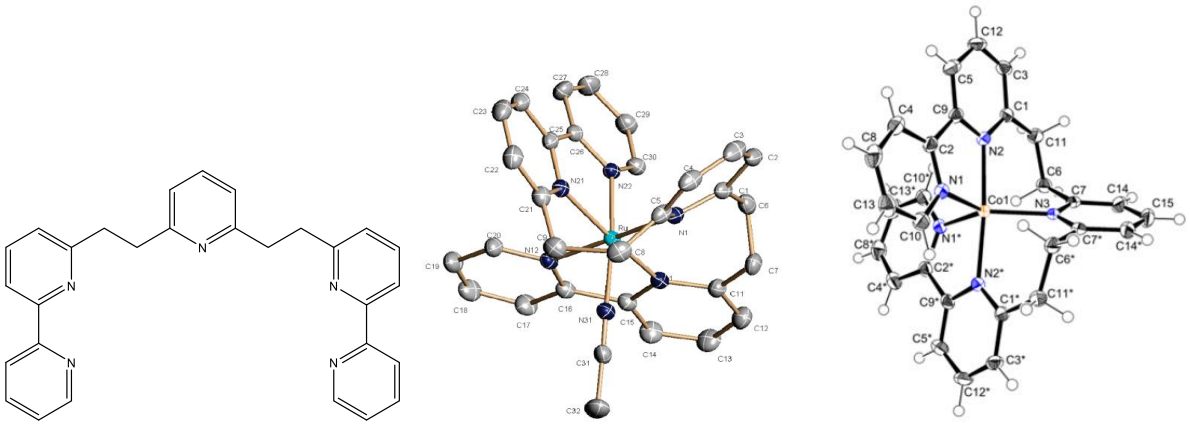

Figure 6. (a). The structure of the N_5 ligand (2,6-bis[2-(2,2′-bipyridin-6′-yl)ethyl]pyridine). (b). Crystal structure of the Ru(II) complex of the N_5 ligand. (c). Crystal structure of the Co complex of the N_5 ligand.

Interestingly, in a later study of the Co(II) complex of this ligand,[15] the complex obtained was found to exhibit a five-coordinate trigonal bipyramidal geometry without an additional monodentate ligand (Figure 6, c).

1.2 Heptadentate ligands.

A rational design is required to successfully synthesize seven coordinate complexes containing transition metal ions from the first row since they have a relatively small size. Many strategies have been used to achieve such syntheses including the use of acyclic or macrocyclic pentadentate ligands, acyclic heptadentate ligands, N, N′-disubstituted pentazamacrocycles, acyclic ligands that stabilize the pentagonal bipyramid by π-π-stacking interactions and hexadentate ligands based on ethylenediaminetetraacetate forming seven-coordinated complexes with a water molecule occupying the seventh coordination position.[16] Our group has long been interested in ligands with all donor atoms being nitrogen[10,17,18] and we have prepared several tetra-, penta- and hexadentate nitrogen donor ligands, and their corresponding complexes with first-row transition-metals. Heptadentate ligands with all seven donor atoms being nitrogen and seven-coordinated complexes with all seven nitrogen atoms bonded to the metal centre are relatively uncommon and it would be interesting to discover the steric and geometric properties of these complexes.

The earliest reports arousing the interest of chemists on seven-coordinate complexes and heptadentate ligands came in the 1960s[19–22] when the crystal structures of several seven-coordinate complexes containing multidentate ligands were obtained. Examples include those reported by Hoard et al., who successfully determined the structures of some hexadentate seven-coordinate anionic ethylenediaminetetraacetate complexes of Mn(II) ($Mn_3(HY)_2 \cdot 10H_2O$) and Fe(III) ($RbFe(OH_2)Y \cdot H_2O$), where Y^{4-}= the ethylenediaminetetraacetate tetraanion. As shown in the structures given in Figure 7, both exhibit a crude pentagonal bipyramidal geometry.

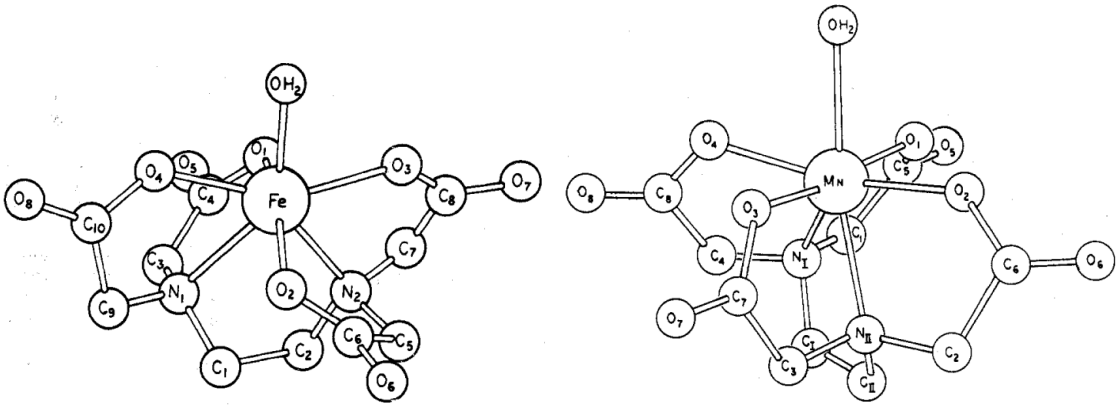

Figure 7. Crystal structures of the seven-coordinate $[Fe(OH_2)Y]^-$ (left) and $[Mn(OH_2)Y]^{2-}$ (right) complex anions.[20,21]

Soon, the first seven-coordinate species containing an N_7 heptadentate ligand, was reported by Wilson et al. in 1968.[23] As shown in Figure 8, the complex cation, $[Ni(tren\text{-}py)]^{2+}$, has a helical capped octahedral C_3 geometry with three imine nitrogen atoms and three pyridine nitrogen atoms being disposed approximately at the apices of an octahedron. The apical N atom, N_7, is acting as the 'cap' with an extremely long bond distance to nickel (3.25 Å) compared to the other 6 metal-nitrogen distances (2.10 Å).

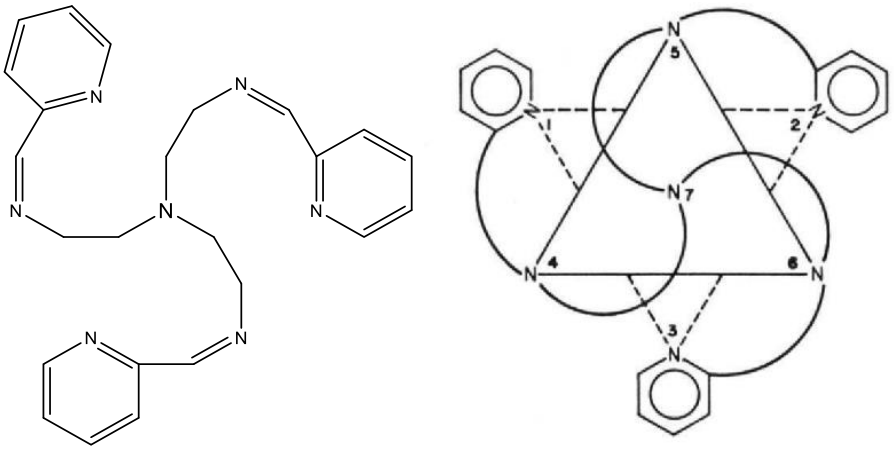

Figure 8. The heptadentate ligand tren-py, $N(CH_2CH_2N{=}CHC_5H_4N)_3$ (left) and the complex ion $[Ni(tren\text{-}py)]^{2+}$ showing the helical C_3 geometry (right).

In 1981 Drew et al.[24] prepared the N_7 ligand shown in Figure 9(A) and reported complexes of this with the first-row transition metals Mn(II), Fe(II), Co(II), Ni(II), Cu(II) and Zn(II). The Cu(II) complex was characterized by x-ray crystallography, which showed the metal ion to be seven-coordinate and to exhibit a pentagonal-bipyramidal geometry. The pyridine, imine and secondary N atoms make up an approximately planar equatorial girdle with the axial positions occupied by the two primary amine nitrogen atoms (Figure 9, (B)).

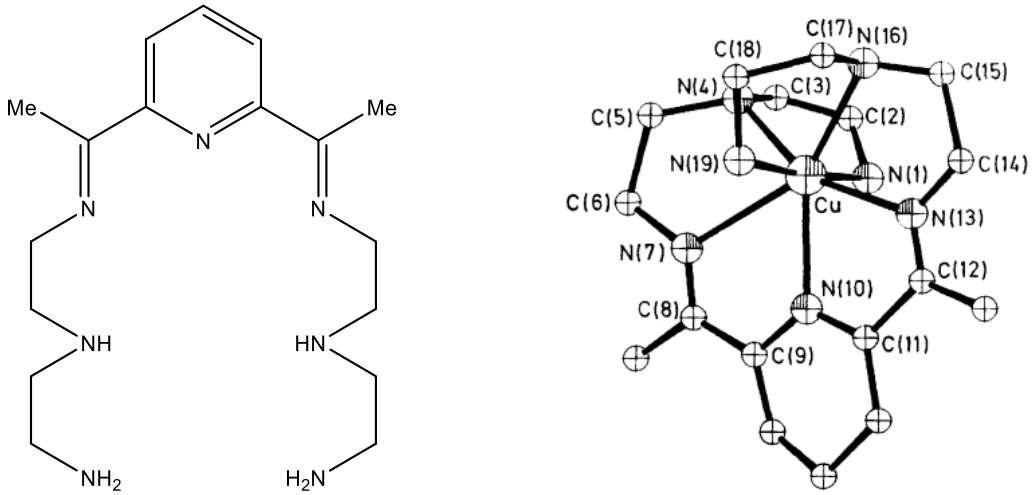

(A) (B)

Figure 9. (A): The structure of the N7 ligand (L_D) synthesized by Drew et al.; (B): The X-ray structure of $[CuL_D]^{2+}$.

Following these early examples over the past decades, a number of N_7 heptadentate ligands have been characterized shown to have the ability to form seven-coordinate complexes with

all seven nitrogen atoms coordinating to the metal centre.[24–52] In some cases, the arrangement of donor atoms in the heptadentate ligands does not allow for coordination of all the nitrogen atoms, and in such cases, the ligand bonds in a hypodentate[53] fashion to give five- or six-coordinate complexes.[27,54–57] For example, the N_7 ligand tris-(o-aminobenzyl)aminoethylamine binds 6 N atoms in its Ni(II) complex and 5 N atoms in its Cu(II) complex, giving octahedral and square pyramidal geometries, respectively (Figure 10). Similarly, ligands having more than 7 nitrogen atoms can also bind in a hypodentate fashion to form seven-coordinate complexes.[26,58–64]

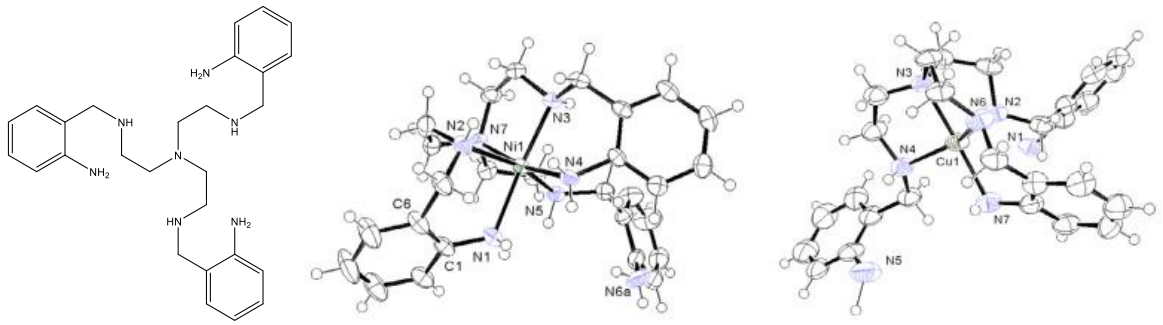

a b c

Figure 10. (a). The structure of tris-(o-aminobenzyl)aminoethylamine (L^4). (b). The structure of $Ni[L^4]^{2+}$. (c). The structure of $Cu[HL^4]^{3+}$.

1.3 Potential applications of seven-coordinate complexes

Transition metal complexes have long been studied as potential catalysts. In particular, transition metal complexes have been used as models for metalloenzymes. For example, superoxide (O_2^-), a by-product of oxygen metabolism, can cause many types of cell damage leading to inflammation, carcinogenesis and aging.[65] Superoxide dismutases (SODs) are metalloenzymes containing Cu, Zn, Mn and Fe which catalyse the degradation of O_2^- and thus defend against the diseases mentioned above. Fe(II)-tetrakis-N,N,N',N'-(2-pyridylmethyl)ethylenediamine (Fe-TPEN) and Fe(III)-tris[N-(2-pyridylmethyl)-2-aminoethyl]amine (Fe-TPAA), are two examples of SOD model complexes,[65] which have been found to be good superoxide dismutase mimics. Studies showed that 0.8 µM Fe-TPEN and 7.5 µM Fe-TPAA were equivalent to 1 unit of SOD activity in the xanthine oxidase-cytochrome c assay, blocking the toxic effect of paraquat on *Escherichia coli* growth, and Fe-TPAA was shown to protect cells from superoxide without the induction of SOD. The high SOD activity of these complexes is considered to be a result of coordination between the

pyridine rings and the central iron, which produces similar environments to those of SODs according to the study of Kimura et al.[66,67]

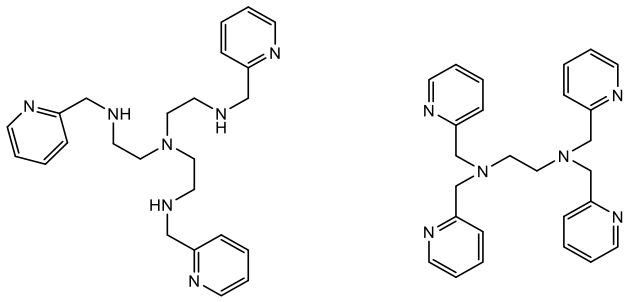

Figure 11. Structures of the N_7 heptadentate ligand TPAA and the N_6 hexadentate ligand TPEN

Heptadentate ligands which form seven-coordinate complexes also appear in the field of industrial catalysts. The tripodal heptadentate Schiff base, tris[N-(2-pyridylmethyl)-2-iminoethyl]amine (Py_3Tren) (Figure 8, left), which can be formed by a metal-assisted oxidative dehydrogenation of TPAA[47] was found to form a Cu complex that was highly active for atom transfer radical polymerization (ATRP). ATRP allows the synthesis of polymers with precise control over molecular weights, molecular weight distributions, complex polymeric architectures and associated functionalities.[68] The Cu complex of the ligand ($CuBr_2/Py_3Tren$) was proved to demonstrate higher activities and reduce the consumption of the metal catalyst compared to the complex of the control ligand.[69]

In addition to use in the fields of catalysis and biology, these ligands and complexes are also useful in luminescence[70] and magnetic[71] studies, including acting as imaging agents and agents for metal recovery, especially for those complexes of lanthanoids. In recent years, seven-coordinate pentagonal bipyramidal complexes of Fe(II), Co(II), Ni(II) and Mo(IV/III) have been shown to possess large magnetic anisotropies, which can be expressed in terms of axial (D) and rhombic (E) zero-field splitting (ZFS).[72] Their large axial magnetic anisotropy can lead to the construction of single-molecule magnets (SMMs) and such complexes can therefore act as ‘nano magnets’ which can potentially have applications in high-density storage media, spintronics and even quantum computing.[72]

1.4 Project Aim

The aim of this project is to carry out fundamental research on new nitrogen-based heptadentate ligands containing 2,2'-bipyridine units. Reductive amination is considered to be a good method to synthesize the newly designed N_7 ligand, N, N'-bis(2,2'-bipyridin-6-ylmethyl)pyridine-2,6-dimethylamine (bmpy) through the reaction between 2,6-diaminomethylpyridine and 2, 2'-bipyridine-6-carboxaldehyde. Should this synthesis be successful, then bmpy and two previously-prepared N_7 ligands, N, N'-bis(2,2'-bipyridin-6-ylmethyl)diethylamine-1,2-dimethylamine (bmdet) and N, N'-bis(6-methyl-2,2'-bipyridin-6'-ylmethyl)diethylamine-1,2-dimethylamine (DMbmdet), will be reacted with several first-row transition metals (Fe, Cu, Ni, Cu and Zn), and the products of these reactions will be studied by a variety of methods, with X-ray crystallography and ESI-MS being the most important detecting methods.

Chapter 2: Experimental

This chapter reports the syntheses of ligand precursors, ligands, and metal complexes used in this study.

2.1 Synthesis of 2,6-dibromomethylpyridine

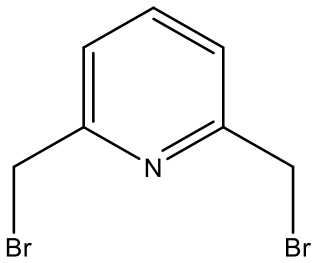

2,6-dibromomethylpyridine

This was prepared both from scratch, and by purification of an existing sample.

Purification of existing samples: Impure 2,6-dibromomethylpyridine (22.598 g) was added to $CHCl_3$ (250 mL), and the resulting mixture was heated to boiling for 30 min, with stirring. The remaining solid was removed by filtration and the filtrate was reduced to dryness (rotavap) to give the product as a white solid (15.111 g).

Synthesis from scratch: The method of Gill[73] was used. 2,6-pyridinedimethanol (7.000 g, 0.0503 mol) was dissolved in concentrated HBr solution (48%-50%, 50 mL, 0.44 mol) and the solution was refluxed with stirring for 18 h. Cooling the brown solution to room temperature resulted in the formation of a white precipitate. Excess solvent was evaporated, concentrated HBr solution (50 mL, 0.440 mol) was added to the crude product, and the solution was then refluxed with stirring for another 18 h. The resulting solution was cooled to room temperature to give a white precipitate, and the mixture was taken to dryness (rotavap). 50 mL 0.1 M NaOH (50 mL) was added to the residue and the mixture was immediately extracted with $CHCl_3$ (7 × 50 mL). The organic layers were combined and evaporated to dryness (rotavap) to give a pale pink solid (9.9389g, yield 74.6%). ^{13}C NMR (100 MHz, $CDCl_3$): δ 156.67, 138.28, 122.89, 33.25 ppm. ^{1}H NMR (400 MHz, $CDCl_3$): δ 7.72 (1H, t), 7.39 (2H, d), 4.55 (4H, s) ppm.

2.2 Synthesis of potassium phthalimide

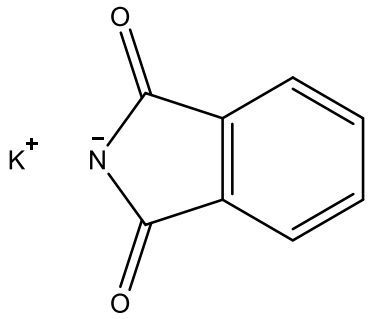

potassium phthalimide

This was prepared by the method of Gill.[73] A solution of phthalimide (8.006 g, 0.0544 mol) in ethanol (160 mL) was refluxed with stirring for 30 min. The hot phthalimide solution was then poured into half of an iced KOH solution (24 mL) containing KOH (6.156 g, 0.110 mol) in water (6 mL) and ethanol (18 mL). A white precipitate formed, which was removed by filtration after the mixture was cooled to room temperature. The white solid obtained was washed with acetone and air-dried. (6.735 g, yield 66.8%). Phthalimide (8.053 g) was added to the filtrate and the solution was refluxed with stirring for 30 min. The hot solution was poured into the remaining half of the KOH solution (12 mL) in an ice bath with stirring. The white precipitate was removed by filtration, washed with acetone, and air-dried. (7.330 g, yield 72.7%).

2.3 Synthesis of 2,6-diaminomethylpyridine

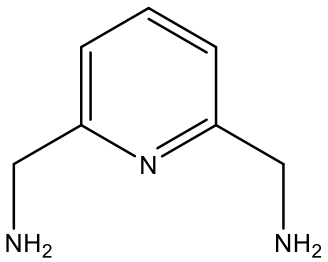

2,6-diaminomethylpyridine

The method of Liu et al.[74] was followed. 2,6-dibromomethylpyridine (2.365 g, 8.927 mmol) and potassium phthalimide (3.304 g, 17.838 mmol) were stirred in DMF (10 mL) at 100 ^{o}C for 48 h. Water (30 mL) was added to the crude product and the resulting white solid was

removed by filtration. The white powder (not totally dry) obtained was dispersed in 30 mL ethanol and hydrazine hydrate solution (50%-60%, 1.67 mL) was added. The mixture was then refluxed with stirring for 24 h. After being cooled to room temperature, 6 M HCl (20 mL) was added to the resulting product and the mixture was then refluxed with stirring for 2 h followed by stirring at room temperature overnight. After the resulting mixture was filtered, 6 M KOH solution (40 mL) was added to the filtrate (pH > 12). The solution was extracted with chloroform (30 mL × 4) and the organic layers were combined and dried over anhydrous Na_2SO_4. The product was obtained as a brown oil following reduction to dryness (0.852 g, yield 68.6%).

2,6-diaminomethylpyridine was found to decompose on storage in the fridge for several months. It was purified on an alumina column starting with $CHCl_3$ as the eluent, and the eluate was collected in fractions. Increasing amounts of MeOH were added to the eluent until 18% MeOH/$CHCl_3$ was reached. TLC and NMR were used to identify the portions containing the pure product. ^{13}C NMR (100 MHz, $CDCl_3$): δ 161.37, 137.05, 119.23, 47.74 ppm. ^{1}H NMR (400 MHz, $CDCl_3$): δ 7.57 (1H, t), 7.09 (2H, d), 3.92 (4H, s), 1.90 (4H, bs) ppm.

2.4 Synthesis of 6-methyl-2, 2'-bipyridine

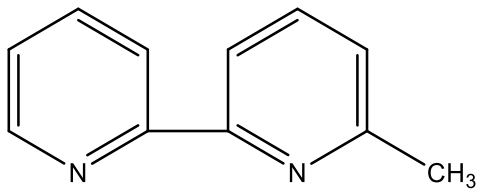

6-methyl-2, 2'-bipyridine

2.4.1 Method A

The method of Schmalzl et al.[75] was used. 2, 2'-bipyridine (18.409 g, 0.118 mol) was dissolved in dry diethyl ether (230 mL) under nitrogen. This solution was then added by cannula to ~100 mL methyllithium solution (3.1 M in diethoxymethane) over a period of 31 min. The resulting dark red solution was stirred at room temperature for 3 h, then added dropwise (caution!) onto ice. The orange ether (top) layer was collected from the resulting two-layered solution. The yellow aqueous (bottom) layer was extracted with diethyl ether (40 mL × 8) and all top layers were combined and evaporated. The brown oil obtained became

sticky on storage overnight. It was triturated with acetone and then the excess solvent was removed (rotavap). The resulting brown oil was stirred in a 90 ^{o}C oil bath for two hours under vacuum to convert any remaining dihydrobipyridine into aromatic 6-methyl-2,2'-bipyridine.

The product was dissolved in ethyl acetate and then loaded onto a silica column and eluted with 6/1 (v/v) hexane/ethyl acetate. This mixture was found to precipitate products on the column and so pure ethyl acetate was then used instead. The eluate was collected in fractions and identified by TLC and NMR. Pure 6-methyl-2, 2'-bipyridine was obtained as a yellow oil (11.887 g, 59.0 % yield). ^{13}C NMR (100 MHz, $CDCl_3$): δ 157.94, 156.52, 155.59, 149.15, 137.05, 136.82, 123.48, 123.24, 121.17, 118.10, 14.66 ppm. ^{1}H NMR (400 MHz, $CDCl_3$): δ 8.68 (1H, d), 8.43 (1H, d), 8.19 (1H, d), 7.82 (1H, t), 7.71 (1H, t), 7.30 (1H, t), 7.18 (1H, d), 2.65 (3H, s) ppm.

2.4.2 Method B

The method of Liao et al.[76] was utilised. 2-bromopyridine (2.385 mL, 0.02501 mol), 2-bromo-6-methylpyridine (1.140 mL, 0.01002 mol), anhydrous LiCl (4.452 g, 0.105 mol) and zinc granules (8.244 g, 0.126 mol) were added to a solution of $NiCl_2{\cdot}6H_2O$ (0.363 g, 1.793 mmol) in DMF (200 mL) at 40 ^{o}C. After the temperature reached 50 ^{o}C, three grains of iodine and 10 drops of acetic acid were added. The mixture was then heated to 60~70 ^{o}C, and a solution consisting of 2-bromopyridine (4.770 mL, 0.0500 mol), 2-bromo-6-methylpyridine (2.280 mL, 0.0200mol) in DMF (200 mL) was added dropwise to the dark blue mixture over a period of 3 h. The resulting mixture was stirred at 60 ^{o}C for 18 h. After being cooled to room temperature, 1 M HCl (150 mL) was slowly added to the crude product. Following stirring for 3 h, the crude material was poured into a new flask, excluding any remaining solid zinc. 25% aqueous ammonia (100 mL) was added to the solution (pH > 10), which was then extracted with CH_2Cl_2 (200mL × 1, 100 mL × 2 and 50 mL × 4). The organic layers were combined, dried over Na_2CO_3 and reduced to dryness (rotavap) to give a sticky dark red oil. This was diluted with toluene (50 mL) and reduced to dryness (2 x) to help remove the remaining DMF. Analysis of the crude product showed that it did not contain the desired 6-methyl-2, 2'-bipyridine product.

2.5 Synthesis of 2, 2'-bipyridine-6-carboxaldehyde

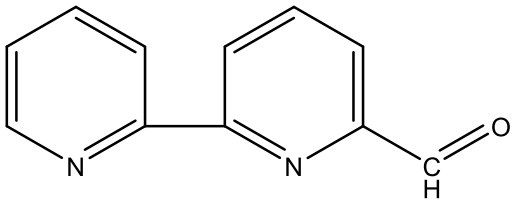

2, 2'-bipyridine-6-carboxaldehyde

The method of Heirtzler et al.[77] was followed. SeO_2 (2.796 g, 0.0252 mol) and water (460 µL, 0.0255 mol) were added to a solution of 6-methyl-2, 2'-bipyridine (2.671 g, 0.0157 mol) in dioxane (74 mL). The mixture was refluxed under nitrogen with stirring for 3 h. The reaction mixture was cooled to room temperature, more SeO_2 (2.793 g, 0.0252 mol) and water (460 µL, 0.0255 mol) were added, and the mixture was refluxed under nitrogen with stirring for another 24 h. Following cooling to room temperature, a black powder was removed by filtration and washed with warm dioxane (12 mL × 3) and warm ethyl acetate (12 mL × 3). The filtrates were combined with the original orange filtrate, and evaporation (rotavap) gave a turbid orange oil. The crude oil was loaded onto a silica column with 85/15(v/v) CH_2Cl_2/EtOAc. The eluate was collected in fractions and those containing pure 2, 2'-bipyridine-6-carboxaldehyde were identified by TLC and NMR. The product was obtained as a very pale pink solid (1.9876 g, yield 68.8 %) after evaporating the eluate to dryness. ^{13}C NMR (100 MHz, $CDCl_3$): δ 193.63, 156.23, 154.73, 152.36, 148.99, 138.05, 137.54, 125.32, 124.44, 121.56, 121.50 ppm. ^{1}H NMR (400 MHz, $CDCl_3$): δ 10.13 (1H, s), 8.65 (2H, m), 8.51 (1H, d), 7.93 (2H, m), 7.84 (1H, t), 7.34 (1H, t) ppm.

2.6 Synthesis of N, N'-bis(2,2'-bipyridin-6-ylmethyl)pyridine-2,6-dimethylamine (bmpy)

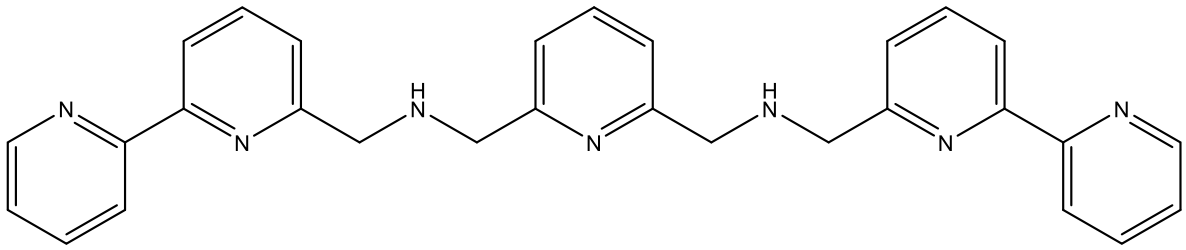

N, N'-bis(2,2'-bipyridin-6-ylmethyl)pyridine-2,6-dimethylamine (bmpy)

2.6.1 Method A

The synthesis of this ligand utilised an adaptation of the method of Baird et al used in preparing a similar molecule.[78] 2,6-diaminomethylpyridine (0.207 g, 1.507 mmol) and 2,2'-bipyridine-6-carbaldehyde (0.556 g, 3.017 mmol) were each dissolved in MeOH (12 mL). The two solutions were mixed, and the resulting mixture was refluxed with stirring for 10 min. It was then stirred at room temperature for 1.5 h, being monitored by TLC during this time. $NaBH_4$ (0.135 g, 3.566 mmol) was then added and stirring was continued for 2 h. The resulting orange solution was evaporated to dryness (rotavap) and water (20 mL) and $CHCl_3$ (20 mL) were added. The chloroform layer was collected, and the water layer was extracted with $CHCl_3$ (2 x 10 mL). All organic layers were combined, dried over Na_2SO_4 and reduced to dryness (rotavap) to give the product as a yellow oil.

2.6.2 Method B

An adaptation of the procedure used by Walther et al.[79] was utilised. A solution of 2,6-diaminomethylpyridine (0.106 g, 0.773 mmol) in MeOH (6 mL) was mixed with a solution of 2,2'-bipyridine-6-carbaldehyde (0.286 g, 1.551 mmol) in MeOH (6 mL). To this solution in an ice bath were added, with stirring, glacial acetic acid (0.275 mL, 4.80 mmol) and $NaBH_3CN$ (0.405 g, 6.437 mmol). Stirring was continued at room temperature until the bubbling had stopped. The mixture was then refluxed with stirring for 45 min and then stirred at room temperature overnight. TLC was used to monitor the reaction. Concentrated HCl (36%) was added dropwise to the resulting solution until the evolution of hydrogen had ceased, and then solid NaOH was added slowly to give pH > 12. The solution was reduced to a small volume, water (20 mL) was added, and the mixture was extracted with $CHCl_3$ (2 x 20 mL). The organic layers were combined, dried over Na_2SO_4 and evaporated to dryness (rotavap) to obtain the product as a yellow oil.

2.6.3 Purification

Products from both methods A and B were found to be impure on the basis of both NMR and MS spectra. The impure product oil was diluted a little with chloroform and loaded onto a silica column in 5% MeOH/$CHCl_3$ (1% NH_4OH). The percentage of MeOH used in the mobile phase was gradually increased to 8% during the process. The eluent was collected in fractions and identified by TLC and NMR. The pure product was obtained as a pale yellow

oil (0.214 g). ^{13}C NMR (100 MHz, $CDCl_3$): δ 159.31, 159.09, 156.22, 155.51, 149.07, 137.29, 136.86, 136.77, 123.59, 122.19, 121.19, 120.45, 119.20, 54.82, 54.75 ppm. ^{1}H NMR (400 MHz, $CDCl_3$): δ 8.64 (2H, d), 8.43 (2H, d), 8.24 (2H, d), 7.73 (4H, m), 7.60 (1H, t), 7.32 (2H, d), 7.24 (4H, m), 4.04 (8H, d), 2.84 (2H, bs) ppm.

2.7 Purification of N, N'-bis(2,2'-bipyridin-6-ylmethyl)diethylamine-1,2-dimethylamine (bmdet)

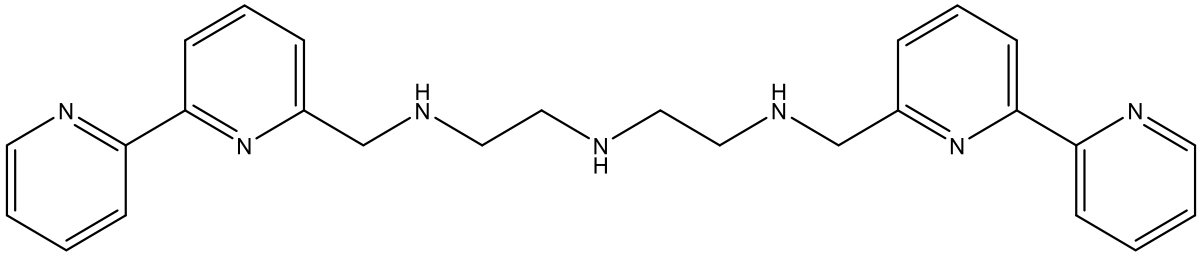

N, N'-bis(2,2'-bipyridin-6-ylmethyl)diethylamine-1,2-dimethylamine (bmdet)

N, N'-bis(2,2'-bipyridin-6-ylmethyl)diethylamine-1,2-dimethylamine (bmdet) was prepared by the method of Schrumpf.[80] The crude material was loaded onto an alumina column in $CHCl_3$, and the product was eluted with 2% MeOH/$CHCl_3$, gradually increasing to 10% MeOH/$CHCl_3$. The product was obtained as a yellow oil (0.287 g) after the evaporation of fractions found to contain pure bmdet. ^{13}C NMR (100 MHz, CDCl3): δ 159.31, 156.25, 155.54, 149.11, 137.29, 136.80, 123.61, 122.18, 121.16, 119.21, 55.13, 49.53, 49.16 ppm.

2.8 Purification of N, N'-bis(6-methyl-2,2'-bipyridin-6'-ylmethyl)diethylamine-1,2-dimethylamine (DMbmdet)

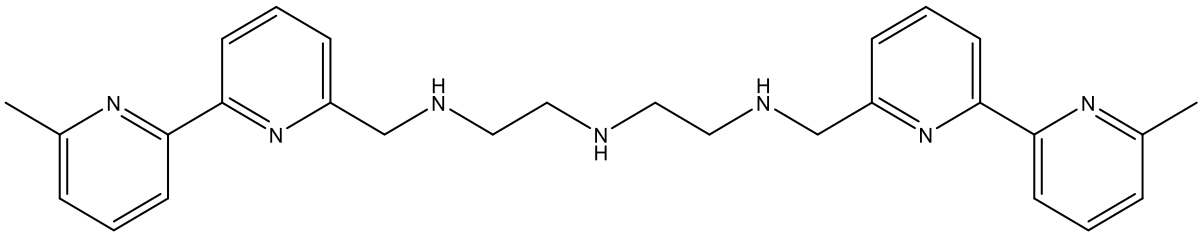

N, N'-bis(6-methyl-2,2'-bipyridin-6'-ylmethyl)diethylamine-1,2-dimethylamine (DMbmdet)

N, N'-bis(6-methyl-2,2'-bipyridin-6'-ylmethyl)diethylamine-1,2-dimethylamine (DMbmdet) was prepared by the method of Schrumpf.[80] The crude material was loaded onto an alumina column in 6% MeOH/CH_2Cl_2. The eluate was collected in fractions and the pure product was

obtained as a yellow oil (0.741 g) ^{13}C NMR (100 MHz, $CDCl_3$): δ 159.11, 157.83, 155.89, 155.66, 137.21, 136.95, 123.16, 121.98, 119.28, 118.15, 55.09, 49.41, 49.03, 24.65 ppm. ^{1}H NMR (400 MHz, $CDCl_3$): δ 8.25 (2H, d), 8.20 (2H, d), 7.72 (2H, t), 7.65 (2H, t), 7.27 (2H, d), 7.12 (2H, d), 3.97 (4H, s), 2.81 (8H, m), 2.61 (6H, s), 2.29 (3H, bs) ppm.

2.9 Studies of bmpy complexes

The initially-prepared bmpy ligand was thought to be relatively pure. This was due to the fact that the compound gave a fairly clean ^{13}CNMR spectrum, although the ^{1}HNMR spectrum was inconclusive. Therefore, initial investigations into the coordination properties of this ligand unwittingly used impure samples. However, subsequent acquisition of HRMS data indicated that the product containing significant mono- and diimine impurities, where reduction was incomplete. The product was then purified on a column. Data obtained using the impure material are given in section 2.9.1, while those obtained with pure bmpy are detailed in section 2.9.2.

2.9.1 Preparation of solutions of complexes

2.9.1.1 Attempted syntheses of Cu(II), Fe(II), Co(II), Ni(II), Zn(II), Mn(II), and Pd(II) complexes in mixed solutions of MeOH / acetonitrile or MeOH / water

Bmpy (not columned) and metal salts were dissolved in MeOH (1.5 mL) and acetonitrile (1 mL) (water is used when dissolving K_2PdCl_4) in two vials respectively. The amounts used are given in the table below.

Ratio (ligand : metal)	Mass of bmpy / g	Metal salt	Mass of metal salt / g
1:1	0.0509	$Cu(ClO_4)_2{\cdot}6H_2O$	0.0403
1:2	0.0518		0.0836
1:3	0.0537		0.1270
1:1	0.0513	$Fe(ClO_4)_2{\cdot}6H_2O$	0.0288
1:2	0.0562		0.0626
1:3	0.0536		0.0885
1:1	0.0543	$Co(ClO_4)_2{\cdot}6H_2O$	0.0438
1:2	0.0518		0.0815

1:3	0.0511		0.1201
1:1	0.0516	$Ni(ClO_4)_2 \cdot 6H_2O$	0.0408
1:2	0.0512		0.0796
1:3	0.0508		0.1198
1:1	0.0561	$Zn(ClO_4)_2 \cdot 6H_2O$	0.0456
1:2	0.0523		0.0829
1:3	0.0521		0.1231
1:1	0.0502	$Mn(ClO_4)_2$	0.0278
1:2	0.0530		0.0571
1:3	0.0516		0.0832
1:1	0.0510	K_2PdCl_4	0.0354
1:2	0.0501		0.0692
1:3	0.0521		0.1082

The solution of bmpy and the solution of the metal salt were mixed and the resulting solution was stirred for several minutes. If any precipitate formed immediately, this was removed by filtration and the filtrate would be kept in a new vial. All solutions were kept in the fume hood and left to evaporate slowly. The residues were analysed by NMR (where possible) and MS.

2.9.1.2 Attempted synthesis of Cu(II), Fe(II), Co(II), Ni(II) complexes in 1:1, 1:2 and 1:3 ratios in acetonitrile

Bmpy and the metal salt were dissolved in acetonitrile (1 mL) in separate vials. A hot water bath was used to assist dissolution of the ligand. The amounts used are given in the table below.

Ratio (ligand : metal)	Mass of bmpy / g	Metal salt	Mass of metal salt / g
1:1	0.0535	$Cu(ClO_4)_2 \cdot 6H_2O$	0.0423
1:2	0.0498		0.0782
1:3	0.0518		0.1218
1:1	0.0502	$Fe(ClO_4)_2 \cdot 6H_2O$	0.0275
1:2	0.0510		0.0552
1:3	0.0513		0.0835
1:1	0.0505	$Co(ClO_4)_2 \cdot 6H_2O$	0.0392

1:2	0.0508		0.0785
1:3	0.0519		0.1201
1:1	0.0502	$Ni(ClO_4)_2 \cdot 6H_2O$	0.0389
1:2	0.0509		0.0788
1:3	0.0503		0.1207

The two solutions were mixed and the resulting solution was stirred for several minutes. They were then all placed in a fume hood for slow evaporation see if any crystals formed.

$NaSbF_6$ (0.0544 g, 2 equivalents) and 15 drops of acetonitrile were added to the residue of the 1:2 Cu sample, and the solution was left to evaporate.

2.9.1.3 Attempted synthesis of a Co(III) complex of bmpy

2.9.1.3.1 Method A

Bmpy (0.0518 g) was dissolved in MeOH (2 mL) and $Co(ClO_4)_2 \cdot 6H_2O$ (0.0410 g) was dissolved in water (1 mL). The cobalt(II) solution was poured into the ligand solution and then the air was blown through the turbid brown solution through a Pasteur pipette overnight. The resulting sandy brown solid was removed by filtration and washed with isopropanol. The solid was then air-dried to give the product as a light brown powder (0.0321 g). Attempts to record the NMR of the product in d7-DMF gave only broad peaks, suggesting the product contained Co(II).

2.9.1.3.2 Method B

Bmpy (0.0524 g) was dissolved in MeOH (1.5 mL) and $Co(ClO_4)_2 \cdot 6H_2O$ (0.0412 g) was dissolved in water (1 mL). To the turbid brown solution formed by pouring the Co solution into the bmpy solution, PbO_2 (0.0275 g) was added. The mixture was stirred overnight and filtered to give a brownish grey solid and dark brown solution. The brown oil obtained after the evaporation of the filtrate was loaded onto a Sephadex SP-C25 column. Two bands were formed and collected separately with 0.4 M $NaClO_4$ as the mobile phase. The second band collected was evaporated to obtain an orange oil and colourless crystals.

2.9.2 MS studies of bmpy complexes

2.9.2.1 MS studies in a mixed solution of MeOH and acetonitrile with Cu(II), Fe(II), Co(II), Ni(II) and Zn(II) in 1:1, 1:2 and 1:3 ratios

A solution of bmpy with a concentration of 1.19 mg/mL was made by adding 0.0119 g bmpy to a 10 mL volumetric flask and making up to the mark with MeOH. Five acetonitrile solutions of metal salts with 10 times the molarity of the bmpy solution were made with 0.0936 g $Cu(ClO_4)_2 \cdot 6H_2O$, 0.0925 g $Co(ClO_4)_2 \cdot 6H_2O$, 0.0923 g $Ni(ClO_4)_2 \cdot 6H_2O$, 0.0916 g $Fe(ClO_4)_2 \cdot 6H_2O$ and 0.0938 g $Zn(ClO_4)_2 \cdot 6H_2O$, respectively, in five 10 mL volumetric flasks. These five solutions were then diluted 10 times by adding 1 mL of each solution to a new 10 mL volumetric flask and making up to the mark with acetonitrile. 10 µL of bmpy solution was mixed with 10 µL (1:1), 20 µL (1:2) and 30 µL (1:3) of every diluted metal salt solution in three Eppendorf tubes respectively. 10 µL of every mixed solution was then added to an MS vial and diluted with 990 µL MeOH. MS data were then obtained for all samples.

2.9.2.2 Attempted synthesis of Co(II) and Fe(II) complexes of bmpy

Bmpy (0.0520 g) was dissolved in MeOH (3 mL) and $Co(ClO_4)_2 \cdot 6H_2O$ (0.0408 g) was dissolved in acetonitrile (2 mL). The two solutions were mixed and MeOH (2 mL) was used to rinse the vial. After being stirred for several minutes, the mixed solution was left to evaporate.

The same process was carried out with bmpy (0.0505 g) and $Fe(ClO_4)_2 \cdot 6H_2O$ (0.0393 g).

Powders were obtained in both vials. Recrystallisation of these powders from hot water, MeOH, acetonitrile and acetone was attempted, but no crystalline material was obtained. Ether diffusion of an acetone solution of the Fe complex was attempted, but again no crystalline material was obtained.

2.10 MS studies of bmdet complexes

A 1.042 mg/mL bmdet solution was made with 0.01042 g bmdet and MeOH in a 10 mL volumetric flask. Five acetonitrile solutions of metal salts with 10 times the molarity of the bmdet solution were made with 0.0882 g $Cu(ClO_4)_2 \cdot 6H_2O$, 0.0872 g $Co(ClO_4)_2 \cdot 6H_2O$, 0.0868 g $Ni(ClO_4)_2 \cdot 6H_2O$, 0.0862 g $Fe(ClO_4)_2 \cdot 6H_2O$ and 0.0888 g $Zn(ClO_4)_2 \cdot 6H_2O$, respectively, in five 10 mL volumetric flasks. These five solutions were then diluted 10 times by adding 1

mL of every solution to a new 10 mL volumetric flask and making up to the mark with acetonitrile. 10 µL bmdet solution was mixed with 10µL (1:1), 20µL (1:2) and 30 µL (1:3) of every diluted metal salt solution in three Eppendorf tubes respectively. 10 µL of every mixed solution was then added to an MS vial and diluted with 990 µL MeOH. All samples were then tested by MS.

2.11 MS studies of DMbmdet complexes

The same method as bmdet was used for the DMbmdet ligand with 0.0108 g DMbmdet, 0.0860 g $Cu(ClO_4)_2 \cdot 6H_2O$, 0.0850 g $Co(ClO_4)_2 \cdot 6H_2O$, 0.0846 g $Ni(ClO_4)_2 \cdot 6H_2O$, 0.0838 g $Fe(ClO_4)_2 \cdot 6H_2O$ and 0.0860 g $Zn(ClO_4)_2 \cdot 6H_2O$.

2.12 Attempted synthesis of a Cu(II) complex of 2, 6-dibromomethylpyridine

2.12.1 Method A

2,6-dibromomethylpyridine (0.104 g) and $Cu(ClO_4)_2 \cdot 6H_2O$ (0.140 g) were dissolved in THF (2 mL) in two different vials. The two solutions were mixed with stirring, and the resulting green solution was left to evaporate. A blueish green powder was obtained.

2.12.2 Method B

2,6-dibromomethylpyridine (0.0997 g) and $Cu(ClO_4)_2 \cdot 6H_2O$ (0.134 g) were dissolved separately in two portions of 1 mL THF. The two solutions were mixed with stirring and then $NaSbF_6$ (0.188 g) and THF (2 mL) were added. A light green powder was obtained after one day.

Both samples were checked by NMR and MS. The MS failed to show any evidence of formation of a Cu complex.

Chapter 3: Results and Discussion

This chapter contains an outline of the results obtained from the procedures described in Chapter 2, and a discussion of these.

3.1 Syntheses of ligand precursors

3.1.1 2,6-dibromomethylpyridine

It was initially planned to use samples of 2,6-dibromomethylpyridine that had been previously prepared in the laboratory, and which had been in storage for a few months. However, these appeared to be largely insoluble in chloroform and only slightly soluble in D_2O. ^1H NMR spectra obtained in the latter solvent were messy and no desired peaks could be detected. Given that 2,6-dibromomethylpyridine should be completely soluble in chloroform, a small amount of the solid material was stirred in chloroform for a while, the mixture was filtered, and the filtrate was reduced to dryness (rotavap). The solid obtained from this procedure proved to be pure 2,6-dibromomethylpyridine by comparison of the NMR data with those of an authentic sample. This procedure was then repeated with heating, which was found to give a higher yield, and a larger scale treatment was applied as recorded in the procedure section.

After the purified previously prepared samples had been used up, more 2,6-dibromomethylpyridine were made following the method of Gill.[73] This was prepared from the reaction of 2,6-pyridinedimethanol and HBr solution. The pure product was then obtained by rapid chloroform extraction of a basified solution of the reaction mixture following removal of the excess solvent. It was important to carry out this process as quickly as possible owing to possible base-catalysed hydrolysis of the dibromo product back to the dialcohol starting material.

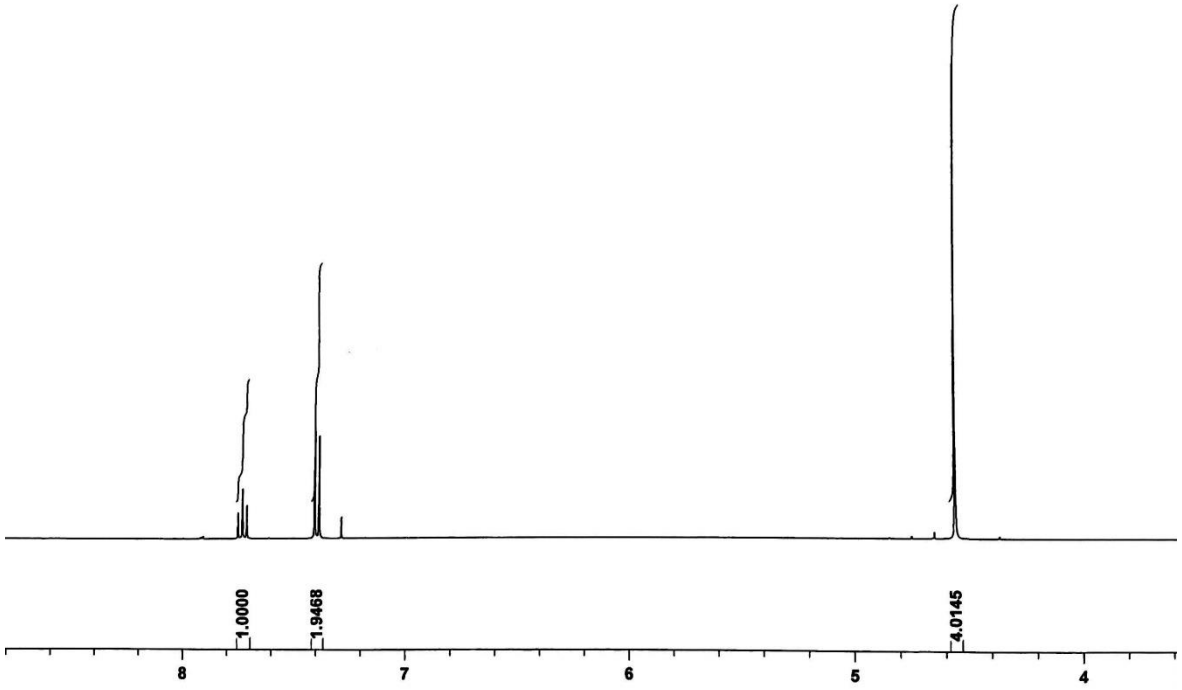

Figure 12: ^{1}H NMR spectrum of 2,6-dibromomethylpyridine

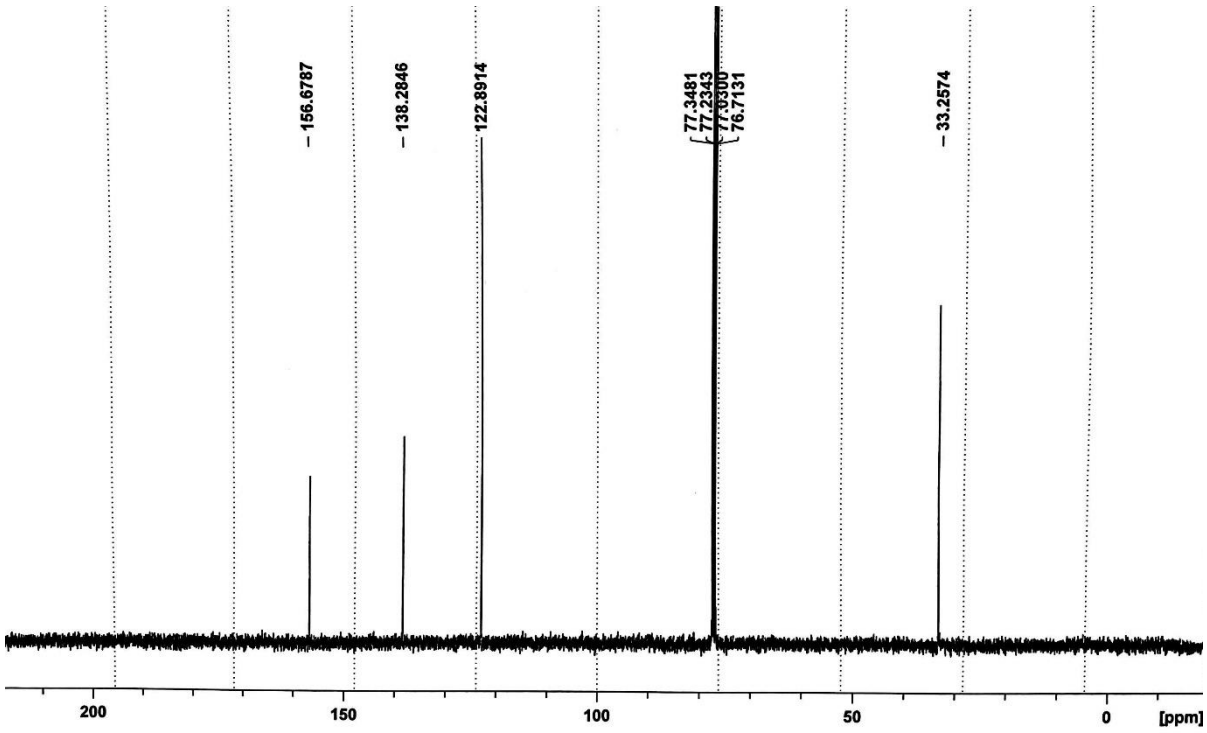

Figure 13: ^{13}C NMR spectrum of 2,6-dibromomethylpyridine

The ^{1}H NMR and ^{13}C NMR spectra of the pure material are given above. In the ^{1}H NMR spectrum, 3 peaks are observed; a one proton triplet at δ 7.7254 ppm, a two proton doublet at δ 7.3937 ppm and a four proton singlet at δ 4.5569 ppm. The triplet is assigned to the hydrogen atom *para* to the nitrogen atom and the doublet arises from the two *meta* hydrogen atoms. The upfield singlet was assigned to the methylene protons. 4 peaks were shown in the ^{13}C NMR spectrum, three in the aromatic region, and one upfield peak corresponding to the methylene carbon atom.

3.1.2 2,6-diaminomethylpyridine

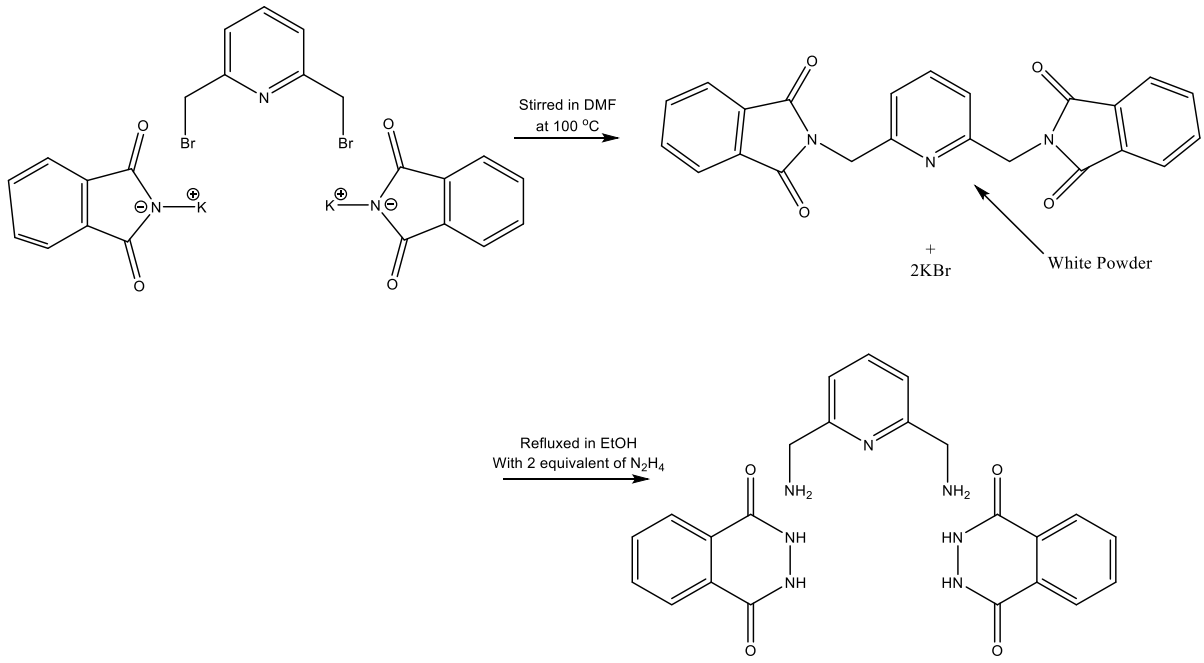

Figure 14: Procedure of synthesizing 2,6-diaminomethylpyridine

2,6-diaminomethylpyridine was prepared from the reaction of 2,6-dibromomethylpyridine with potassium phthalimide in DMF. This gave the diphthaloyl intermediate as a white powder, and this was then reacted with hydrazine hydrate in EtOH, thus removing the phthaloyl protecting groups and giving the product as a brown oil. When refluxing the diphthaloyl intermediate with hydrazine hydrate, a big block of white solid always formed on top of the brown solution and remained stationary even on vigorous stirring. Even after crushing with a glass rod, the solid block always reforms. However, comparison of the yields of products obtained on crushing the solid versus doing nothing showed little difference.

Although the NMR data were consistent with the product being 2,6-diaminomethylpyridine, when the brown oil obtained was dissolved in $CDCl_3$, a white powder formed. Therefore, the brown oil product was dissolved in a little chloroform and the turbid brown solution was filtered through celite and the filtrate reduced to a thick brown oil. However, the white precipitate formed again when dissolving this in $CDCl_3$. It is not known what the white precipitate is, but it could simply be some excess KOH.

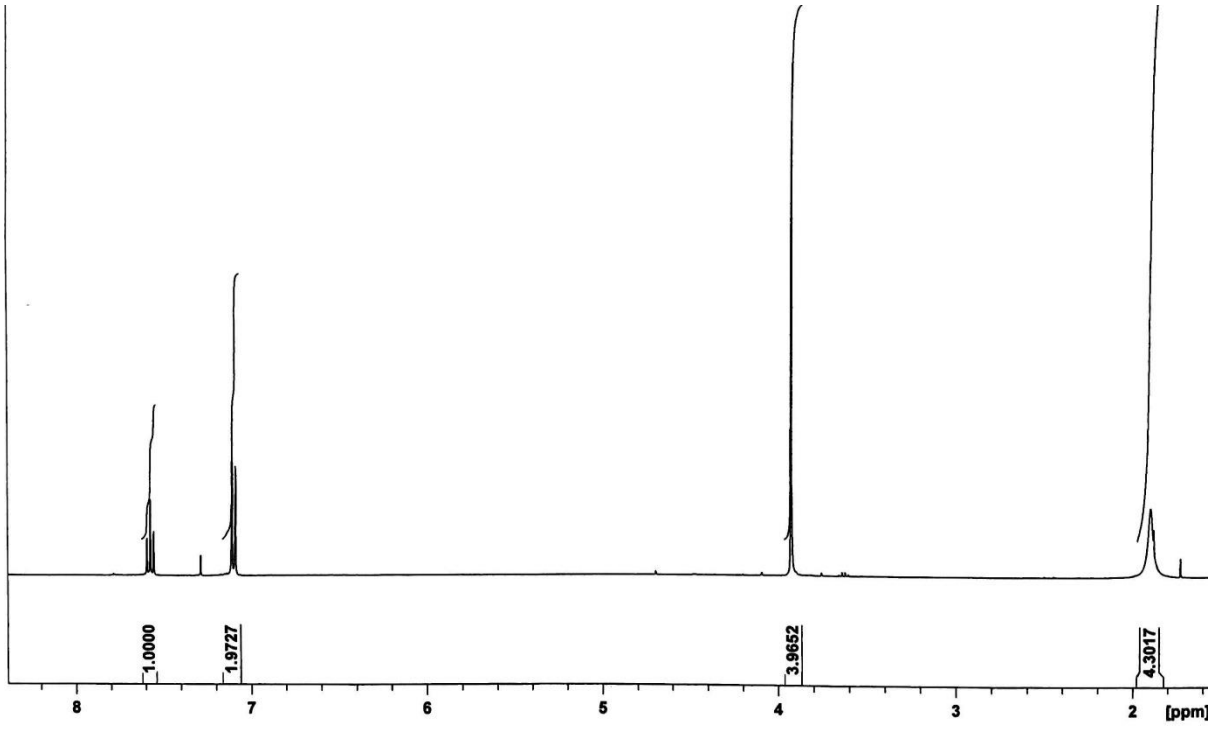

Figure 15: ^1H NMR spectrum of 2,6-diaminomethylpyridine

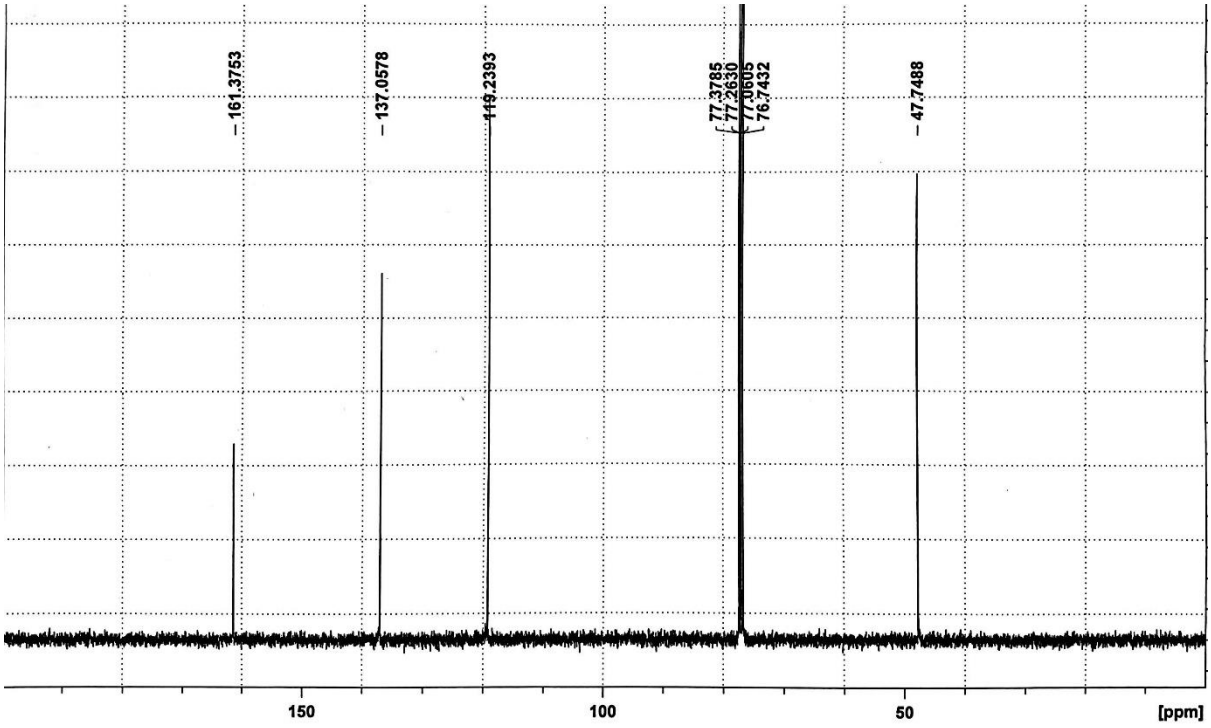

Figure 16: ^{13}C NMR spectrum of 2,6-diaminomethylpyridine

The ^{1}H NMR and ^{13}C NMR spectra of 2,6-diaminomethylpyridine are given above. A one-proton triplet, a two-proton doublet, a four-proton singlet, and a broad four-proton singlet were apparent in the ^{1}H NMR spectrum. The triplet at δ 7.5724 ppm is due to the hydrogen at the *p*-position, the doublet at δ 7.0995 ppm to the protons at the two *m*-positions, the singlet at δ 3.9252 ppm to the two sets of methylene protons, and the broad singlet at δ 1.9044 ppm to the amine hydrogen atoms. 4 resonances were displayed in the ^{13}CNMR spectrum. The peak at 47.7488 ppm can be assigned to the methylene C atoms while the other three peaks in the aromatic region (161.3753 ppm, 137.0578 ppm and 119.2393 ppm) correspond to the carbons on the pyridine at the *o*-, *m*- and *p*- positions relative to the nitrogen atom, respectively.

3.1.3 6-methyl-2,2'-bipyridine

6-methyl-2,2'-bipyridine was first made from the reaction between 2,2'-bipyridine and methyllithium (Method A). The resulting solution was added to ice and the top layer of the product was collected to be extracted by diethyl ether. The top layer was collected and a crude product was obtained as a brown oil after evaporation. Storage of this overnight led to a material that was sticky and insoluble in both diethyl ether and chloroform. A solid product

was obtained by trituration with acetone, but this was shown to not be the desired product. Given that the product was apparently decomposing on storage, the following purification process was carried out immediately following isolation of the crude product.

The brown oil obtained after removing the solvent (rotavap) from the triturated product was stirred at 90 ^{o}C under vacuum. The crude oil was then dissolved in ethyl acetate (in contrast to what is stated in the original preparation, it is not soluble in 6/1 (v/v) hexane/ethyl acetate). Even so, it still took a long time and a large amount of solvent to dissolve it (an ultrasonic bath was used), resulting in a long loading process, which led to poor separation. A number of bands stretched down the whole column, gradually changing from brown to red to yellow. The low solubility may be caused by the impurities in the crude product. Fortunately, the pure product was finally obtained from this column.

Given the problems experienced in the above synthesis, it was decided to attempt the synthesis of 6-methyl-2,2'-bipyridine by the reaction of 2-bromopyridine and 2-bromo-6-methylpyridine in the presence of LiCl, $NiCl_2 \cdot 6H_2O$, iodine, acetic acid and zinc granules in DMF (Method B). However, this synthesis failed in our hands. The original synthesis used zinc dust (which was not available) rather than zinc granules, and this might well be the main reason why the synthesis failed. As a catalyst, zinc granules have a much smaller surface area than zinc dust, which leads to a slower reaction rate. This also caused the problem that it would take too long to remove the zinc using HCl. Ammonia solution was then used to make the solution basic after all zinc was removed. The NMR spectra of the product obtained from the extraction with DCM were not consistent with formation of the product; while the ^{13}C NMR spectrum displayed a methyl group peak at around 24 ppm, the rest of the spectrum was extremely messy, presumably due to the presence of unreacted starting materials.

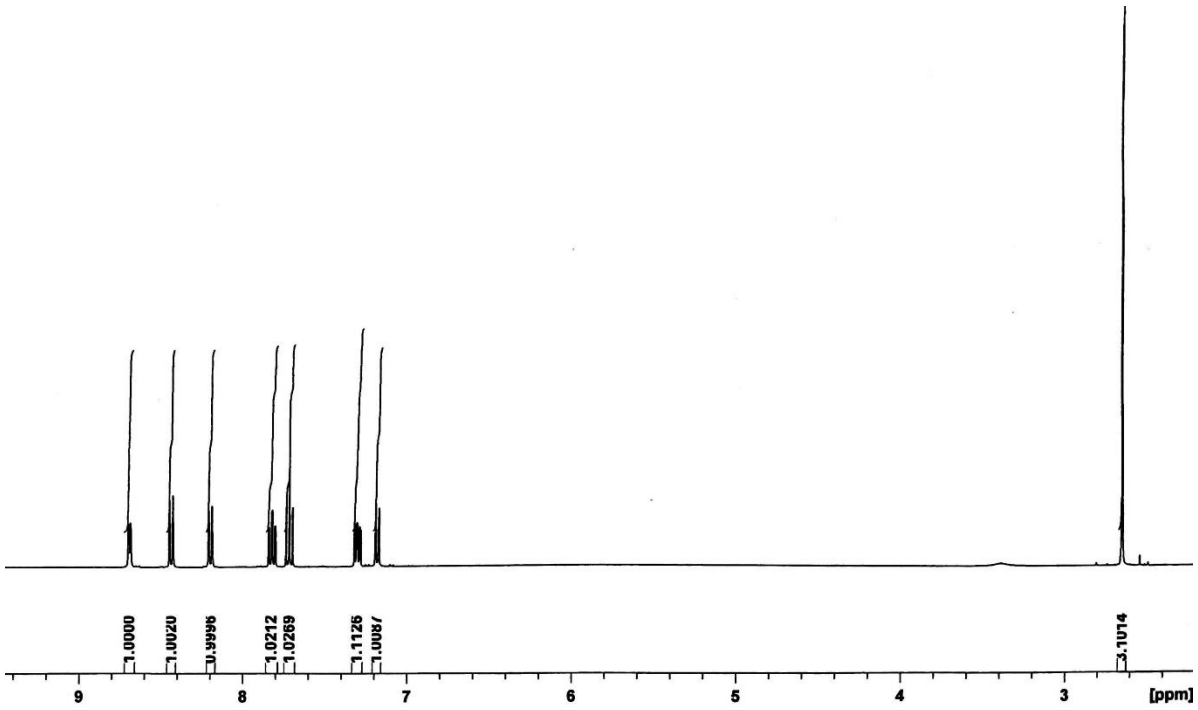

Figure 17: ^{1}H NMR spectrum of 6-methyl-2, 2'-bipyridine

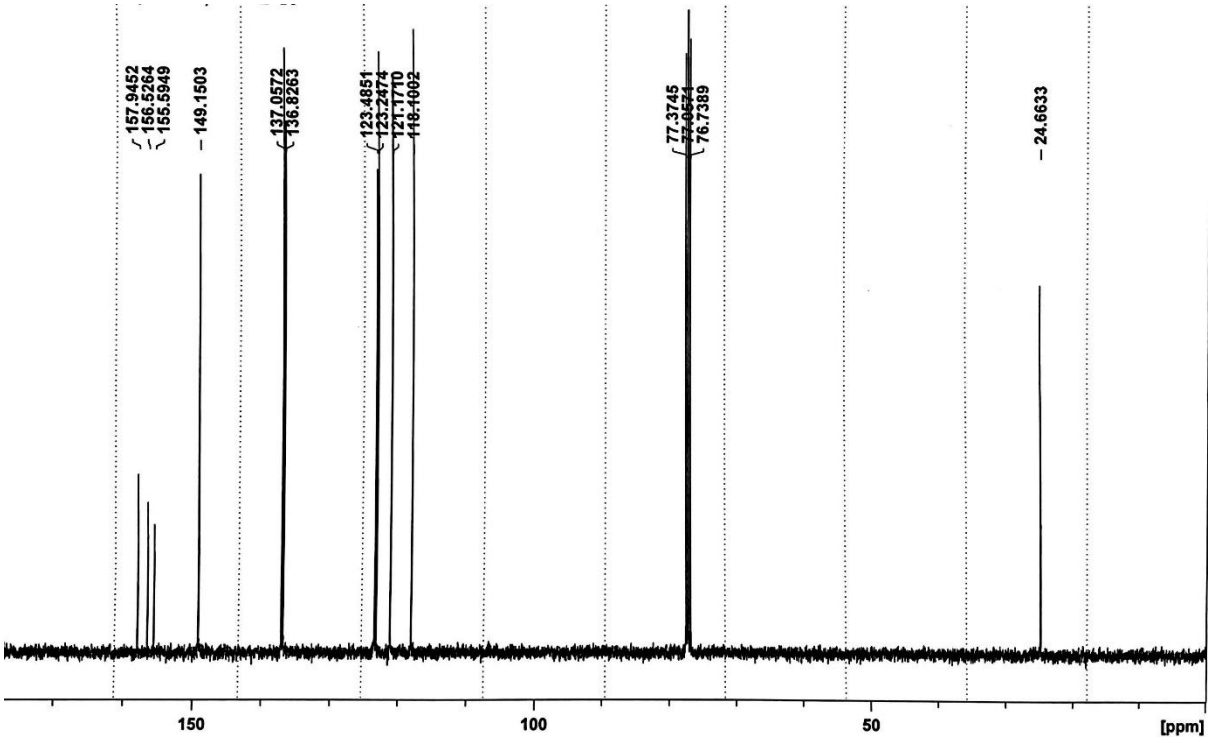

Figure 18: ^{13}C NMR spectrum of 6-methyl-2, 2'-bipyridine

The ^{1}H NMR and ^{13}C NMR spectra of pure 6-methyl-2,2'-bipyridine are given in Figures 17 and 18. In the ^{1}H NMR, the three one proton triplets be assigned to the hydrogens on carbons 4, 4' and 5' and the four one proton doublets come from the hydrogens on carbons 3, 5, 3' and 6'. The only singlet (three protons), which is upfield of the rest, is assigned to the three hydrogens on the methyl group. The 10 resonances observed in the downfield region of the ^{13}C NMR spectrum are assigned to the 10 carbons on the bipyridine skeleton, and the upfield peak (24.6633 ppm) is assigned to the methyl group.

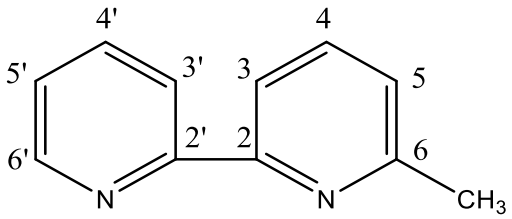

Figure 19: Structure and atom numbering of 6-methyl-2, 2'-bipyridine

3.1.4 2,2'-bipyridine-6-carboxaldehyde

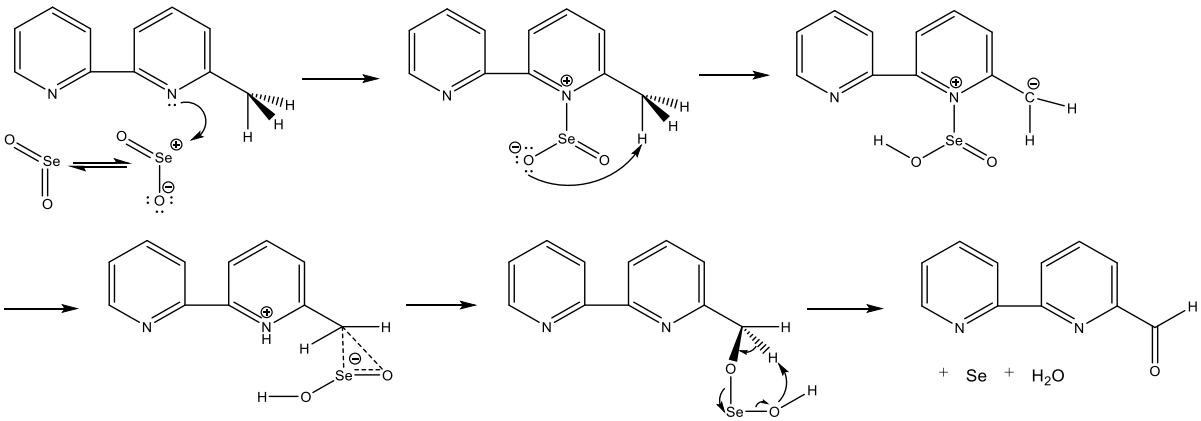

Figure 20: Proposed mechanism for the SeO_2 oxidation of 6-methyl-2, 2'-bipyridine[81]

2, 2'-bipyridine-6-carboxaldehyde was prepared by the reaction of 6-methyl-2, 2'-bipyridine with SeO_2 and water in dioxane under nitrogen. In the first attempt to synthesize this aldehyde, water was not added while adding SeO_2. Despite this, the yield obtained from this attempt is the same as that obtained when the literature procedure was followed exactly.

Regardless of whether or not water was added, sticky orange crude products were found to form in the flasks after filtration of the reaction mixture and before evaporating the resulting filtrate. While much of the crude product was soluble in chloroform, a significant amount was

not, but rather was water soluble. ^{1}H NMR of the water soluble portion in D_2O showed a characteristic aldehyde peak at > δ 10 ppm, suggesting that this portion might well contain the aldehyde product, but protonated on one of the N atoms. Therefore, this portion was then dissolved in a basic aqueous solution and extracted with chloroform. Two portions of crude products were then purified using two columns, and both gave the pure 2, 2'-bipyridine-6-carboxaldehyde product.

^{1}H NMR and ^{13}C NMR spectra of the pure product are given below. The ^{1}H NMR spectrum shows the aldehyde peak at δ 10.1300, a one proton doublet and two one proton triplets at δ 8.5143, δ 7.8493 and δ 7.3409, and two proton multiplets at δ 8.6565 and at δ 7.9392 ppm. In the ^{13}C NMR spectrum, the 10 downfield peaks in the range between 156.2359 ppm and 121.5070 ppm arise from the ten aromatic carbons on the bipyridine skeleton, while the peak at 193.6363 ppm is due to the carbon of the aldehyde group.

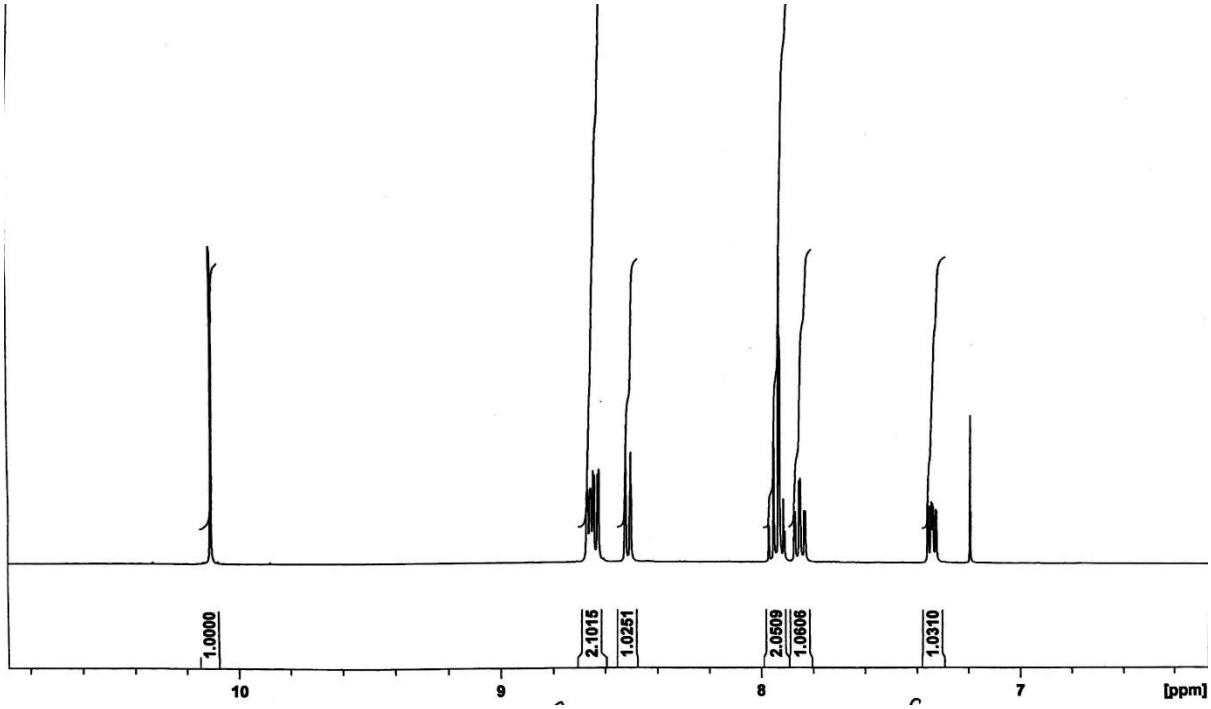

Figure 21: ^{1}H NMR spectrum of 2, 2'-bipyridine-6-carboxaldehyde

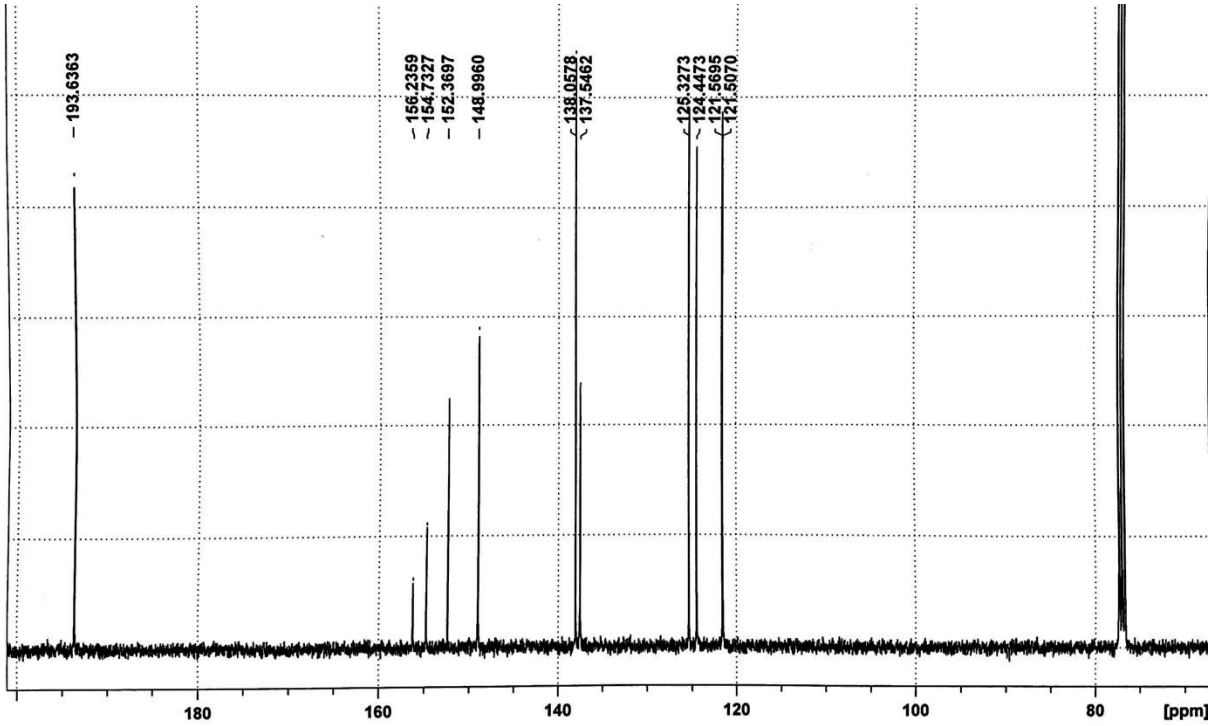

Figure 22: ^{13}C NMR spectrum of 2, 2'-bipyridine-6-carboxaldehyde

3.2 Ligand synthesis: N, N'-bis(2,2'-bipyridin-6-ylmethyl)pyridine-2,6-dimethylamine (bmpy)

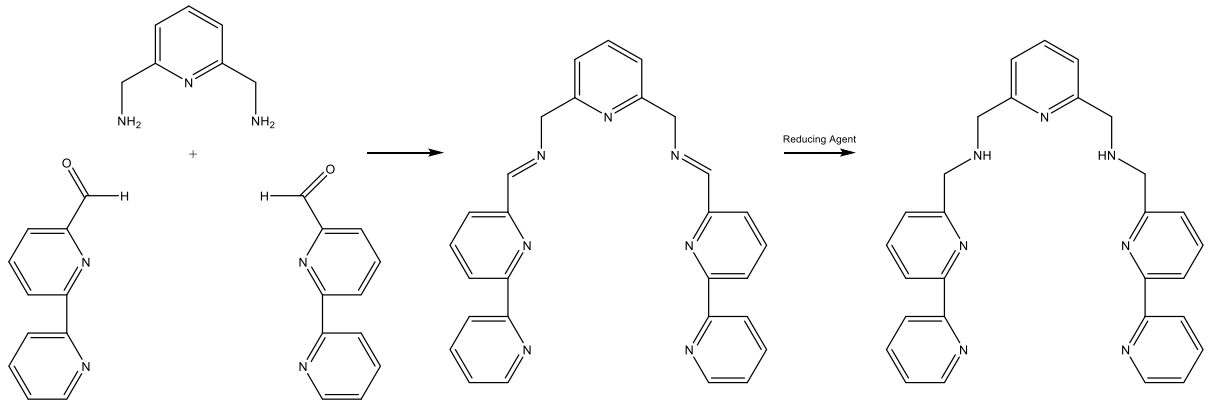

Figure 23: Procedure used to synthesise N, N'-bis(2,2'-bipyridin-6-ylmethyl)pyridine-2,6-dimethylamine (bmpy)

The new ligand N, N'-bis(2,2'-bipyridin-6-ylmethyl)pyridine-2,6-dimethylamine (bmpy) was prepared following the procedure above using the reductive amination of two carbonyl compounds and a primary diamine. The aldehyde and the primary amine were first reacted to give an imine. This was then reduced to give the secondary amine.

Many attempts were made to obtain pure bmpy. Initially, $NaBH_4$ was used as the reducing agent, and the reflux time was varied to investigate the effect on the reaction. However, NMR of the product obtained from these trials results always showed the presence of impurities in addition to peaks of the product, suggesting under-reduction. The MS results show only a small peak at *m/z* 474.2398 and the large peaks at 352.1409 and 845.3244 cannot be assigned. However, a moderately sized peak at 472.2006 suggests that something close to the desired product is present in the mixture.

Norminal Mass: 474
Molecular Mass: 474.580605
Monoisotopic Mass: 474.2406189337

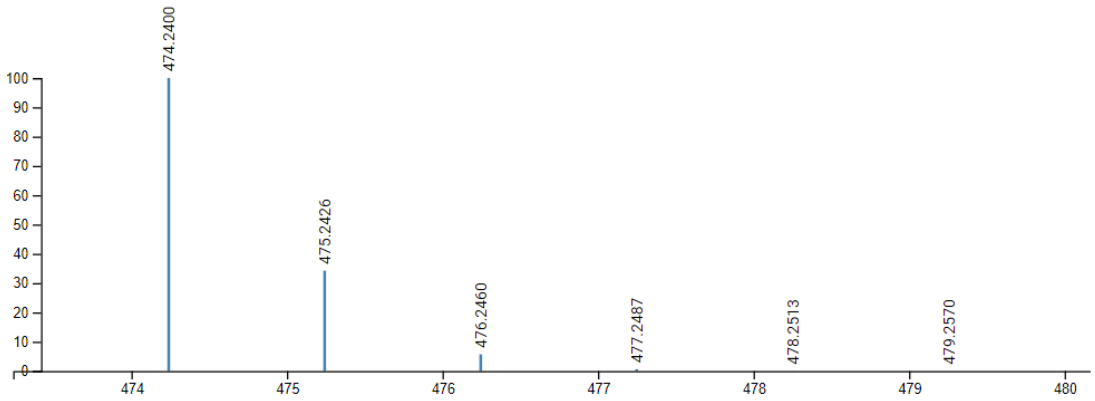

Figure 24: Predicted spectrum (Molecular Formula: $C_{29}H_{28}N_7$, Charge: +1)

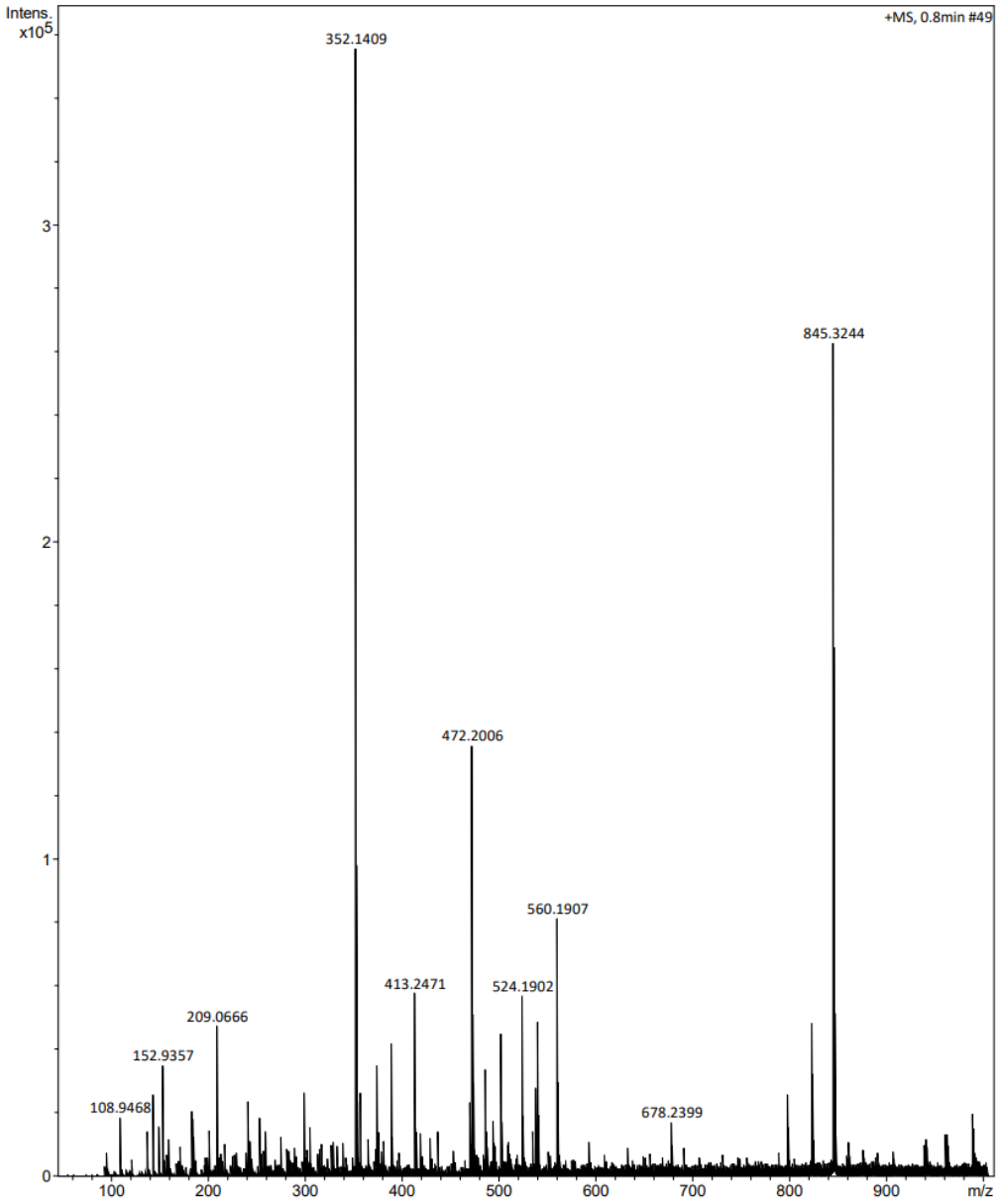

Figure 25: HRMS result of the product (impure)

Column chromatography was considered as a method to purify the product. TLC using a series of eluents from 2% MeOH/$CHCl_3$ (v/v) to 20% MeOH/$CHCl_3$, with and without triethylamine was tried on both silica and alumina sheets, but none of them gave a good separation – indeed mostly streaking was observed with these combinations. However, any less polar mobile phase resulted in the spot not moving. Therefore, both silica and alumina columns were considered not good options. Instead, it was proposed that the product be protonated using aqueous HCl, isolated, and then purified on a cation exchange column (Dowex 50W x2). However, NMR spectra of the fractions collected using this method were not consistent with the desired product.

In one of the early attempts at preparing the ligand, the reaction mixture suddenly gave a cream precipitate after being stirred for several minutes, which had never happened in other attempts. The precipitate was filtered off and NMR showed that both the white solid and yellow filtrate obtained contained large amounts of the starting aldehyde, meaning that formation of the imine was far from complete. It was therefore decided to use TLC to monitor the reaction.

Products from the attempts monitored by TLC were still not pure. It was then decided to use an alumina column with MeOH/$CHCl_3$ ($CHCl_3$ itself was used at first and then the percentage of MeOH was gradually increased to 4% during the process) even though there was not a good separation on TLC sheets. Two yellow bands were formed on the column and collected separately, but the NMR data were ambiguous. Both bands seemed to be the impure ligand as before. HRMS was thus used to identify their differences. As shown in the spectra below, the major peaks occur at *m/z* 474.2398 and *m/z* 472.2245. The former is consistent with the pure ligand. The latter appears to be consistent with a compound in which only one of the two imine groups have been reduced, leading to a molecular formula having two fewer hydrogen atoms than the desired ligand. Similarly, the peak at *m/z* 470.2107 is consistent with the diimine.

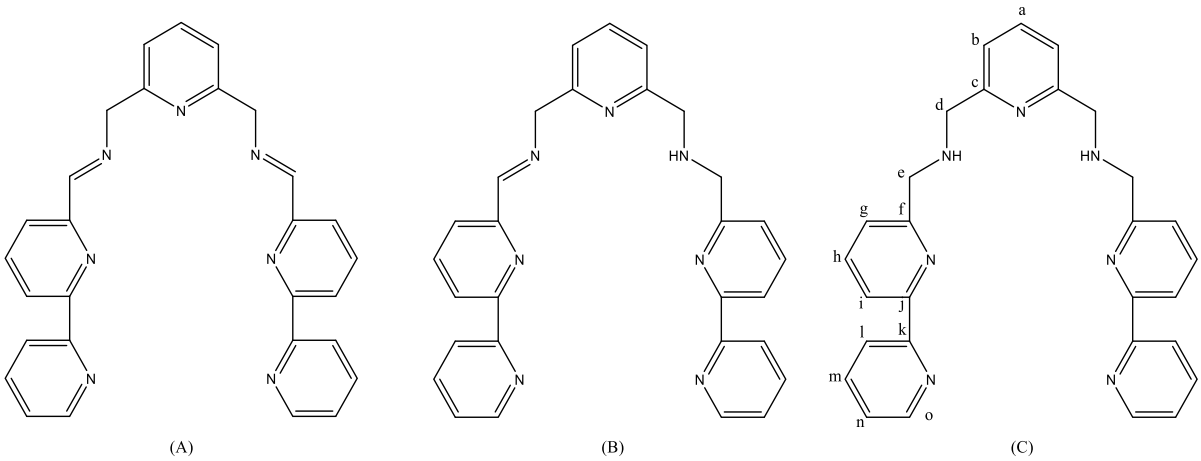

Figure 26: (A): $C_{29}H_{23}N_7$, diimine. (B): $C_{29}H_{25}N_7$, one of the imines being reduced to an amine. (C): $C_{29}H_{27}N_7$, both imines being reduced to amines (desired product)

From the spectra, the desired product was contained more in the first band while the half-reduced product was contained more in the second band, which can indicate that the desired product was moving faster than the half-reduced product on the column.

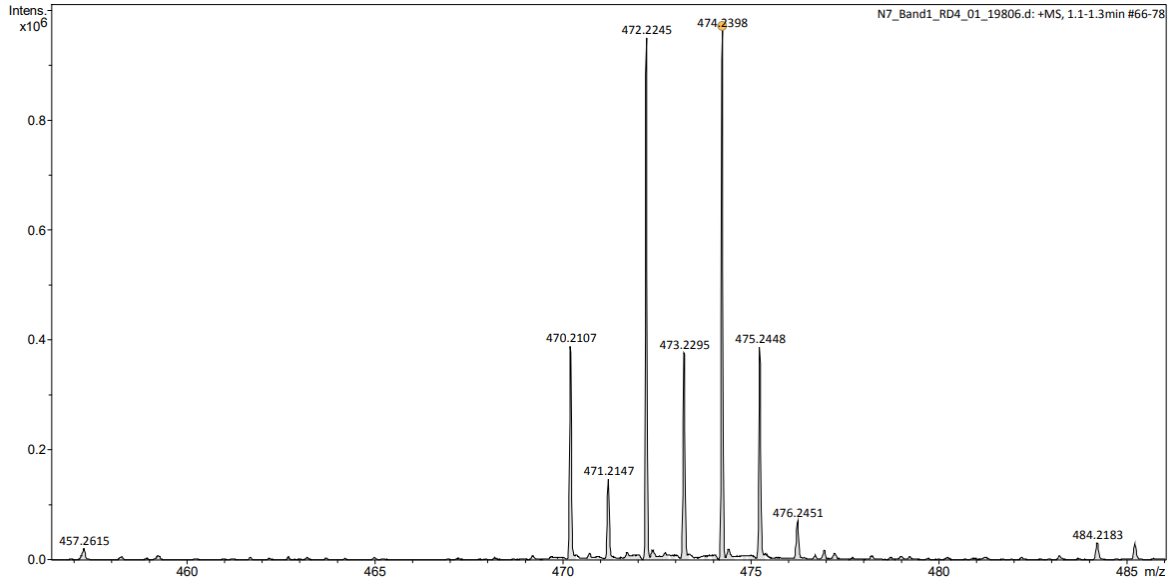

Figure 27: HRMS spectrum of the first band

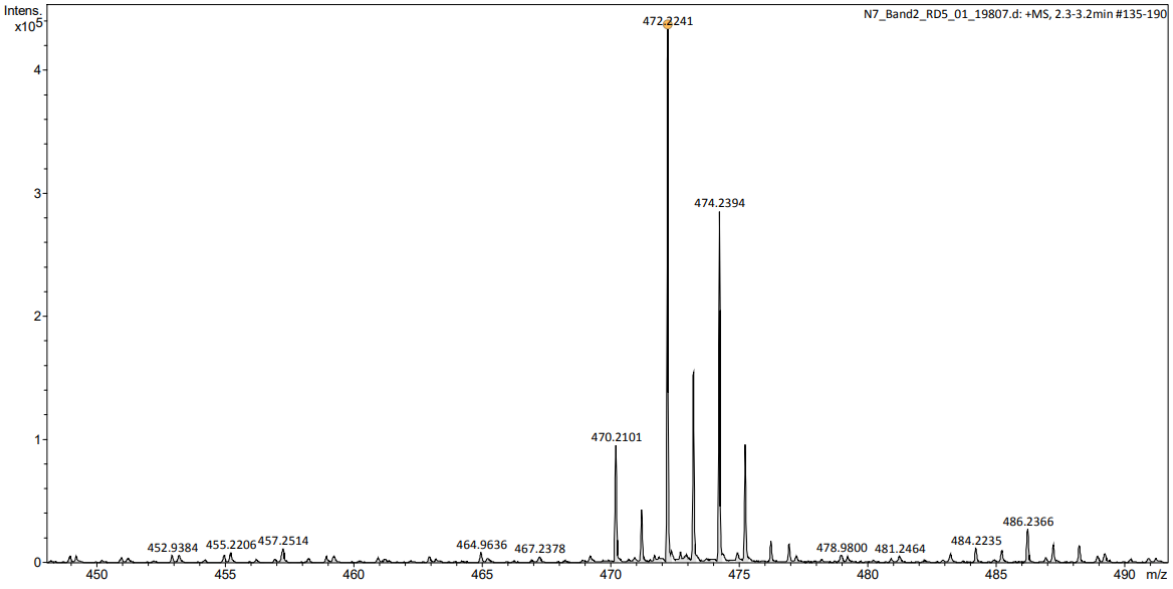

Figure 28: HRMS spectrum of the second band

As a result, the product contained in the second band was reacted with a further two equivalents of $NaBH_4$ in an attempt to reduce the mixture completely. While the NMR of the resulting product did not seem to show any improvement, the *m/z* 472.2241 and m/z 470.2101 peaks appeared to be smaller in the MS spectrum. The product obtained from the

first band was rechromatographed on a new alumina column and all fractions collected were analysed by NMR. However, none of them was found to be absolutely pure.

Since the problem in the synthesis appeared to be occurring in the reducing process, $NaBH_3CN$ was then used as the reducing agent instead of $NaBH_4$, following the method of Walther et al. $NaBH_3CN$ is widely used in the reduction of imines and is well-known for its selectivity. Its reducing ability is weak enough to not react with aldehydes or ketones while strong enough to reduce imines to amines. Therefore, it can be added at the beginning of the reaction together with the 2,6-diaminomethylpyridine and 2,2'-bipyridine-6-carbaldehyde, rather than added after the diimine has already been formed by the diamine and the aldehyde, as was done with $NaBH_4$. However, the NMR results indicated that the products of these attempts were still impure as found when using $NaBH_4$, even though in one attempt more than 10 equivalents of $NaBH_3CN$ were used.

The emphasis was then put back on purification and a silica column was tried. This method is recorded in the experimental procedure section. Pure bmpy was obtained from this column.

The ^{1}H NMR, ^{13}C NMR and MS spectra of the pure product are given below. The mass spectra of two different portions of pure bmpy are surprisingly different, but are both consistent with the presence of the ligand. Portion A shows two main peaks at *m/z* 474.2 and 237.7; the former corresponds to $[M+H]^+$ (Formula: $C_{29}H_{28}N_7^+$, Molecular Mass: 474.581, Monoisotopic Mass: 474.241) and the latter to $[M+2H]^{2+}$ (Formula: $C_{29}H_{29}N_7^{2+}$, Molecular Mass: 475.589, Monoisotopic Mass: 475.248). The spectrum of portion B has *m/z* 237.7 peak as the base peak, and a peak at *m/z* 496.3 which corresponds to the sodiated ligand (Formula: $C_{29}H_{27}N_7Na^+$, Molecular Mass: 496.562, Monoisotopic Mass: 496.223).

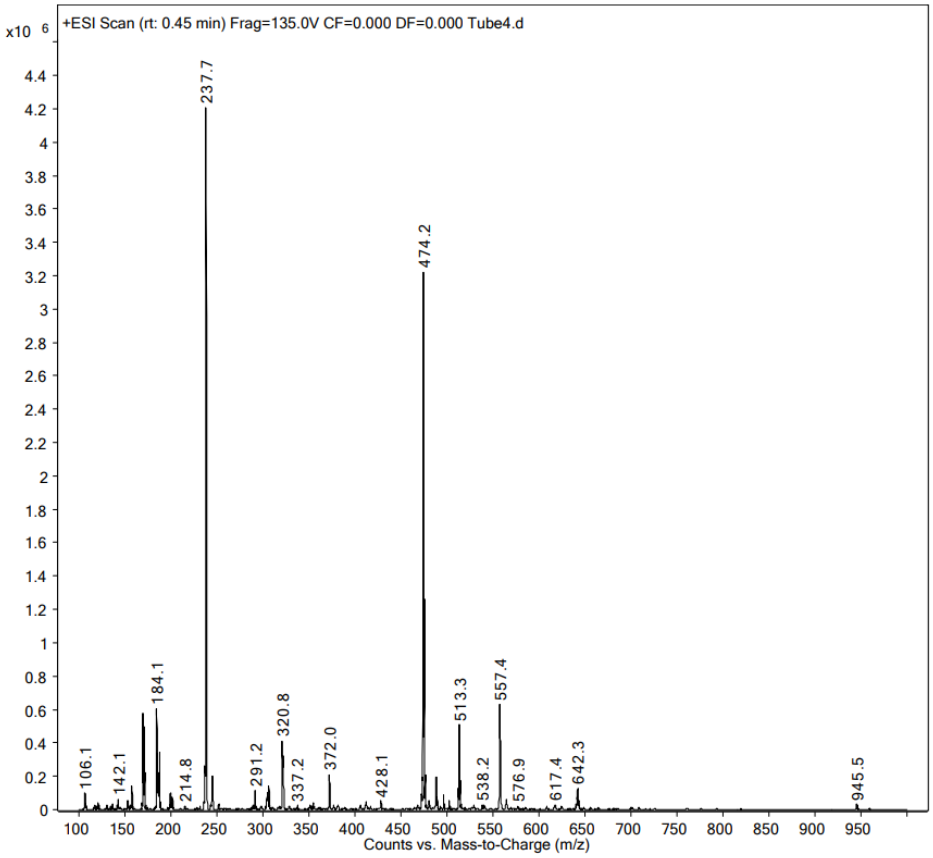

Figure 29: MS spectra of bmpy (portion A)

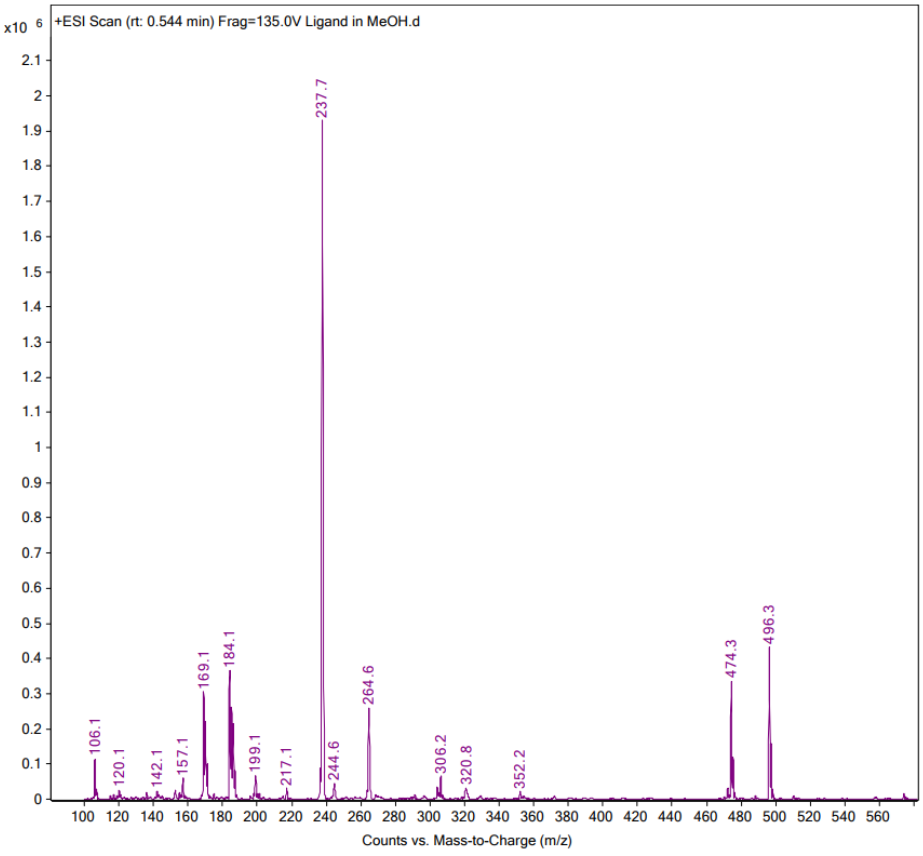

Figure 30: MS spectra of bmpy (portion B)

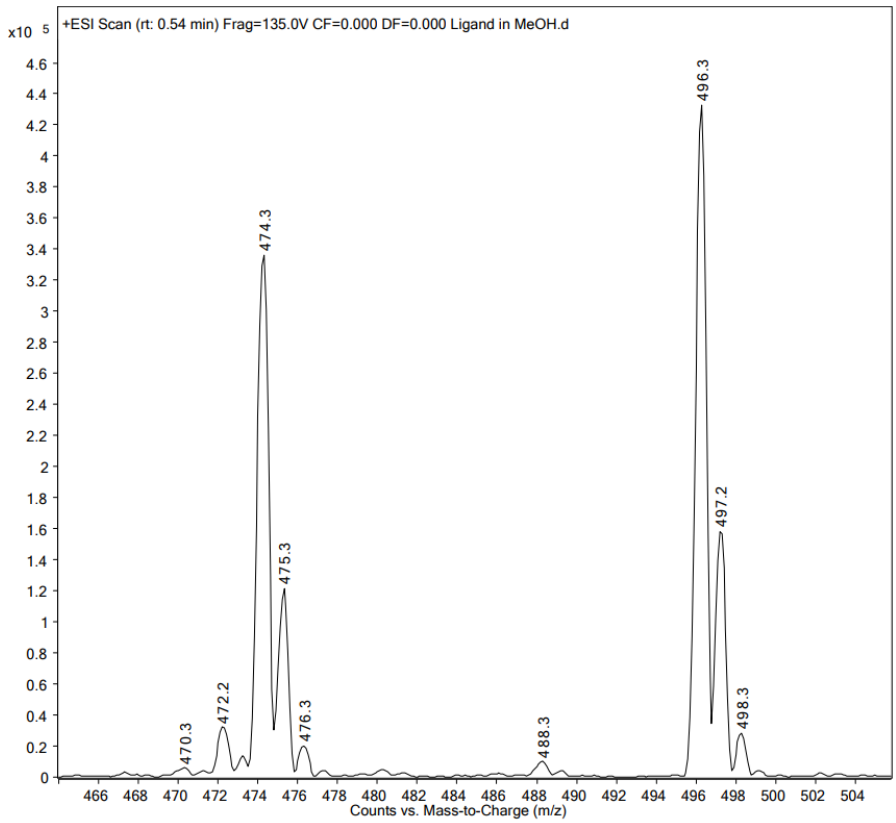

Figure 31: *m/z* 474.3 and *m/z* 496.3 of MS spectra of bmpy (portionB)

The ^{1}H NMR spectrum (Figure 32) shows one doublet and one broad singlet in the upfield region, due to the four hydrogens on the two methylene groups (d and e) and the secondary amine hydrogen atoms, respectively. In the downfield region, four doublets, one triplet and two multiplets can be detected for the aromatic hydrogen atoms; the multiplet at δ 7.7373 looks to be two overlapping triplets and the multiplet at δ 7.2488 appears to be an overlapping doublet and triplet. Therefore, there are five doublets (matching positions b, g, i, l and o) and four triplets (matching positions a, h, m and n) in total. The ^{13}C NMR spectrum of the bmpy ligand is given in Figure 33. From the structure shown in figure 26(C), it can be seen that the bmpy ligand should exhibit 15 peaks in the ^{13}C NMR spectrum. With two bipyridines on the side and one pyridine in the middle, there should be 13 peaks in the downfield region of the ^{13}C NMR spectrum, consistent with the spectrum below. The remaining two upfield peaks at 54.8238 ppm and 54.7574 ppm can be assigned to the two methylene groups.

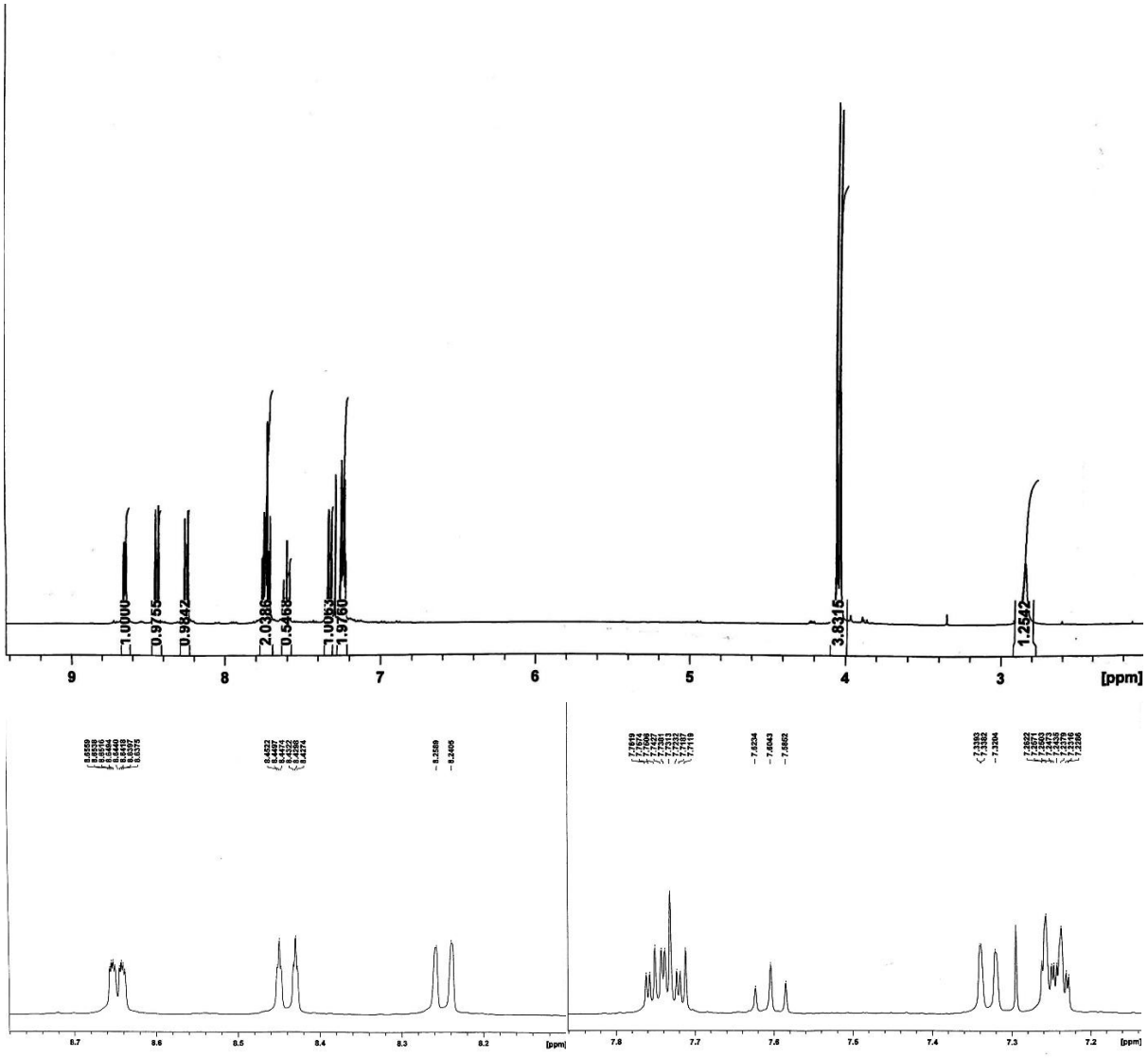

Figure 32: Top: ^{1}H NMR spectrum of N, N'-bis(2,2'-bipyridin-6-ylmethyl)pyridine-2,6-dimethylamine (bmpy)

Bottom: Downfield region of the ^{1}H NMR spectrum

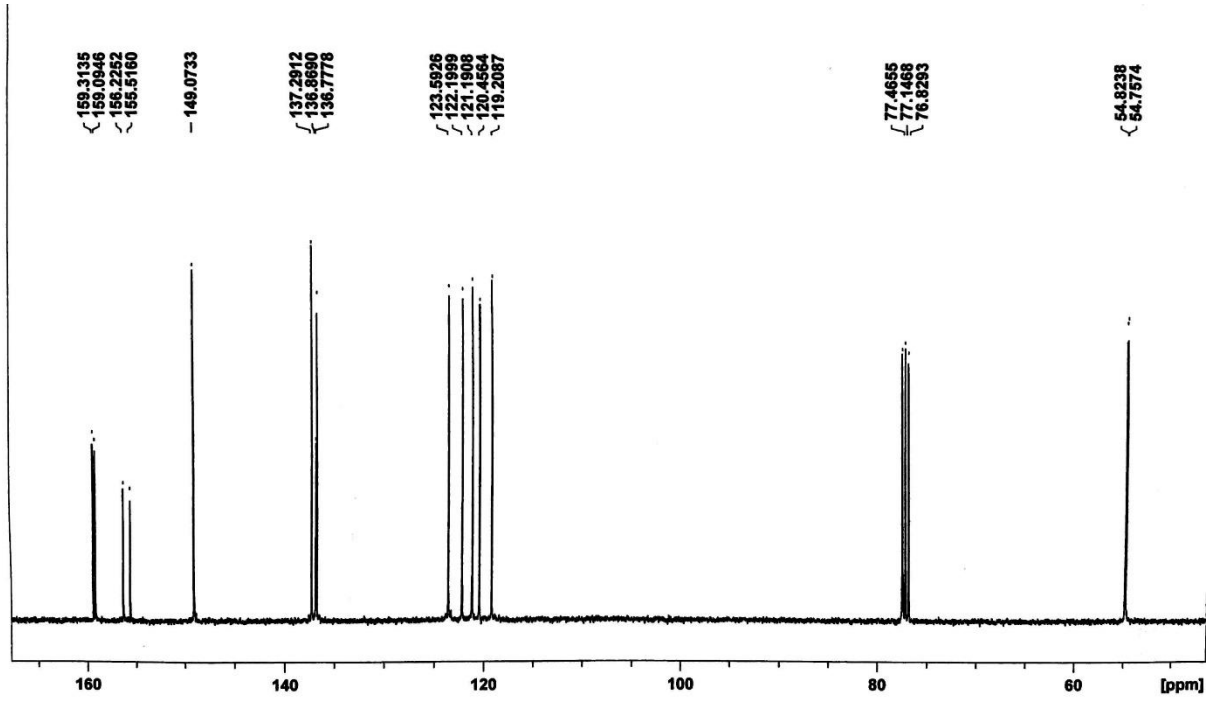

Figure 33: ^{13}C NMR spectrum of N, N'-bis(2,2'-bipyridin-6-ylmethyl)pyridine-2,6-dimethylamine (bmpy)

3.3 Transition metal complexes of bmpy

Initial attempts at preparing transition metal complexes of bmpy used the crude product obtained from the reaction mixture that had not been chromatographed and had simply been washed with water to remove any water soluble impurities. Solutions of ligand and the appropriate metal perchlorate were prepared in 1:1, 1:2 and 1:3 ratios of ligand to metal. Dark blue solutions were obtained for all 1:1, 1:2 and 1:3 mixtures of bmpy and $Cu(ClO_4)_2.6H_2O$. Dark purple solutions were received for all 1:1, 1:2 and 1:3 mixtures of bmpy and $Fe(ClO_4)_2.6H_2O$. Amber solutions were obtained for all three samples with $Co(ClO_4)_2{\cdot}6H_2O$, while brown, brownish green and green solutions were obtained from the mixture of $Ni(ClO_4)_2{\cdot}6H_2O$ with bmpy in 1:1, 1:2 and 1:3 ratios respectively. Using $Zn(ClO_4)_2{\cdot}6H_2O$, yellow solutions were obtained for all three ratios. Solutions formed from mixing $Mn(ClO_4)_2.6H_2O$ with bmpy were brown at all ratios. With K_2PdCl_4, a brown solution was obtained from the 1:1 mixture, but a precipitate was formed in the 1:2 and 1:3 mixtures, and therefore these were filtered before setting aside the filtrate to evaporate. Slow evaporation of all the solutions failed to give crystalline material of X-ray quality, and attempted

recrystallisation from either water or acetonitrile of any solid materials obtained was also unsuccessful.

When it was realised that the bmpy ligand contained some under-reduced product, the above samples were discarded and the chromatographed product was then used with Co(II), Cu(II), Ni(II), Fe(II) and Zn(II). Owing to the fact that only a small amount of pure bmpy was obtained, complexes were prepared on a small scale that was amenable to being tested directly by MS.

3.3.1 Bmpy + $Co(ClO_4)_2 \cdot 6H_2O$

The mass spectra shown in Figure 34 were obtained from the solutions of bmpy: $Co(ClO_4)_2 \cdot 6H_2O$ in 1:1, 1:2 and 1:3 ratios, respectively. It is immediately obvious that the three spectra are essentially identical, meaning that the same product is formed regardless of the mole ratio. The base peak in all cases occurs at *m/z* 266.2. This is consistent with the mononuclear $[Co(bmpy)]^{2+}$ ion (Formula: $[Co(C_{29}H_{27}N_7)]^{2+}$, Molecular Mass: 532.506, Monoisotopic Mass: 532.166). A small peak at *m/z* 631.2 (Figure 35) common to all spectra is consistent with the $[Co(bmpy)(ClO_4)]^+$ ion (Formula: $[Co(C_{29}H_{27}N_7)ClO_4]^+$, Molecular Mass: 631.956, Monoisotopic Mass: 631.114). This peak shows the characteristic isotope pattern of a chlorine-containing species, namely peaks in an approximately 3:1 ratio, 2 *m*/*z* units apart..

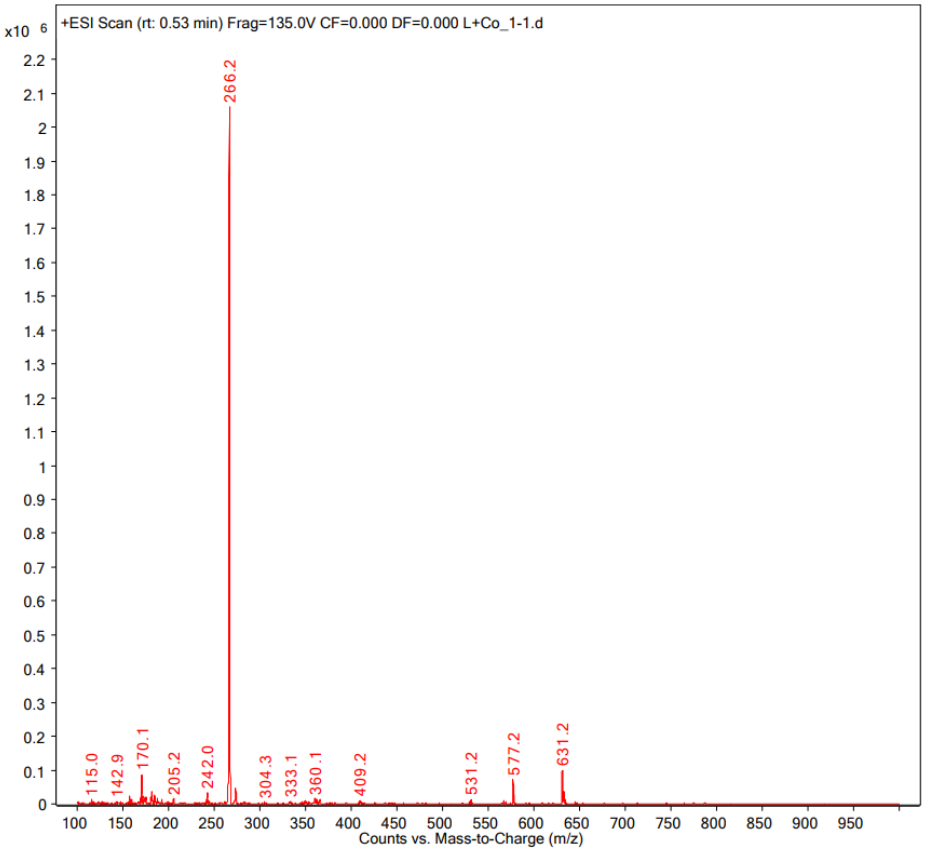
+ESI Scan (rt: 0.53 min) Frag=135.0V CF=0.000 DF=0.000 L+Co_1-1.d
x10 6
266.2
115.0
142.9
170.1
205.2
242.0
304.3
333.1
360.1
409.2
531.2
577.2
631.2
Counts vs. Mass-to-Charge (m/z)

(A)

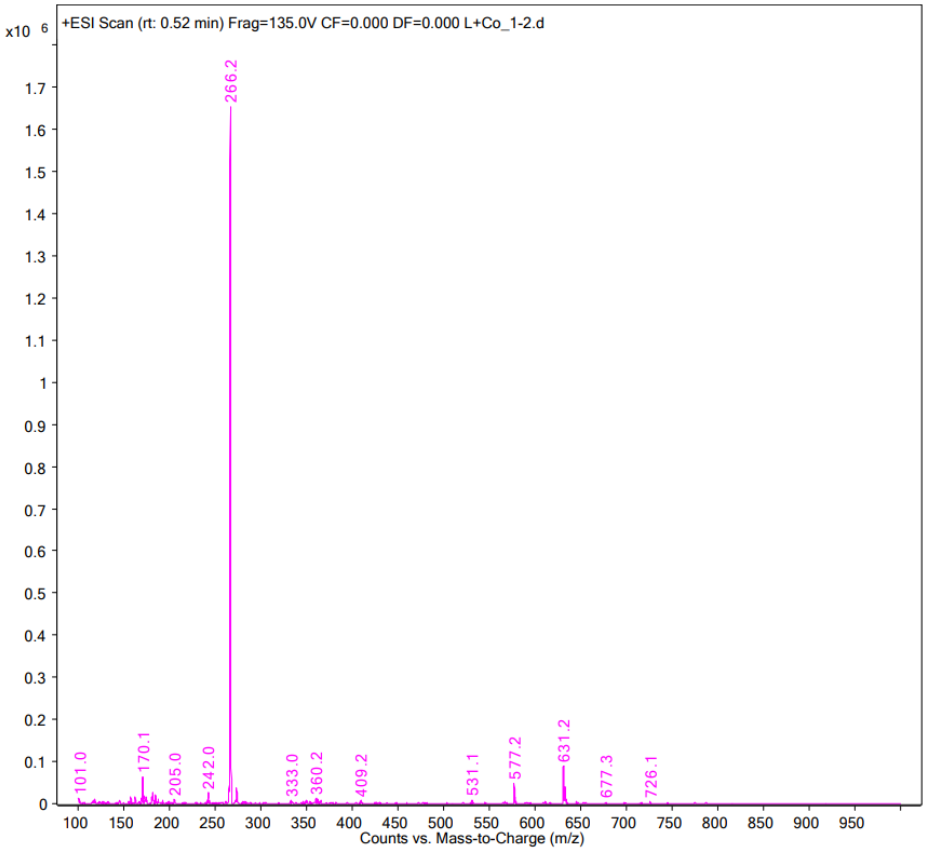
+ESI Scan (rt: 0.52 min) Frag=135.0V CF=0.000 DF=0.000 L+Co_1-2.d
x10 6
266.2
101.0
170.1
205.0
242.0
333.0
360.2
409.2
531.1
577.2
631.2
677.3
726.1
Counts vs. Mass-to-Charge (m/z)

(B)

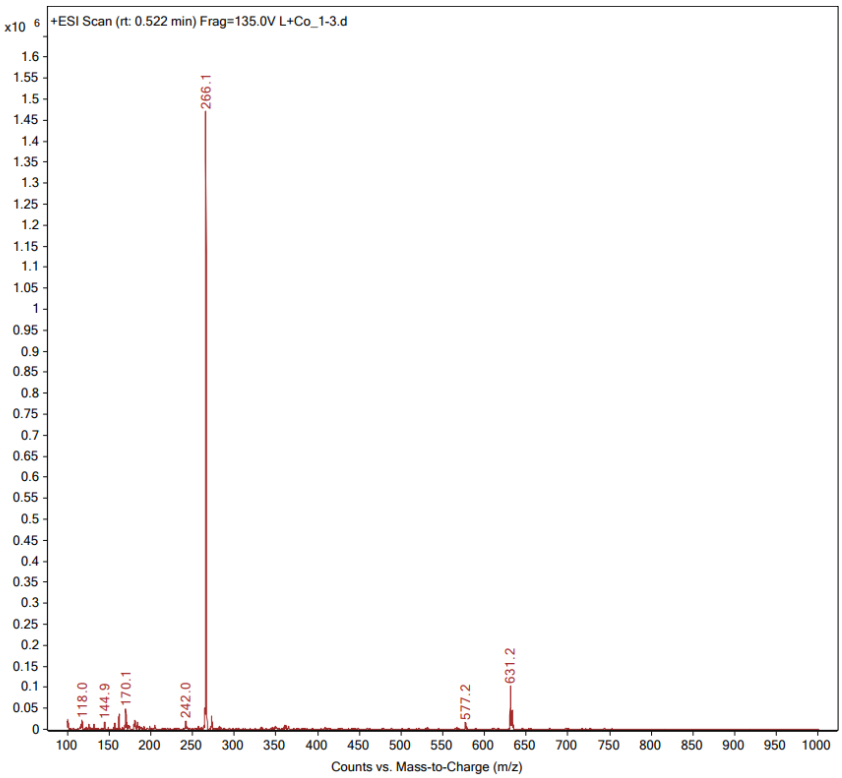

(C)

Figure 34: Mass spectra of solutions containing bmpy and $Co(ClO_4)_2 \cdot 6H_2O$ in differing mole ratios. (A). (1:1), (B). (1:2), (C). (1:3)

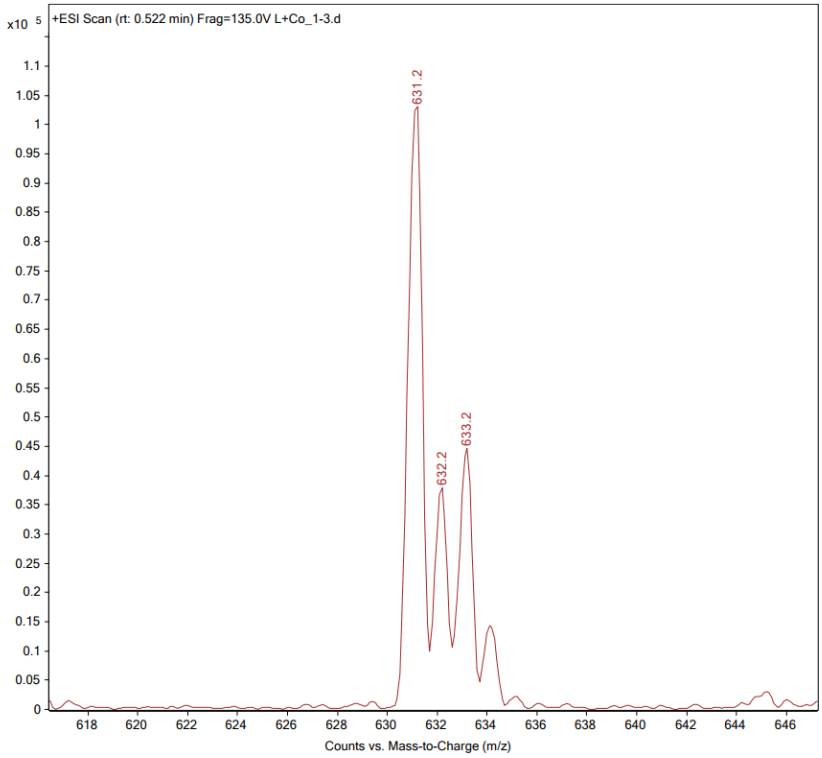

Figure 35: Expansion of the peak at *m/z* 631.2 in the mass spectrum of bmpy: $Co(ClO_4)_2 \cdot 6H_2O$ (1:3)

3.3.2 Bmpy + $Cu(ClO_4)_2 \cdot 6H_2O$

The mass spectra shown in Figure 36 were obtained from the solutions of bmpy: $Cu(ClO_4)_2 \cdot 6H_2O$ in 1:1, 1:2 and 1:3 ratios, respectively. Again, it can be observed that the mole ratio does not influence the nature of the product, with all spectra showing the base peak at *m/z* 298.6, together with a peak of almost equal intensity at *m/z* 299.6. This is consistent with formation of the dinuclear species $[Cu_2(bmpy\text{-}2H)]^{2+}$ in which the ligand has lost two hydrogen atoms (Formula: $[Cu_2(C_{29}H_{25}N_7)]^{2+}$, Molecular Mass: 598.649, Monoisotopic Mass: 597.076). That there are two peaks of almost equal intensity with a 1 *m/z* difference (Figure 37) is consistent with the presence of two copper atoms/ions in the complex.

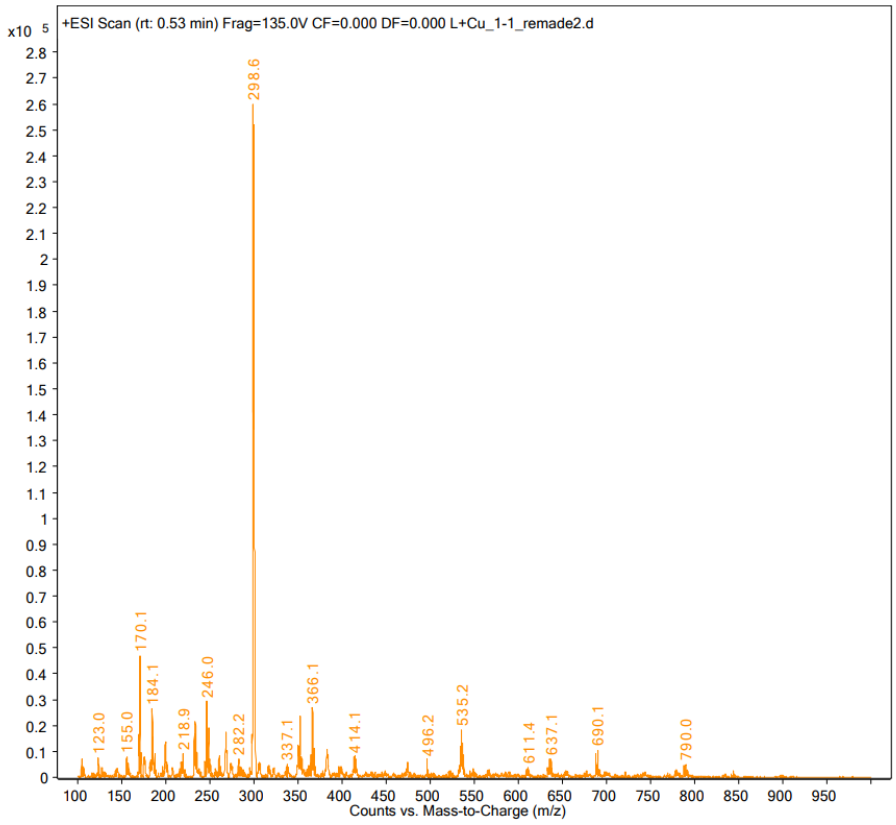

(A)

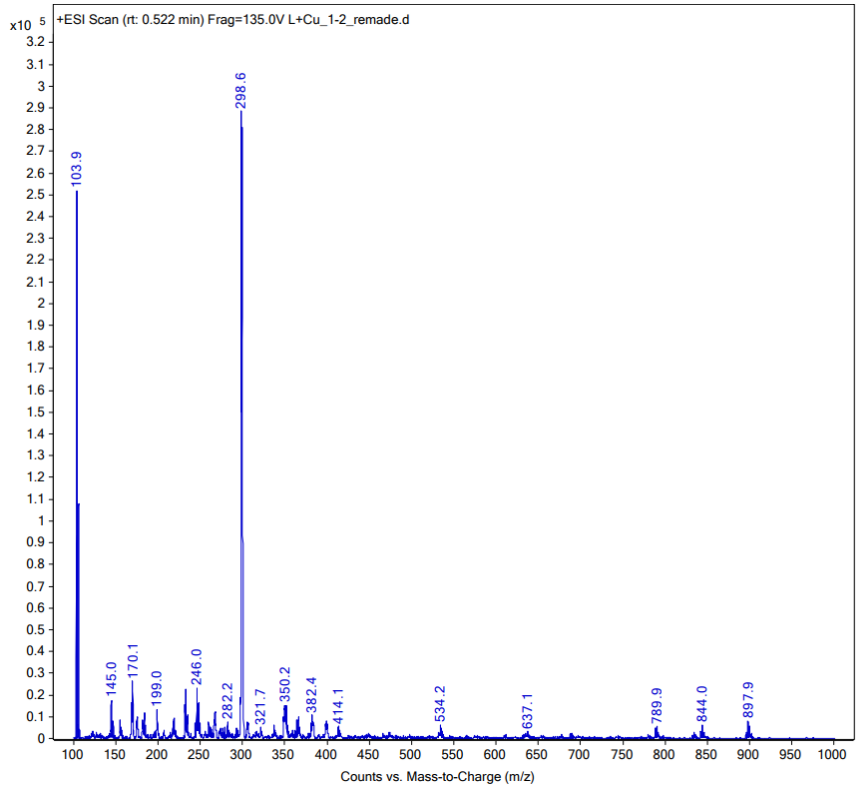

(B)

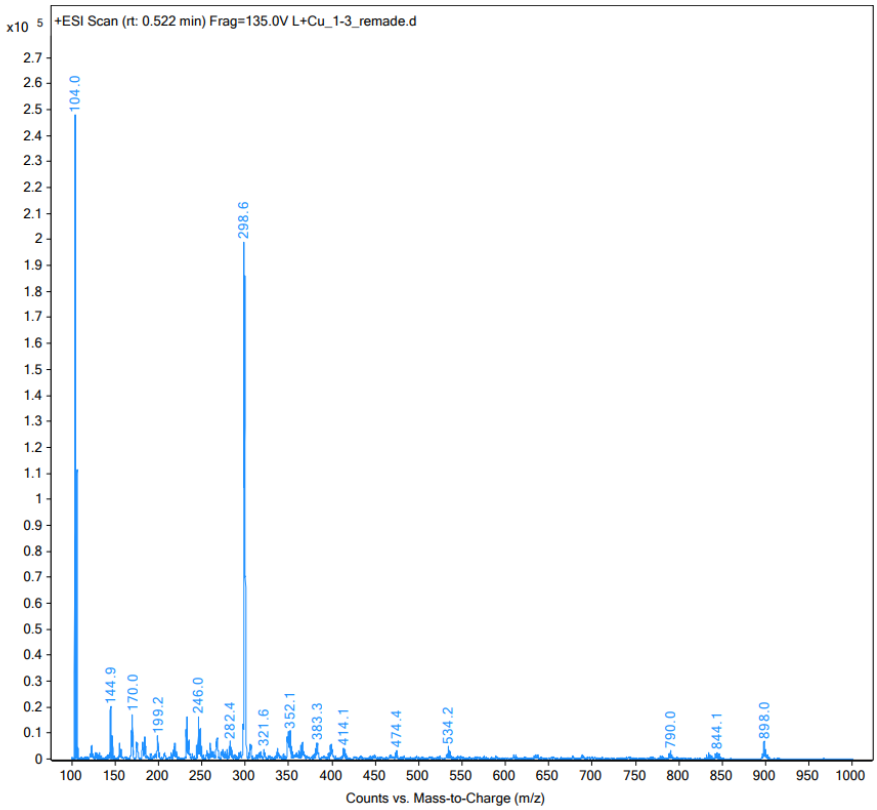

(C)

Figure 36: Mass spectra of solutions containing bmpy and $Cu(ClO_4)_2 \cdot 6H_2O$ in differing mole ratios. (A). (1:1), (B). (1:2), (C). (1:3)

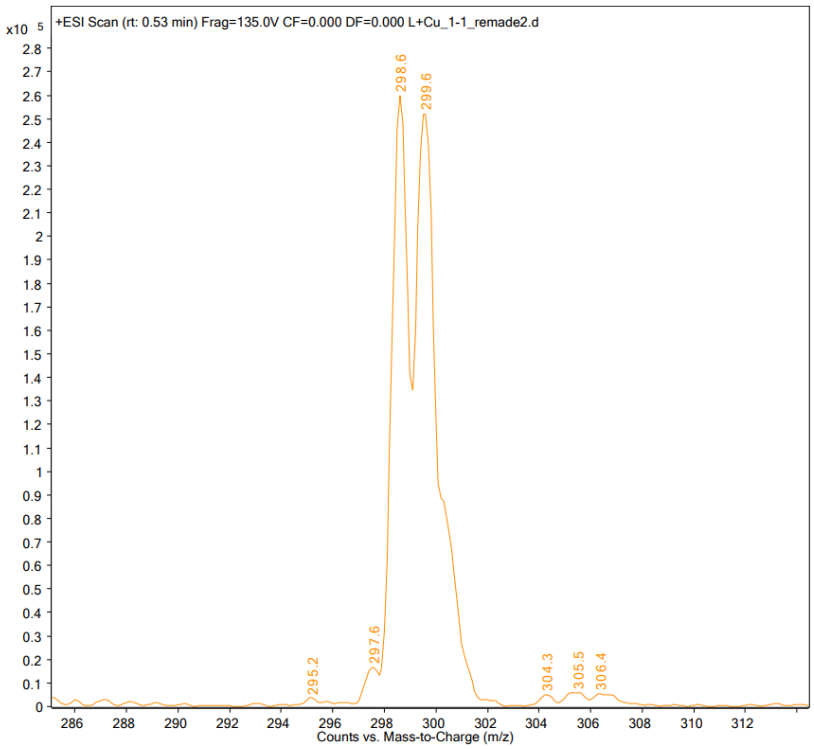

Figure 37: Expansion of the base peak *m/z* 298.6 in the mass spectrum of bmpy:$Cu(ClO_4)_2 \cdot 6H_2O$ (1:1)

3.3.3 Bmpy + $Fe(ClO_4)_2 \cdot 6H_2O$

The mass spectra shown in Figure 38 were obtained from the solutions of bmpy: $Fe(ClO_4)_2 \cdot 6H_2O$ in 1:1, 1:2 and 1:3 ratios, respectively. The base peak in all cases occurs at *m/z* 264.6/264.7, again showing that the major product formed does not depend on the mole ratio. The base peak is consistent with the mononuclear complex $[Fe(bmpy)]^{2+}$ (Formula: $[Fe(C_{29}H_{27}N_7)]^{2+}$, Molecular Mass: 529.418, Monoisotopic Mass: 529.168). A minor peak at *m/z* 628.1 is consistent with the ion $[Fe(bmpy)(ClO_4)]^{+}$ (Formula: $[Fe(C_{29}H_{27}N_7)ClO_4]^{+}$, Molecular Mass: 628.868, Monoisotopic Mass: 628.116).

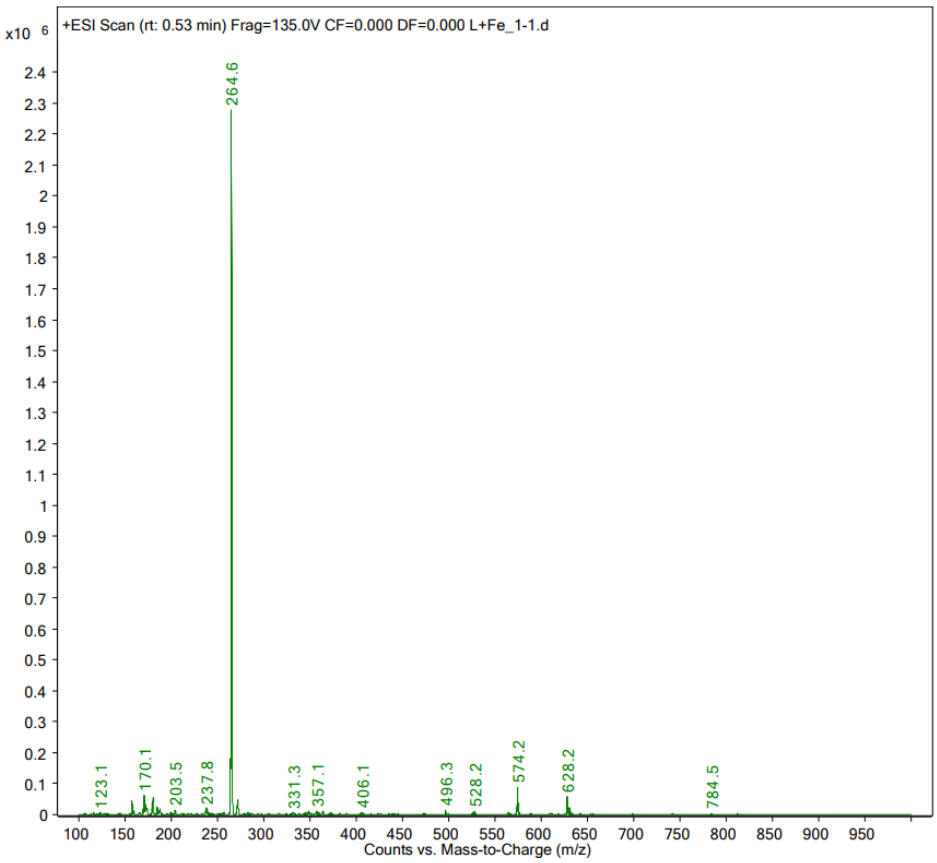
+ESI Scan (rt: 0.53 min) Frag=135.0V CF=0.000 DF=0.000 L+Fe_1-1.d
x10 6
264.6
123.1
170.1
203.5
237.8
331.3
357.1
406.1
496.3
528.2
574.2
628.2
784.5
Counts vs. Mass-to-Charge (m/z)

(A)

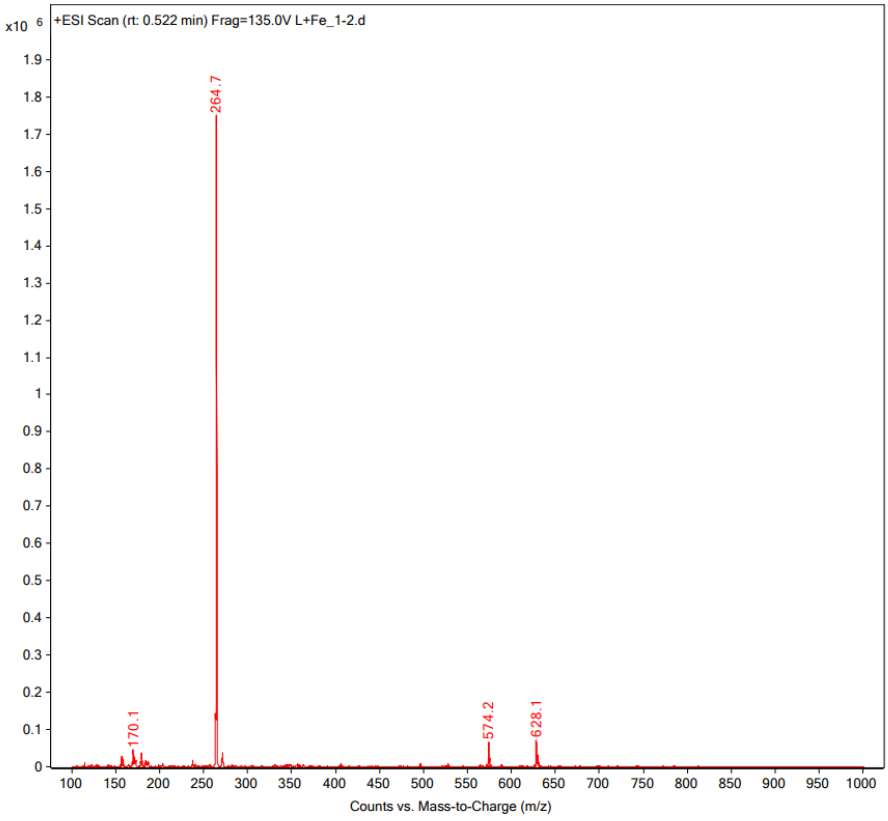
+ESI Scan (rt: 0.522 min) Frag=135.0V L+Fe_1-2.d
x10 6
264.7
170.1
574.2
628.1
Counts vs. Mass-to-Charge (m/z)

(B)

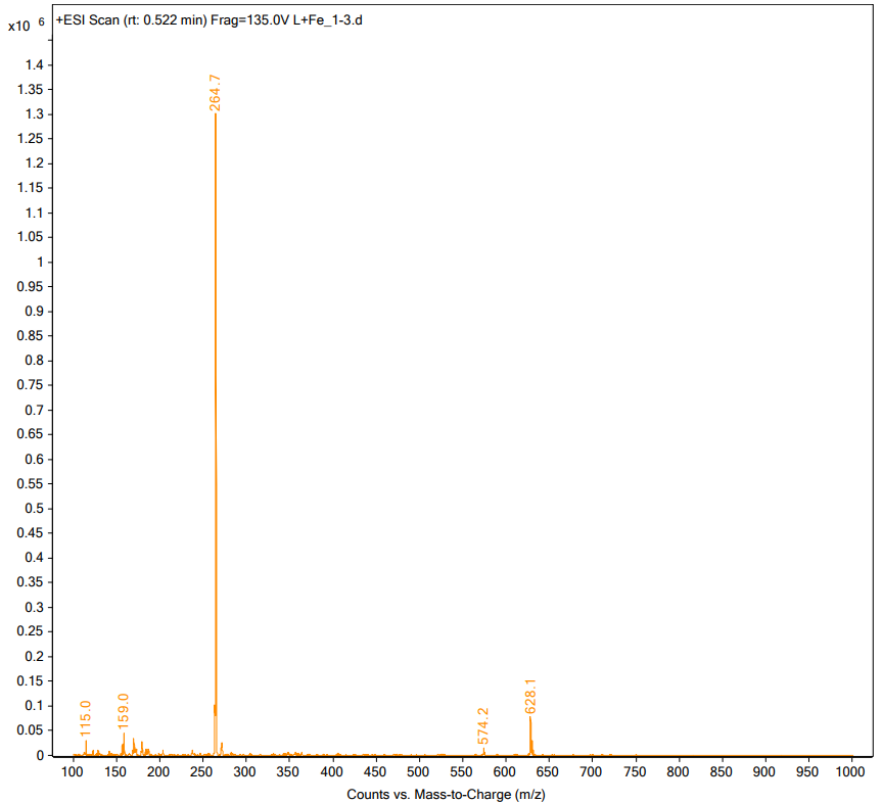

(C)

Figure 38: Mass spectra of solutions containing bmpy and $Fe(ClO_4)_2 \cdot 6H_2O$ in differing mole ratios. (A). (1:1), (B). (1:2), (C). (1:3)

3.3.4 Bmpy + $Ni(ClO_4)_2 \cdot 6H_2O$

The mass spectra shown in Figure 39 were obtained from the solutions of bmpy: $Ni(ClO_4)_2 \cdot 6H_2O$ in 1:1, 1:2 and 1:3 ratios, respectively. In all three spectra, the base peak at *m/z* 265.7 is the only significant peak observed. This is consistent with the ion $[Ni(bmpy)]^{2+}$ (Formula: $[Ni(C_{29}H_{27}N_7)]^{2+}$, Molecular Mass: 532.266, Monoisotopic Mass: 531.168). A peak at *m/z* 630.2 (Figure 29) is also present in all three spectra, and increases in intensity as the amount of metal ion increases. This peak is consistent with the ion $[Ni(bmpy)(ClO_4)]^{+}$ (Formula: $[Ni(C_{29}H_{27}N_7)ClO_4]^{+}$, Molecular Mass: 631.717, Monoisotopic Mass: 630.117). A low intensity peak at *m/z* 530.2 observed in all spectra is consistent with the deprotonated ion $[Ni(bmpy\text{-}H)]^{+}$ (Formula: $[Ni(C_{29}H_{26}N_7)]^{+}$, Molecular Mass: 531.258, Monoisotopic Mass: 530.160).

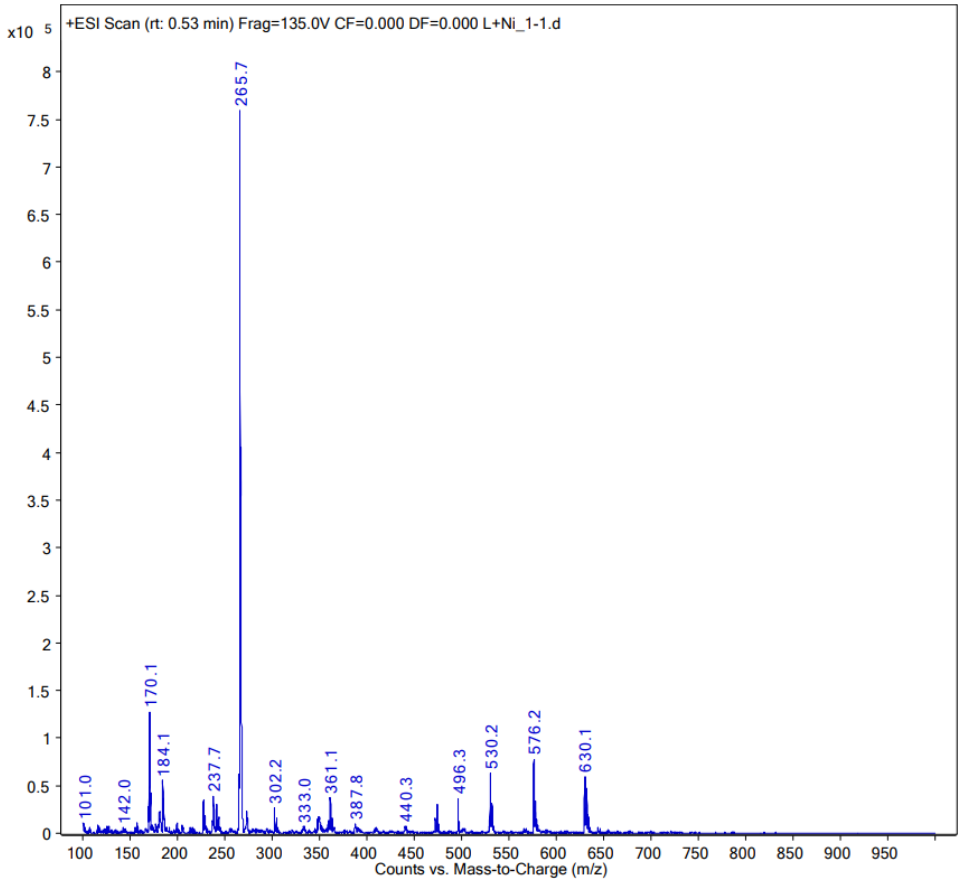
+ESI Scan (rt: 0.53 min) Frag=135.0V CF=0.000 DF=0.000 L+Ni_1-1.d
x10 5
265.7
170.1
184.1
101.0
142.0
237.7
302.2
333.0
361.1
387.8
440.3
496.3
530.2
576.2
630.1
Counts vs. Mass-to-Charge (m/z)

(A)

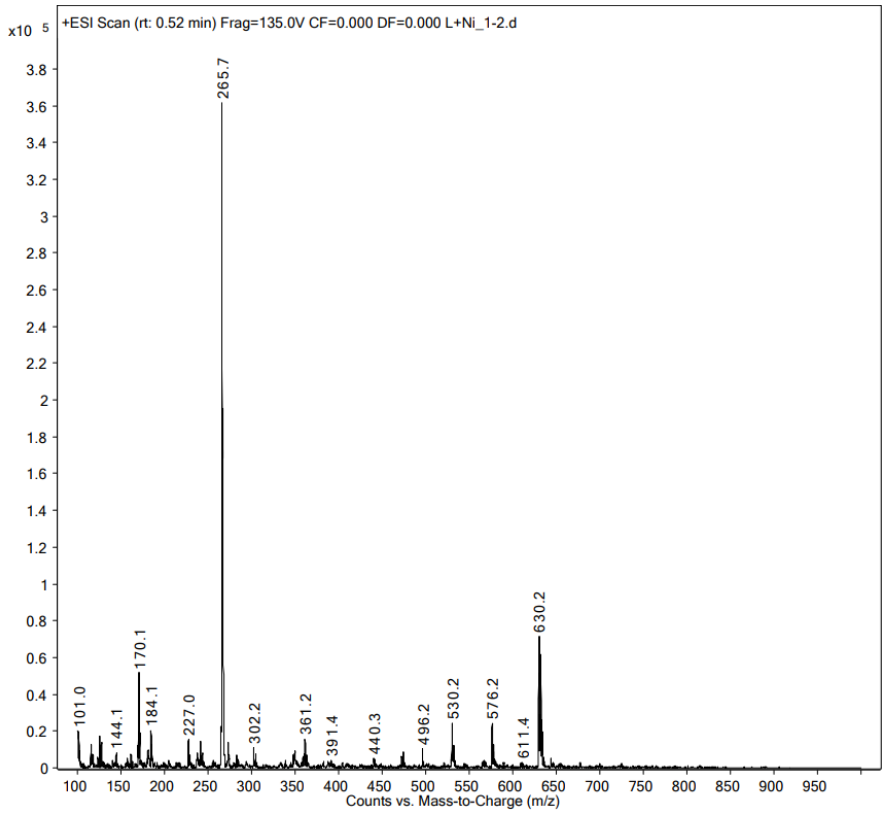
+ESI Scan (rt: 0.52 min) Frag=135.0V CF=0.000 DF=0.000 L+Ni_1-2.d
x10 5
265.7
170.1
184.1
101.0
144.1
227.0
302.2
361.2
391.4
440.3
496.2
530.2
576.2
611.4
630.2
Counts vs. Mass-to-Charge (m/z)

(B)

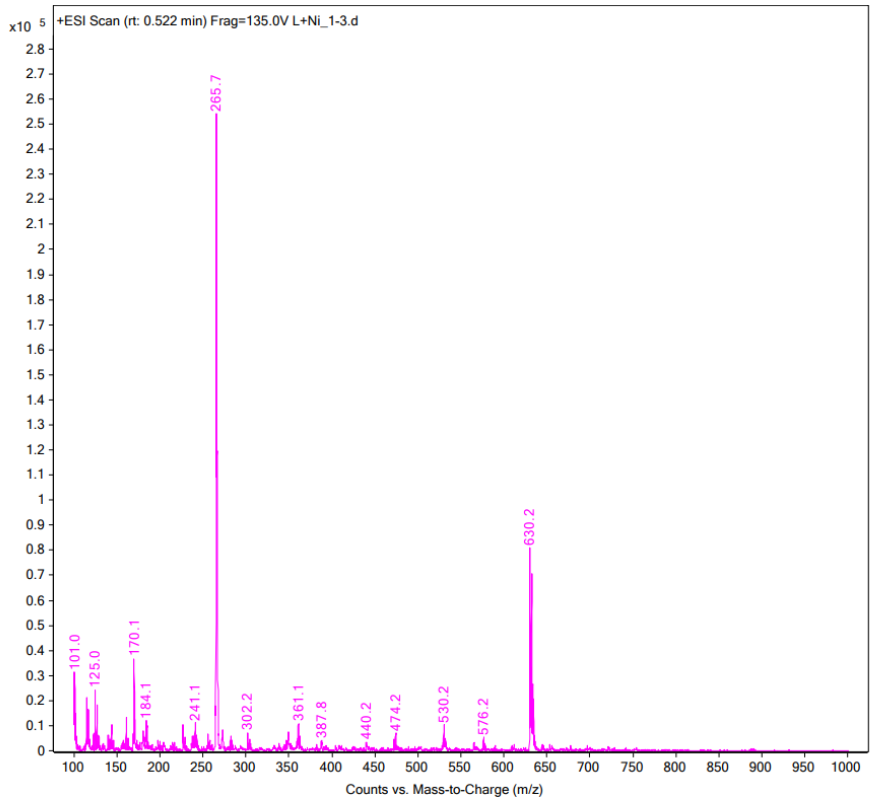

(C)

Figure 39: Mass spectra of solutions containing bmpy and $Ni(ClO_4)_2 \cdot 6H_2O$ in differing mole ratios. (A). (1:1), (B). (1:2), (C). (1:3)

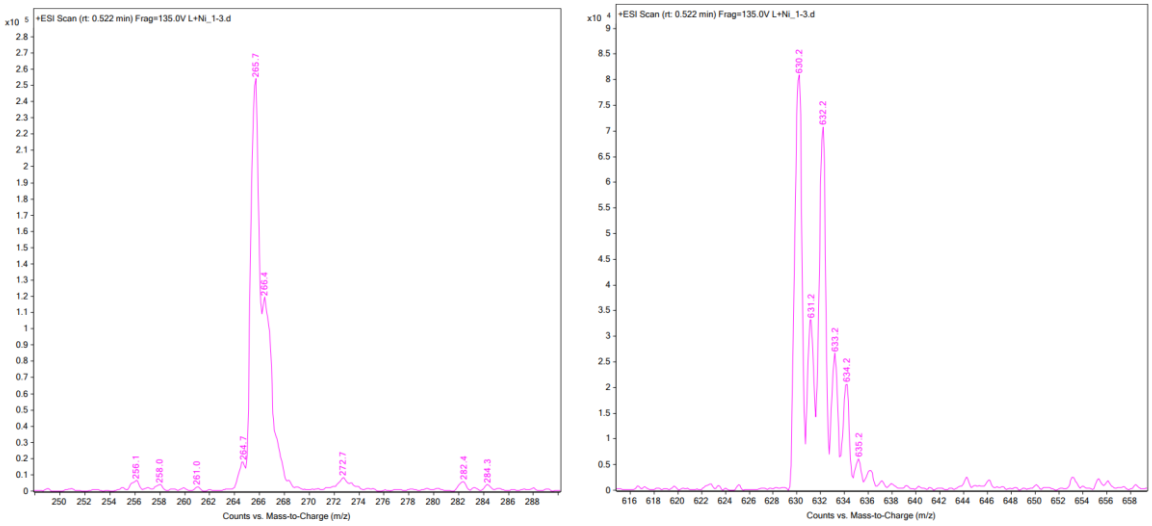

Figure 40: Expansions of the peaks at *m/z* 265.7 and *m/z* 630.2 showing the isotope patterns of bmpy:$Ni(ClO_4)_2 \cdot 6H_2O$ (1:3)

3.3.5 Bmpy + $Zn(ClO_4)_2 \cdot 6H_2O$

The mass spectra shown in Figure 41 were obtained from the solutions of bmpy: $Zn(ClO_4)_2 \cdot 6H_2O$ in 1:1, 1:2 and 1:3 ratios, respectively. In all three spectra, the base peak occurs at *m/z* 268.6, again showing that the mole ratio has no effect on the nature of the major product formed. This peak corresponds to the $[Zn(bmpy)]^{2+}$ ion (Formula: $[Zn(C_{29}H_{27}N_7)]^{2+}$, Molecular Mass: 538.950, Monoisotopic Mass: 537.162). A peak corresponding to the monoprotonated free ligand at *m/z* 496.3 is also observed in all spectra, suggesting that the Zn^{2+} ion binds to bmpy less strongly than the other metal ions investigated. A low intensity peak at *m/z* 636.1/638.2 is consistent with the $[Zn(bmpy)(ClO_4)]^+$ ion (Formula: $[Zn(C_{29}H_{27}N_7)ClO_4]^+$, Molecular Mass: 638.401, Monoisotopic Mass: 636.110).

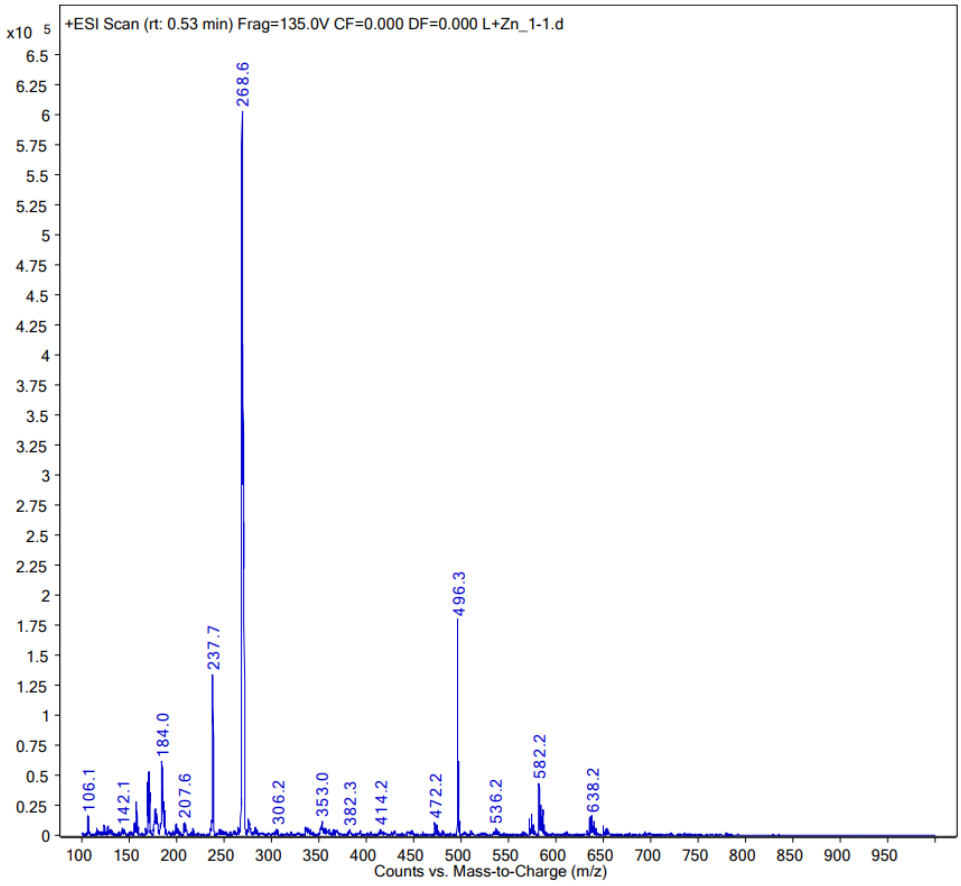

(A)

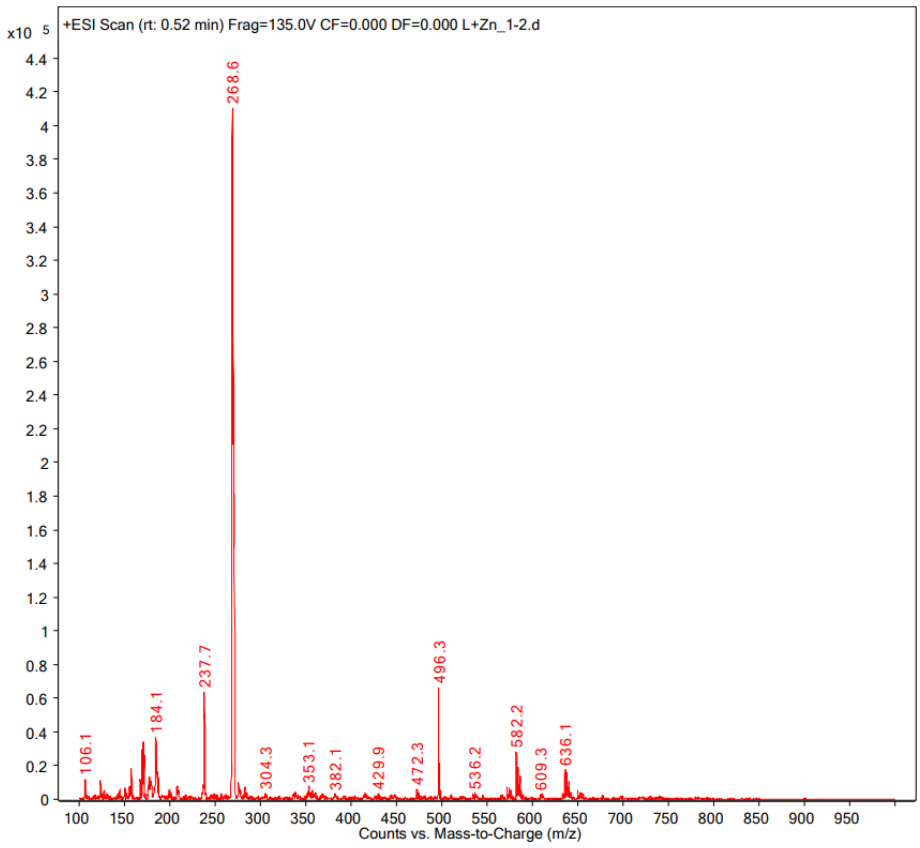

(B)

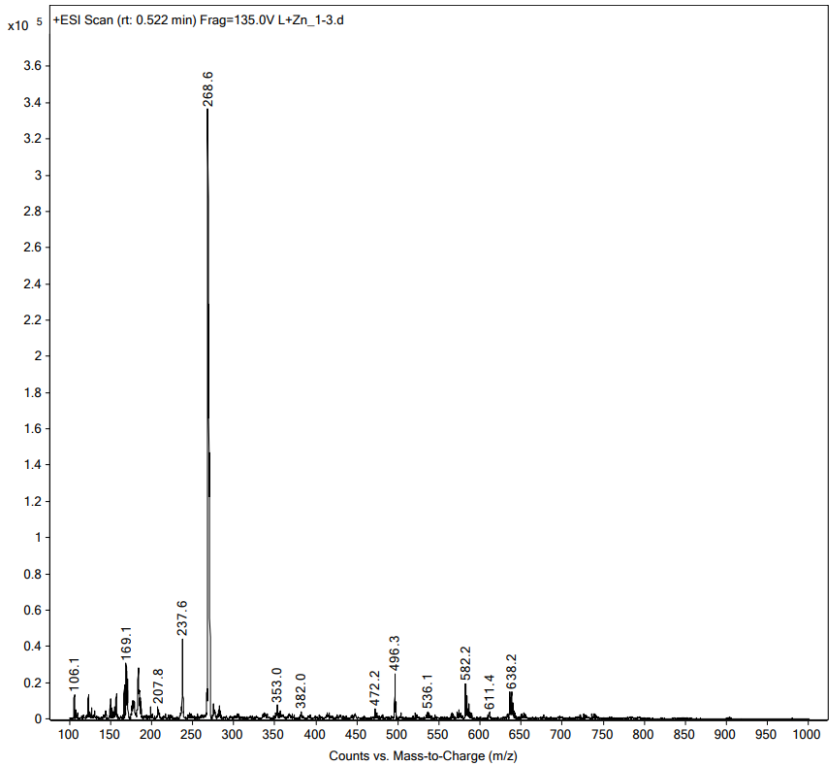

(C)

Figure 41: Mass spectra of solutions containing bmpy and $Zn(ClO_4)_2 \cdot 6H_2O$ in differing mole ratios. (A). (1:1), (B). (1:2), (C). (1:3)

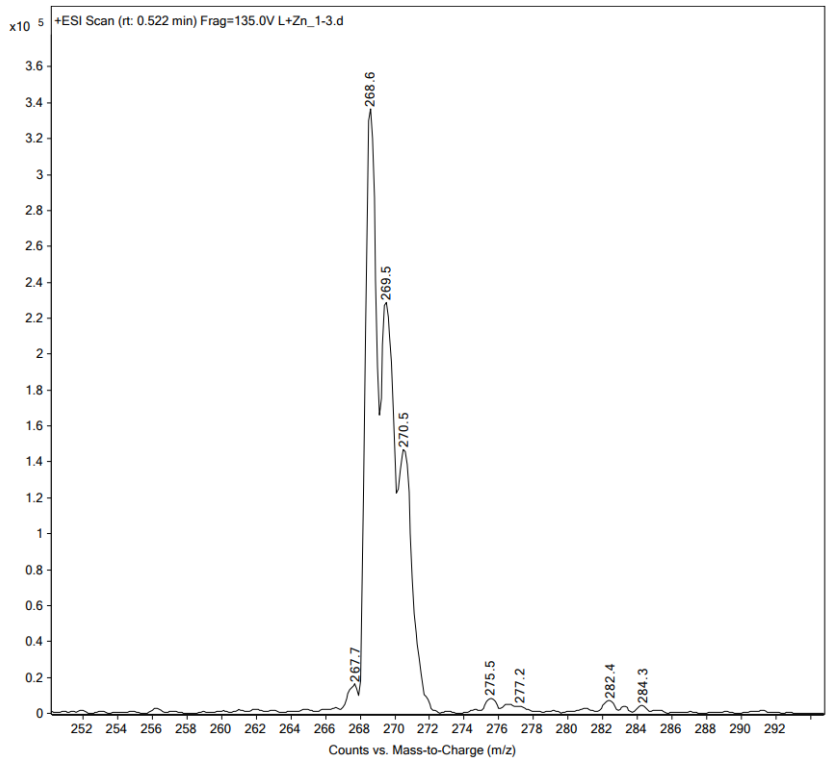

Figure 42: Isotope pattern of the base peak in the mass spectrum of bmpy: $Zn(ClO_4)_2 \cdot 6H_2O$ (1:3)

3.4 Purification of N, N'-bis(2,2'-bipyridin-6-ylmethyl)diethylamine-1,2-dimethylamine (bmdet) and the transition metal complexes of bmdet

Bmdet was prepared by the method of Schrumpf.[80] via the reaction between 2,2′-bipyridine-6-carboxaldehyde and diethylenetriamine with $NaBH_4$ to reduce the imine product. The crude bmdet, which had been prepared previously, was successfully purified on an alumina column on elution with 2% MeOH/$CHCl_3$, gradually increasing to 10% MeOH/$CHCl_3$. ^{13}C NMR was used to check the fractions collected and MS was also used to confirm the identity of the product.

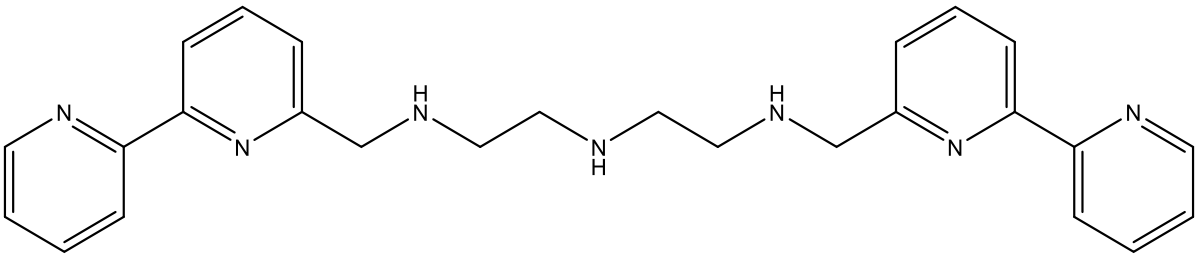

N, N'-bis(2,2'-bipyridin-6-ylmethyl)diethylamine-1,2-dimethylamine (bmdet)

Figure 43: Structure of bmdet

As shown in the chemical structure above, bmdet has 6 aliphatic carbons and 20 aromatic carbons. Because of its symmetrical structure, there should be 10 peaks for aromatic carbons in the downfield region of the ^{13}C NMR and 3 peaks for methylenes in the upfield region. The ^{13}C NMR spectrum of the purified compound shown below is consistent with these predictions.

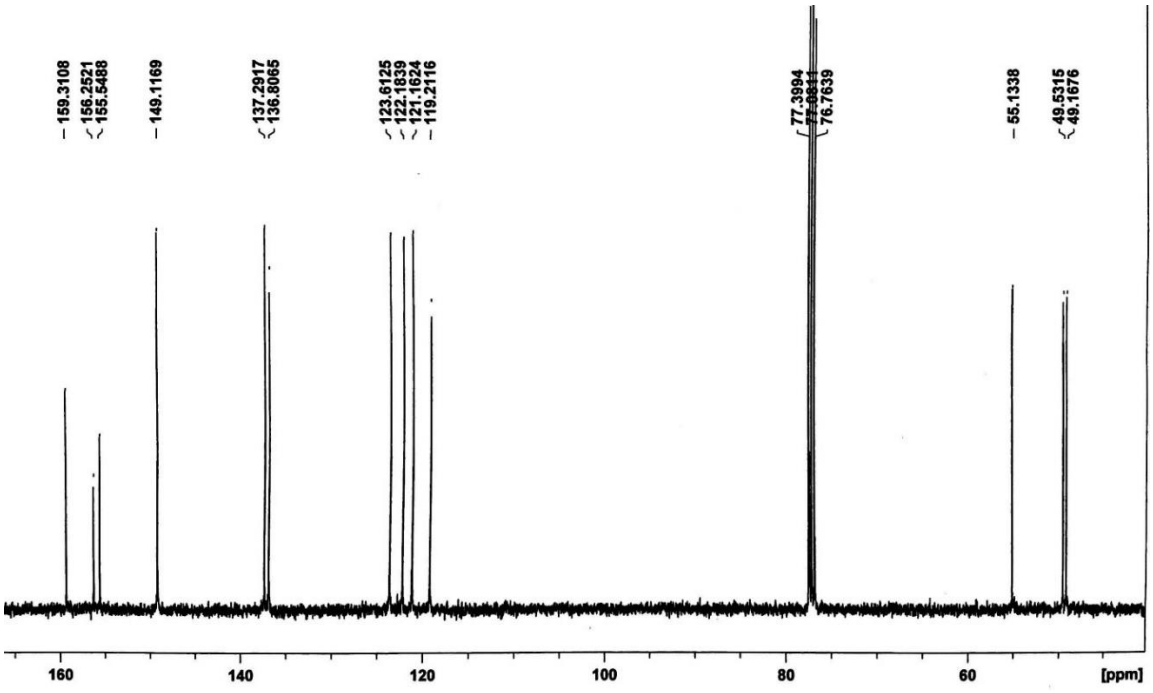

Figure 44: ^{13}C NMR spectrum of N, N'-bis(2,2'-bipyridin-6-ylmethyl)diethylamine-1,2-dimethylamine (bmdet)

In the mass spectrum of bmdet (Figure 45), the base peak is observed at *m/z* 220.8, and this corresponds to doubly protonated bmdet (Formula: $C_{26}H_{31}N_7^{2+}$, Molecular Mass: 441.572, Monoisotopic Mass: 441.264). A less intense peak at *m/z* 440.4 is due to singly protonated bmdet (Formula: $C_{26}H_{30}N_7$, Molecular Mass: 440.564, Monoisotopic Mass: 440.256), while the peak at *m/z* 462.4 corresponds to sodiated bmdet (Formula: $[Na(C_{26}H_{29}N_7)]^+$, Molecular Mass: 462.546, Monoisotopic Mass: 462.238).

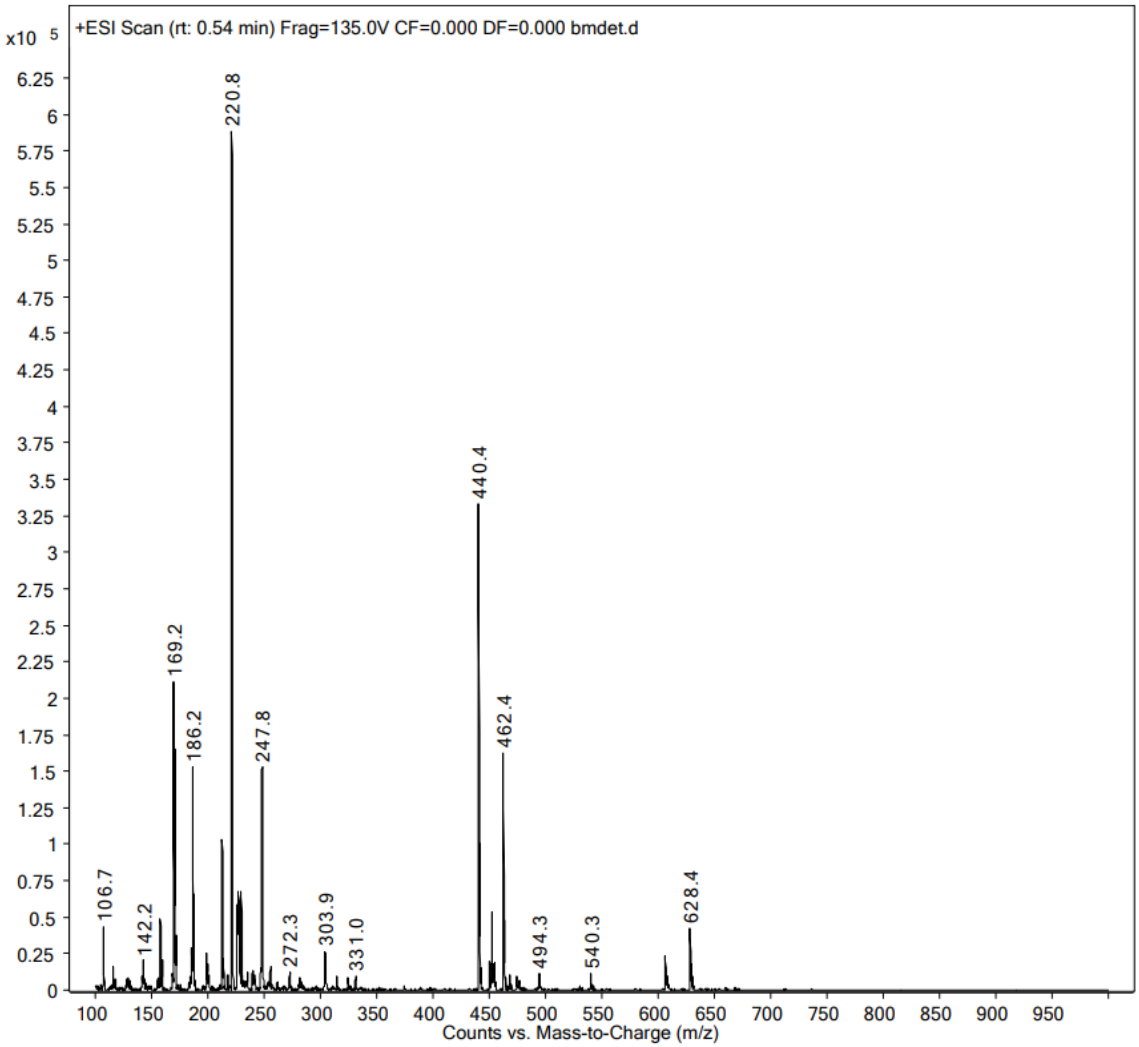

Figure 45: Mass spectrum of N, N'-bis(2,2'-bipyridin-6-ylmethyl)diethylamine-1,2-dimethylamine (bmdet)

In a similar fashion to experiments carried out with bmpy, the purified bmdet product was reacted with Co(II), Cu(II), Fe(II), Ni(II) and Zn(II) on a small scale, with the products being detected by ESI-MS.

3.4.1 Bmdet + $Co(ClO_4)_2 \cdot 6H_2O$

Figure 46 shows the mass spectra obtained from mixtures of bmdet and $Co(ClO_4)_2 \cdot 6H_2O$ in 1:1, 1:2 and 1:3 ratios. The spectra are similar, with the base peak in each occurring at *m/z* 249.2, showing that the mole ratio of reactants does not affect the nature of the products. The base peak is consistent with the mononuclear $[Co(bmdet)]^{2+}$ ion (Formula: $[Co(C_{26}H_{29}N_7)]^{2+}$, Molecular Mass: 498.490, Monoisotopic Mass: 498.182). All three spectra have a low

intensity peak at *m/z* 597.2 and this is consistent with the $[Co(bmdet)(ClO_4)]^+$ ion (Formula: $[Co(C_{26}H_{29}N_7)ClO_4]^+$, Molecular Mass: 597.940, Monoisotopic Mass: 597.130). There is no evidence for the formation of any Co(III) complexes in the reaction mixture.

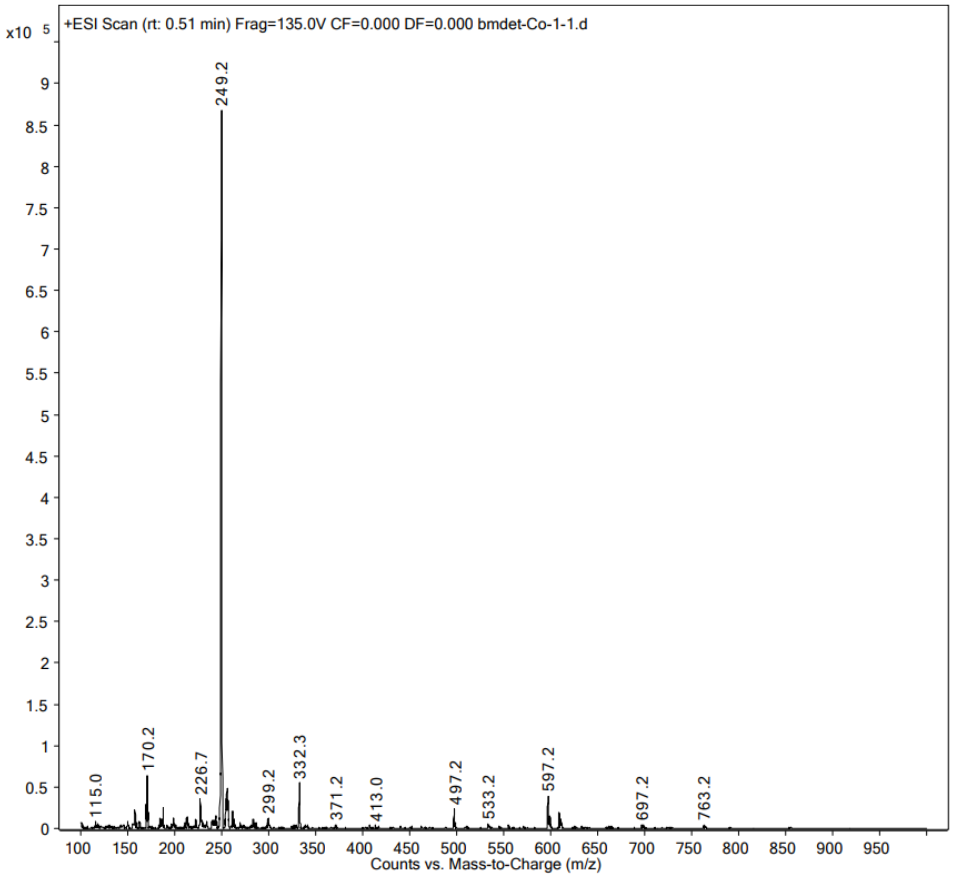

(A)

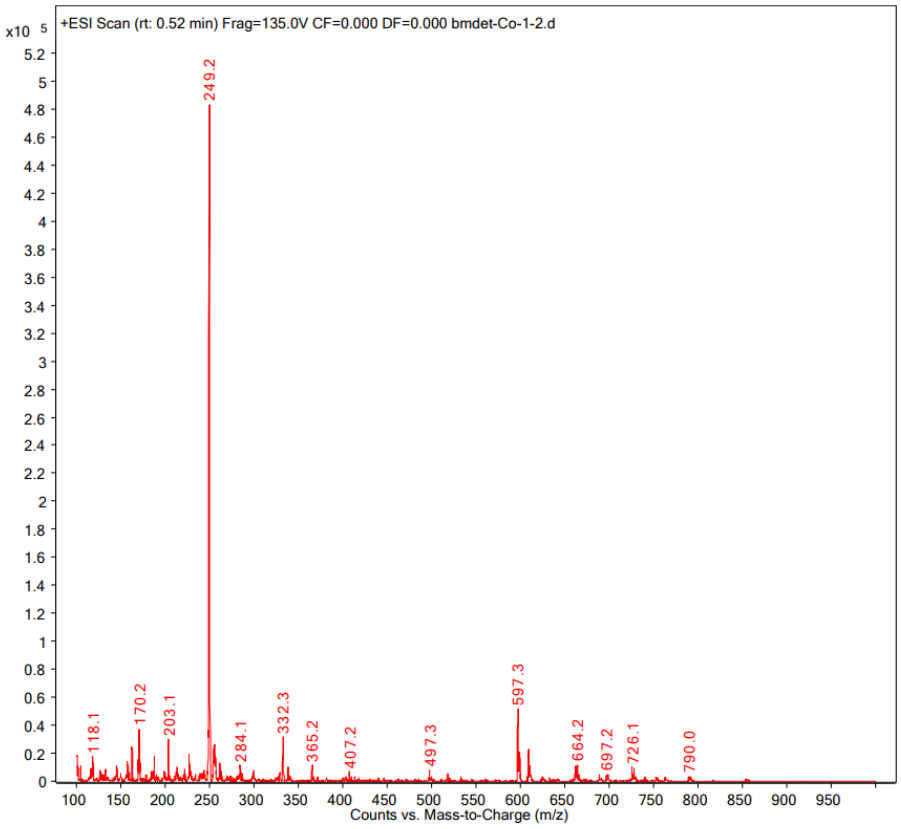

(B)

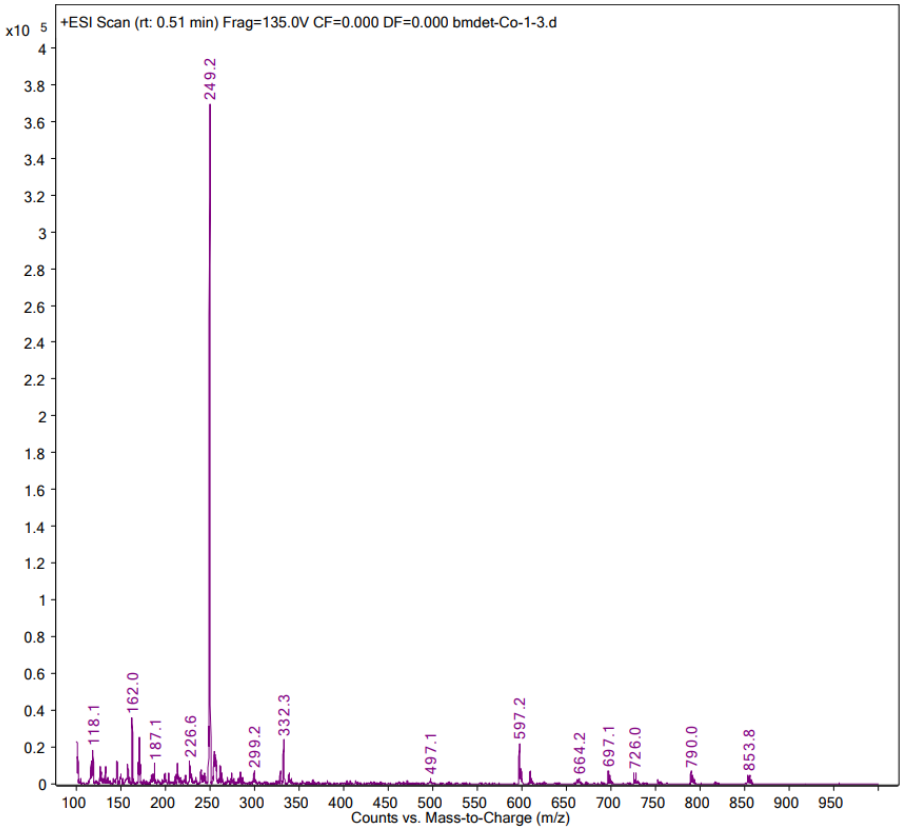

(C)

Figure 46: Mass spectra of Bmdet/$Co(ClO_4)_2 \cdot 6H_2O$ (A). (1/1), (B). (1/2), (C). (1/3).

3.4.2 Bmdet + $Cu(ClO_4)_2 \cdot 6H_2O$

Figure 47 shows the mass spectra obtained from mixtures of bmdet and $Cu(ClO_4)_2 \cdot 6H_2O$ in 1:1, 1:2 and 1:3 ratios. The base peak can be observed in all three spectra at *m/z* 260.1, which is consistent with the $[Cu(bmdet)H_2O]^{2+}$ ion (Formula: $[Cu(C_{26}H_{29}N_7)H_2O]^{2+}$, Molecular Mass: 521.118, Monoisotopic Mass: 520.189). An intense peak at *m/z* 241.2 was observed in the spectrum of the 1:1 ratio mixture, but the intensity of this peak became low in the 1:2 spectrum and it totally disappeared in the 1:3 spectrum. This peak could correspond to the product of fragmentation of bmdet by loss of one bipyridine group and one dimethylamine group (Formula: $C_{14}H_{17}N_4$, Molecular Mass: 241.312, Monoisotopic Mass: 241.145). All spectra also have lower intensity peaks at *m/z* 232.1 and *m/z* 303.2. The former may be due to ions containing deprotonated 6-methylenebipyridine and Cu^{2+} (Formula: $[Cu(C_{11}H_9N_2)]^+$, Molecular Mass: 232.749, Monoisotopic Mass: 232.006), while the latter is consistent with loss of one bipyridine unit from bmdet, with the fragment being protonated and hydrated (Formula: $[(C_{16}H_{23}N_5)H_2O]^+$, Molecular Mass: 303.403, Monoisotopic Mass: 303.206) respectively.

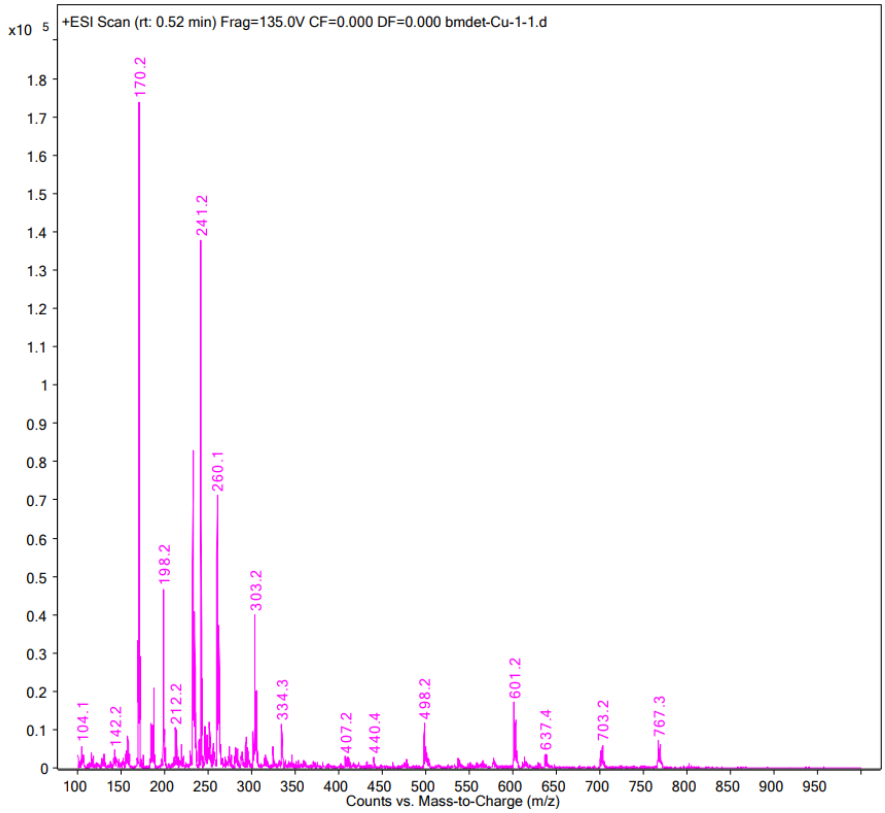

(A)

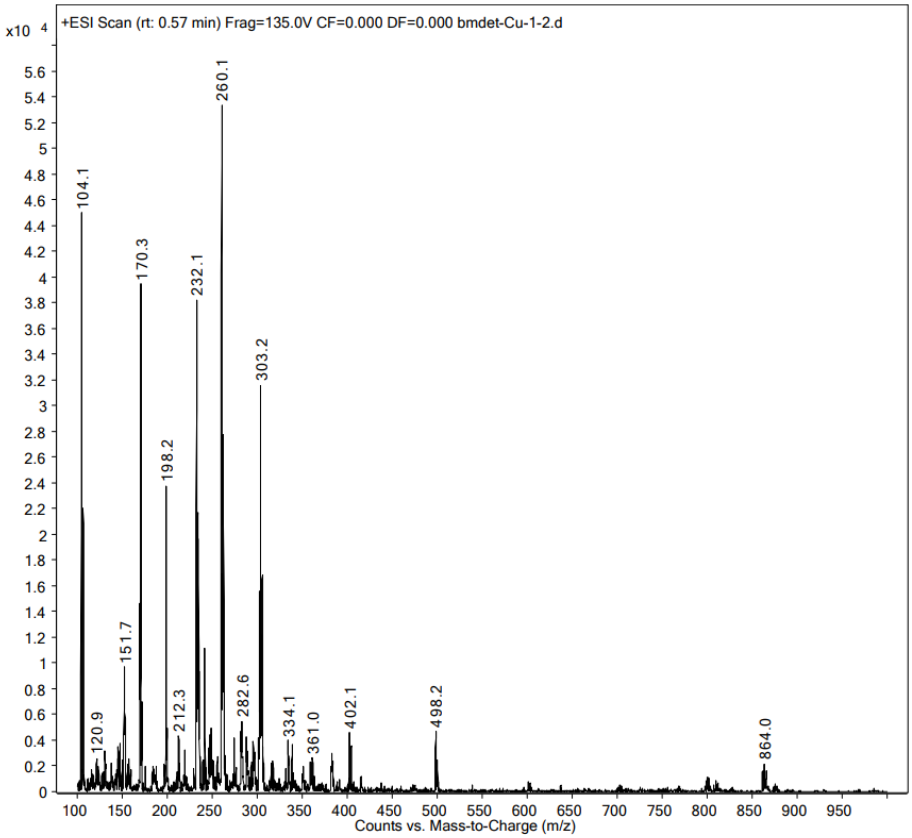

(B)

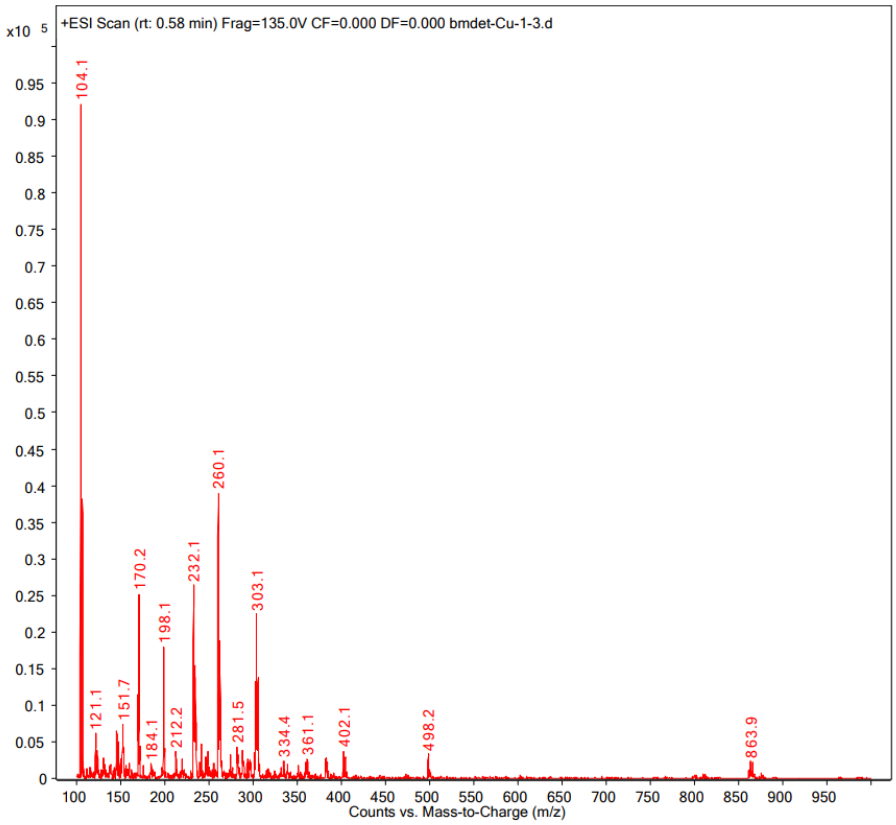

(C)

Figure 47: Mass spectra of Bmdet/$Cu(ClO_4)_2 \cdot 6H_2O$ (A). (1/1), (B). (1/2), (C). (1/3).

3.4.3 Bmdet + $Fe(ClO_4)_2 \cdot 6H_2O$

Figure 48 shows the mass spectra obtained from mixtures of bmdet and $Fe(ClO_4)_2 \cdot 6H_2O$ in 1:1, 1:2 and 1:3 ratios. In all spectra, the base peak is observed at *m/z* 247.7, and this is due to the mononuclear $[Fe(bmdet)]^{2+}$ ion (Formula: $[Fe(C_{26}H_{29}N_7)]^{2+}$, Molecular Mass: 495.401, Monoisotopic Mass: 495.183). The three spectra show that the species formed are independent of the ratio of the starting materials. The minor peak at *m/z* 594.2 in the spectra correspond to the $[Fe(dmbet)(ClO_4)]^{+}$ ion (Formula: $[Fe(C_{26}H_{29}N_7)ClO_4]^{-}$, Molecular Mass: 594.852, Monoisotopic Mass: 594.132). The isotope pattern of Fe is apparent in both peaks.

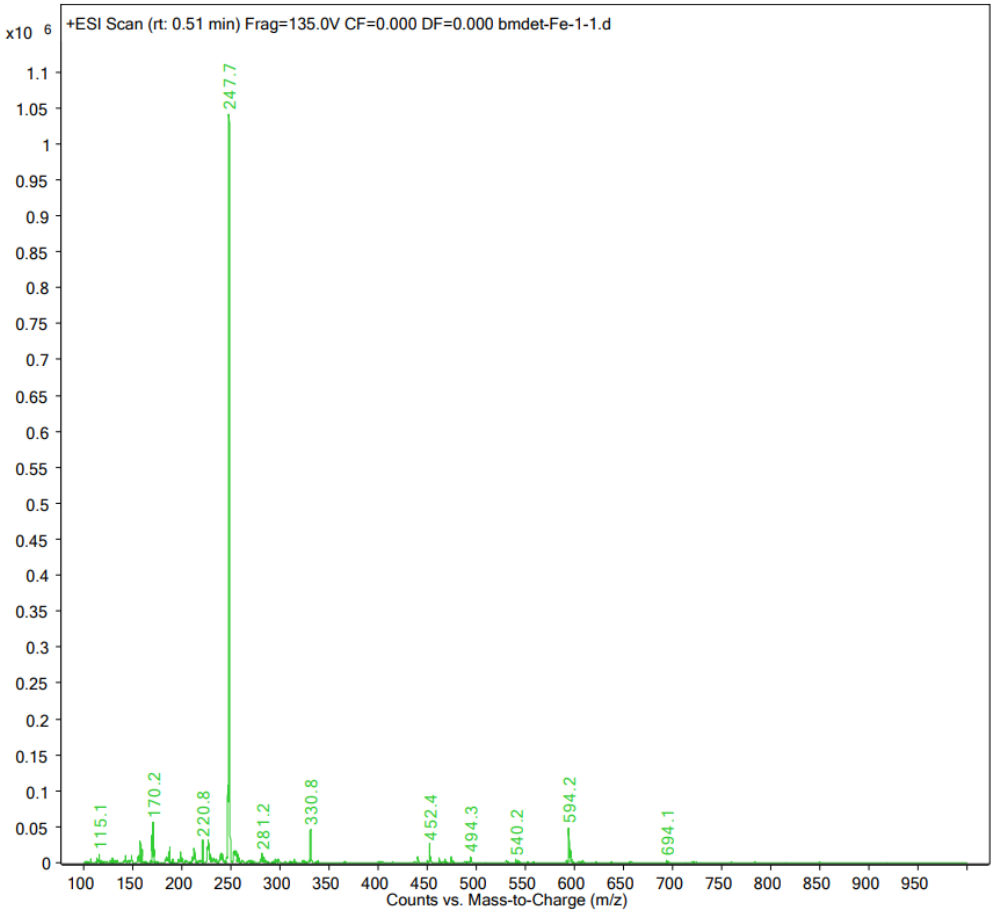

(A)

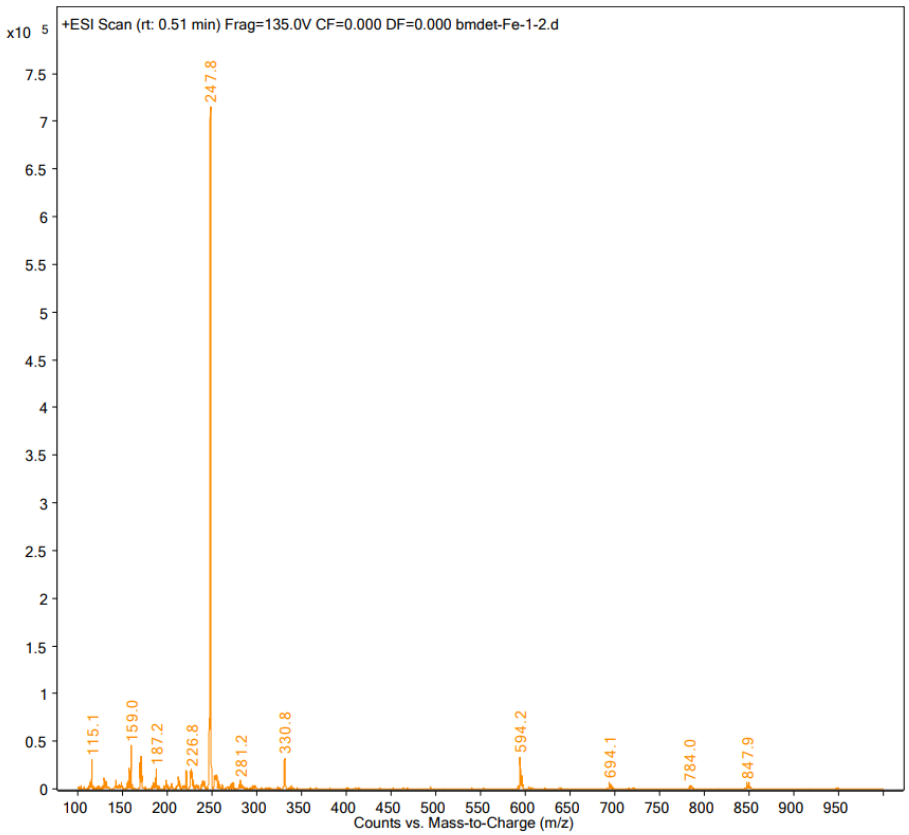

(B)

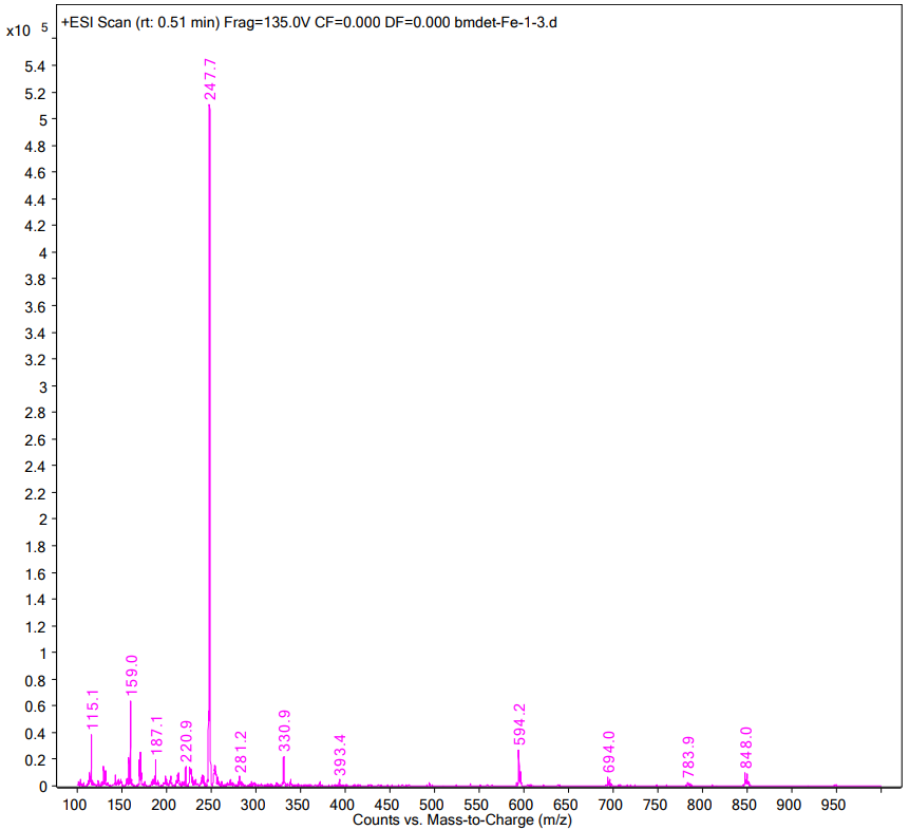

(C)

Figure 48: Mass spectra of Bmdet/$Fe(ClO_4)_2 \cdot 6H_2O$ (A). (1/1), (B). (1/2), (C). (1/3).

3.4.4 Bmdet + $Ni(ClO_4)_2 \cdot 6H_2O$

Figure 49 shows the mass spectra obtained from mixtures of bmdet and $Ni(ClO_4)_2 \cdot 6H_2O$ in 1:1, 1:2 and 1:3 ratios. The base peak at *m/z* 248.8 can be observed in all three spectra, which indicates that different mole rations of the metal and ligand do not affect the nature of the species formed. The base peak is due to the mononuclear $[Ni(bmdet)]^{2+}$ ion (Formula: $[Ni(C_{26}H_{29}N_7)]^{2+}$, Molecular Mass: 498.250, Monoisotopic Mass: 497.184) the isotope pattern consistent with Ni is apparent (Figure 50). A peak at *m/z* 440.3 was observed in the spectrum obtained from the 1:1 ratio mixture, but disappeared from the 1:2 and 1:3 spectra. This arises from the protonated bmdet ligand, which suggests that the ligand was not completely bound to the Ni^{2+} ion at low concentrations of the metal ion. The signal at *m/z* 596.2 observed in all three spectra corresponds to the $[Ni(bmdet)(ClO_4)]^+$ ion (Formula: $[Ni(C_{26}H_{29}N_7)ClO_4]^+$, Molecular Mass: 596.700, Monoisotopic Mass: 596.132).

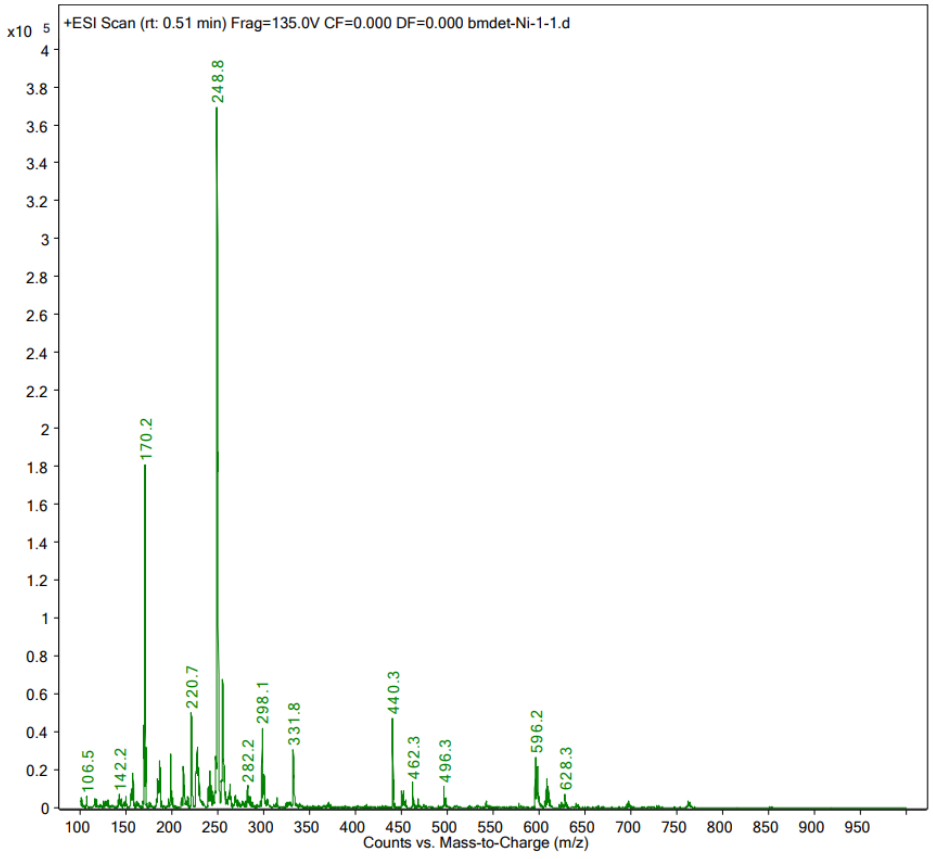

(A)

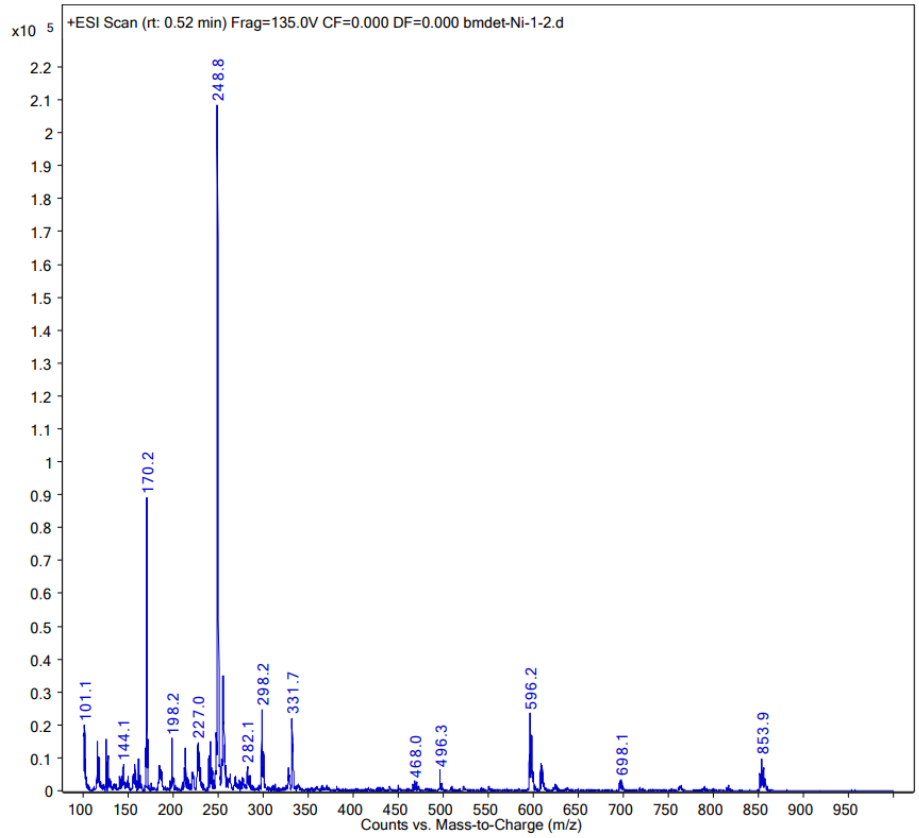

(B)

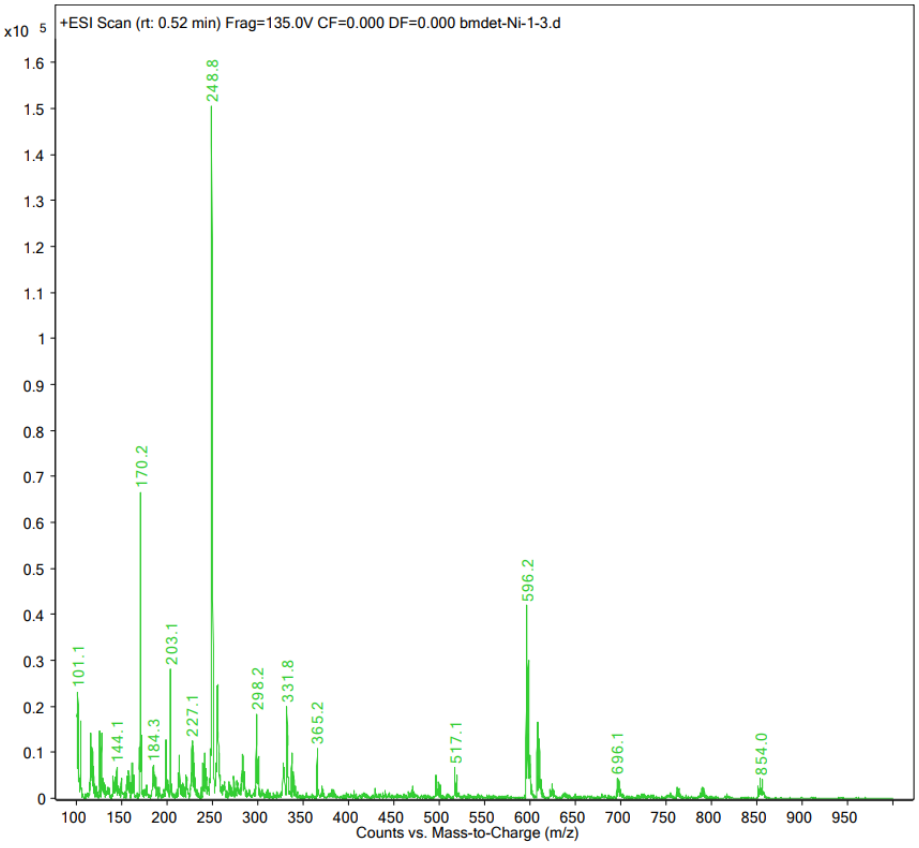

(C)

Figure 49: Mass spectra of Bmdet/$Ni(ClO_4)_2 \cdot 6H_2O$ (A). (1/1), (B). (1/2), (C). (1/3).

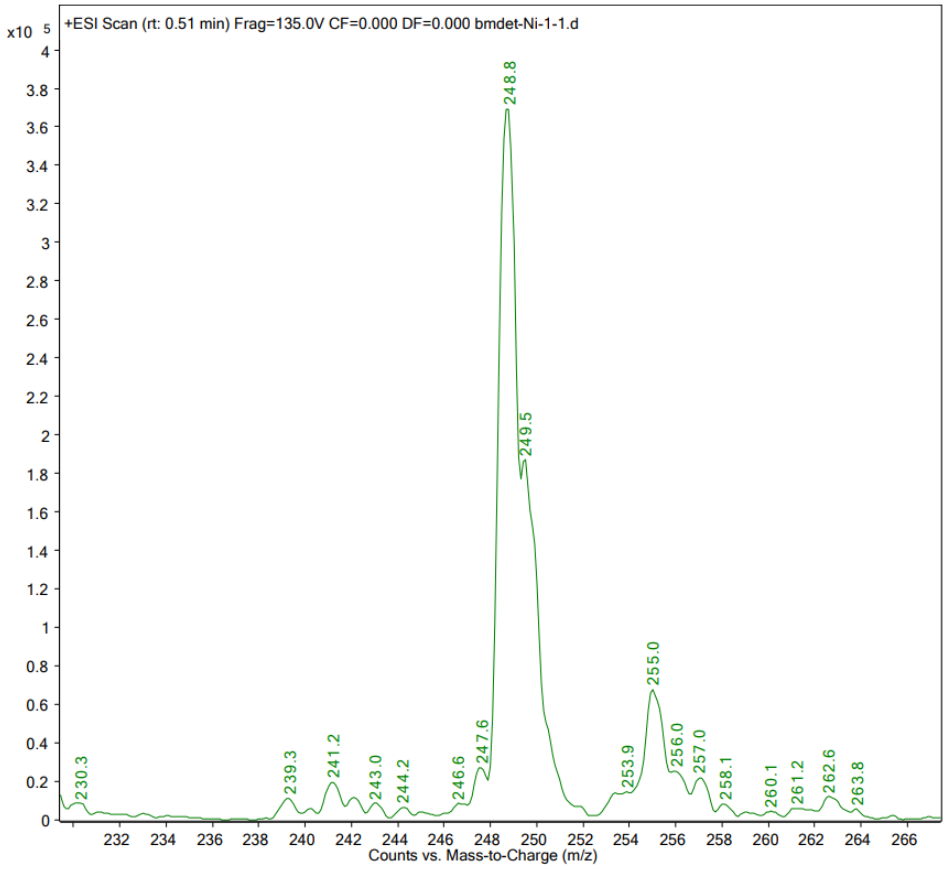

Figure 50: Expansion of the peaks at *m/z* 248.8 and *m/z* 249.5 in the mass spectrum of Bmdet/$Ni(ClO_4)_2 \cdot 6H_2O$ (1/1).

3.4.5 Bmdet + $Zn(ClO_4)_2 \cdot 6H_2O$

Figure 51 shows the mass spectra obtained from mixtures of bmdet and $Zn(ClO_4)_2 \cdot 6H_2O$ in 1:1, 1:2 and 1:3 ratios. The base peak in all three spectra is observed at *m/z* 251.7, and corresponds to the mononuclear $[Zn(bmdet)]^{2+}$ ion (Formula: $[Zn(C_{26}H_{29}N_7)]^{2+}$, Molecular Mass: 504.934, Monoisotopic Mass: 503.178). The Zn isotope pattern is apparent (Figure 52). The very low intensity peaks at *m/z* 602.2/604.2 arise from the $[Zn(bmdet)(ClO_4)]^+$ ion (Formula: $[Zn(C_{26}H_{29}N_7)ClO_4]^+$, Molecular Mass: 604.385, Monoisotopic Mass: 602.126).

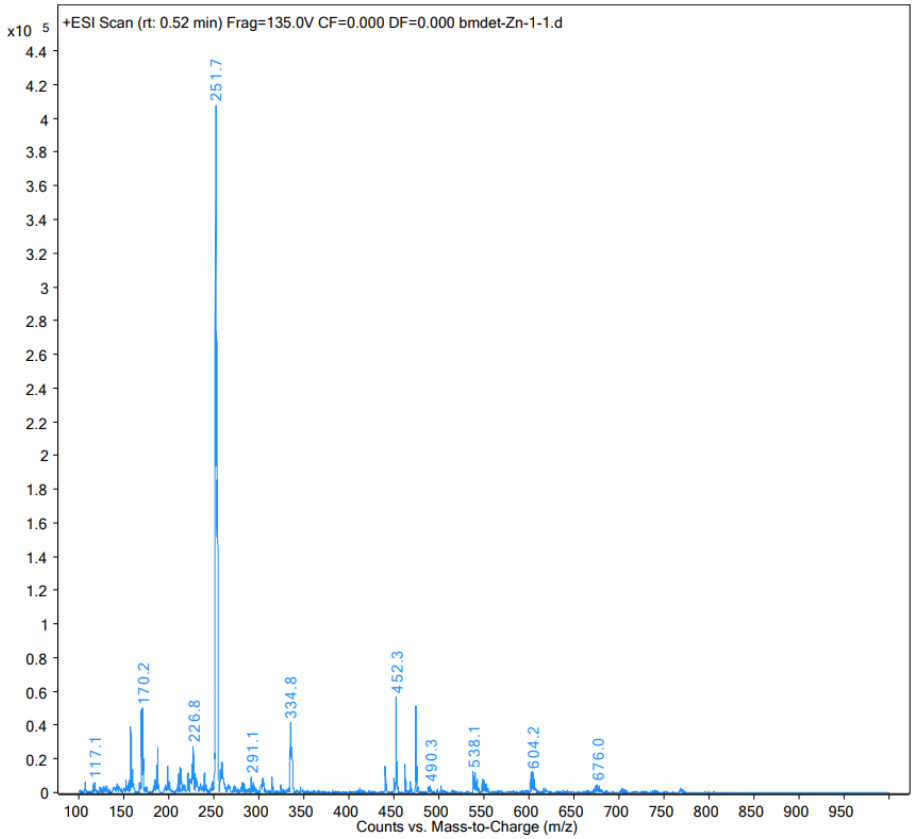
+ESI Scan (rt: 0.52 min) Frag=135.0V CF=0.000 DF=0.000 bmdet-Zn-1-1.d
x10 5
251.7
170.2
226.8
334.8
452.3
117.1
291.1
490.3
538.1
604.2
676.0
Counts vs. Mass-to-Charge (m/z)

(A)

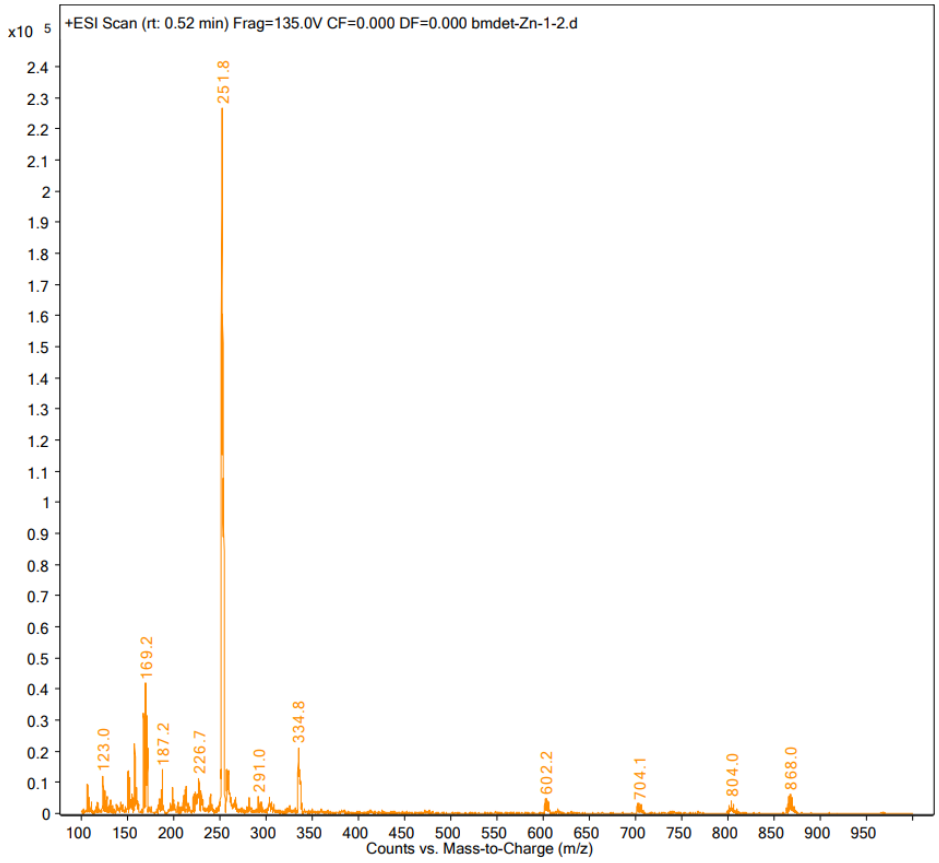
+ESI Scan (rt: 0.52 min) Frag=135.0V CF=0.000 DF=0.000 bmdet-Zn-1-2.d
x10 5
251.8
169.2
123.0
187.2
226.7
291.0
334.8
602.2
704.1
804.0
868.0
Counts vs. Mass-to-Charge (m/z)

(B)

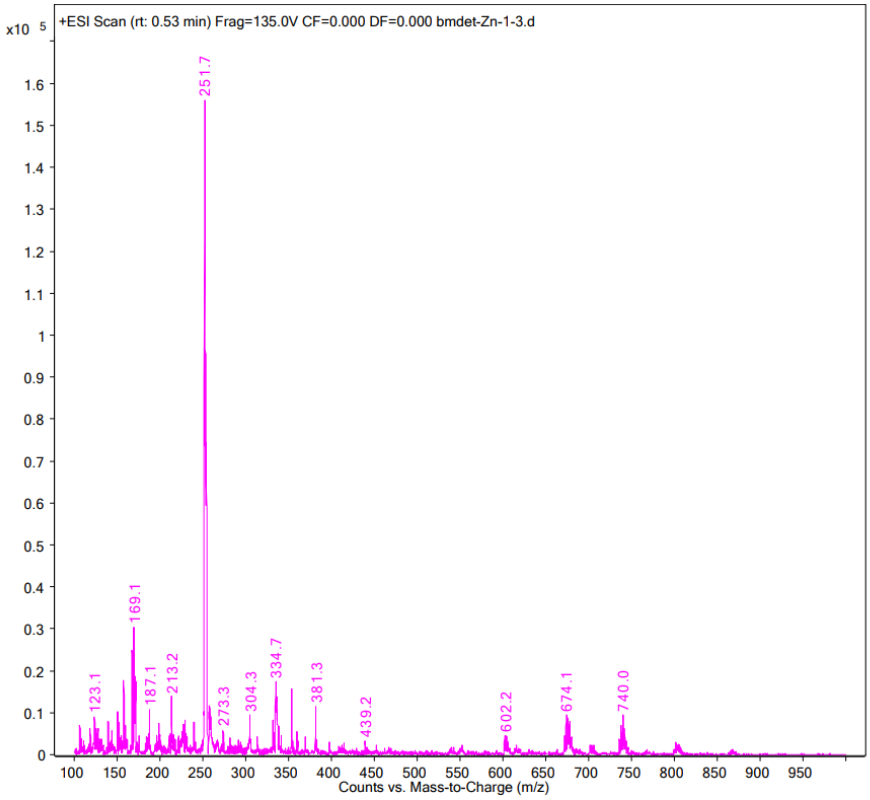

(C)

Figure 51: Mass spectra of Bmdet/$Zn(ClO_4)_2 \cdot 6H_2O$ (A). (1/1), (B). (1/2), (C). (1/3).

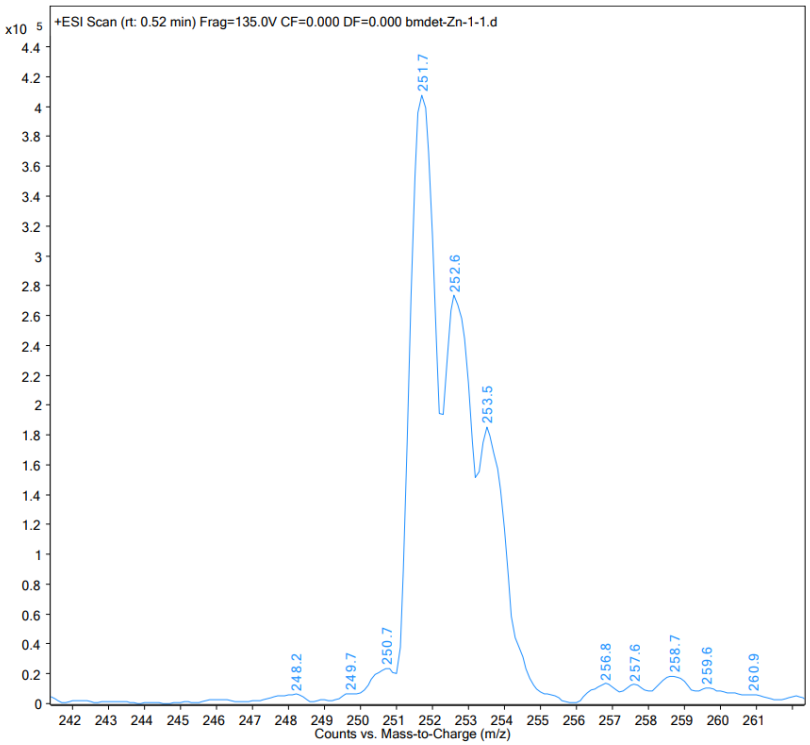

Figure 52: Expansion of the peaks at *m/z* 251.7, and *m/z* 252.6 and *m/z* 253.5 in the mass spectrum of Bmdet/$Zn(ClO_4)_2 \cdot 6H_2O$ (1/1)

3.5 Purification of N, N'-bis(6-methyl-2,2'-bipyridin-6'-ylmethyl)diethylamine-1,2-dimethylamine (DMbmdet) and the complexes of DMbmdet

The crude DMbmdet ligand was previously prepared by the method of Schrumpf.[80] via the reaction between 6′-methyl(2,2′-bipyridine)-6-carboxaldehyde and diethylenetriamine with $NaBH_4$ as the reducing agent for the Schiff base product obtained. It was purified on an alumina column and the ^1H NMR and ^{13}C NMR spectra of the pure product are given below.

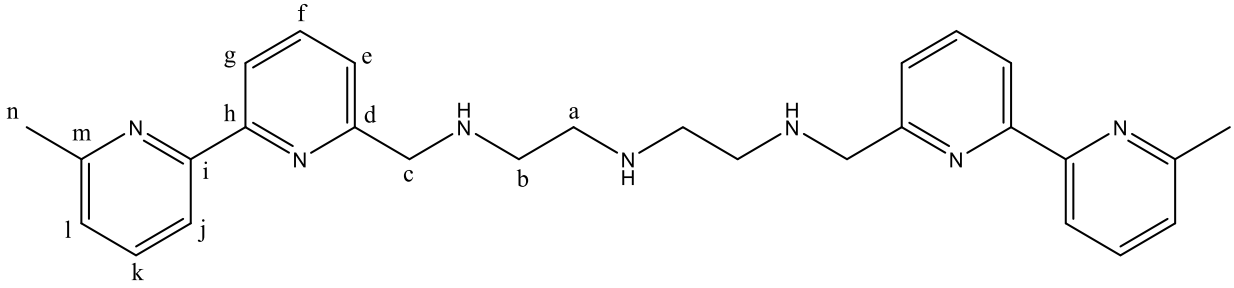

N, N'-bis(6-methyl-2,2'-bipyridin-6'-ylmethyl)diethylamine-1,2-dimethylamine (DMbmdet)

Figure 53: Structure of DMbmdet

The chemical formula of the ligand is $C_{28}H_{33}N_7$. Given that the compound is symmetrical about the central N atom, only 14 peaks should be observed in the ^{13}C NMR spectrum. Figure 55 shows this to be the case; there are 10 aromatic peaks at low field, and 4 peaks due to the methyl and methylene carbon atoms. In the ^1H NMR spectrum (Figure 54), two triplets at δ 7.7219 and δ 7.6526 are due to the hydrogen atoms on carbons k and f, while the four downfield doublets arise from the rest of the aromatic hydrogens. The multiplet at δ 2.8153 comes from the four hydrogens on carbons a and b. The broad singlet at δ 2.2978 can be associated with the hydrogens on nitrogen. The singlets at δ 2.6147 and δ 3.9711 can come from the hydrogen on carbons n and c, respectively.

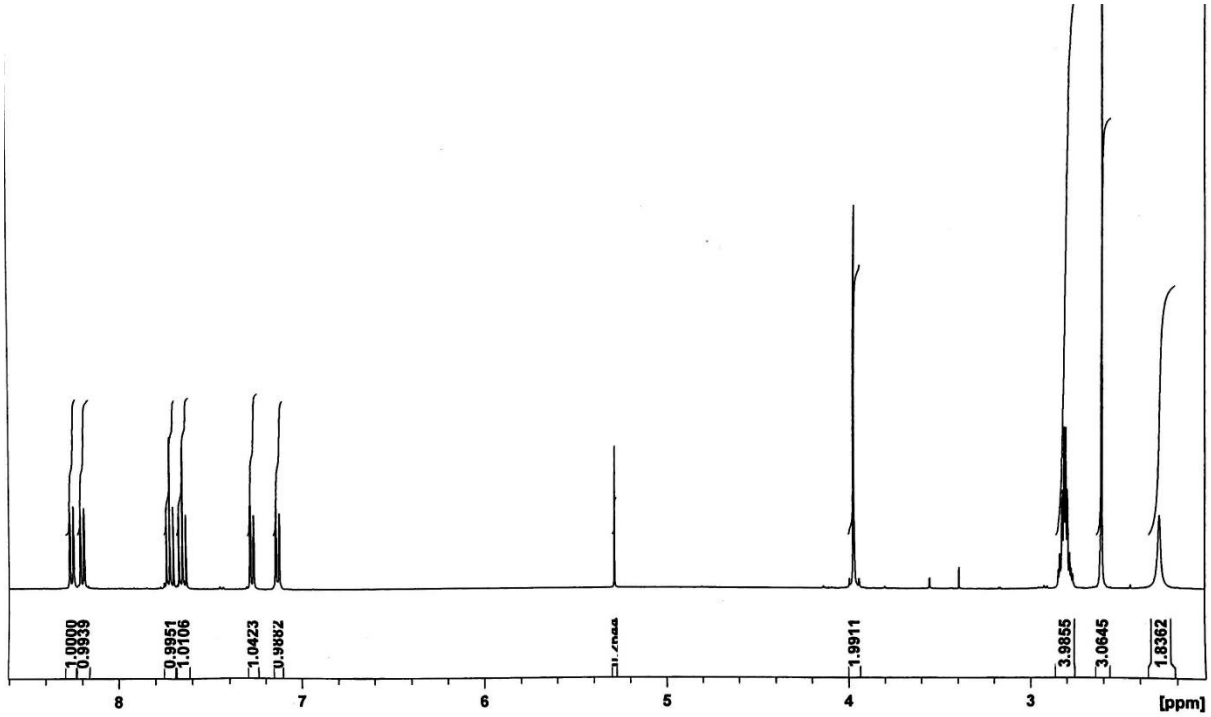

Figure 54: ^{1}H NMR spectrum of DMbmdet

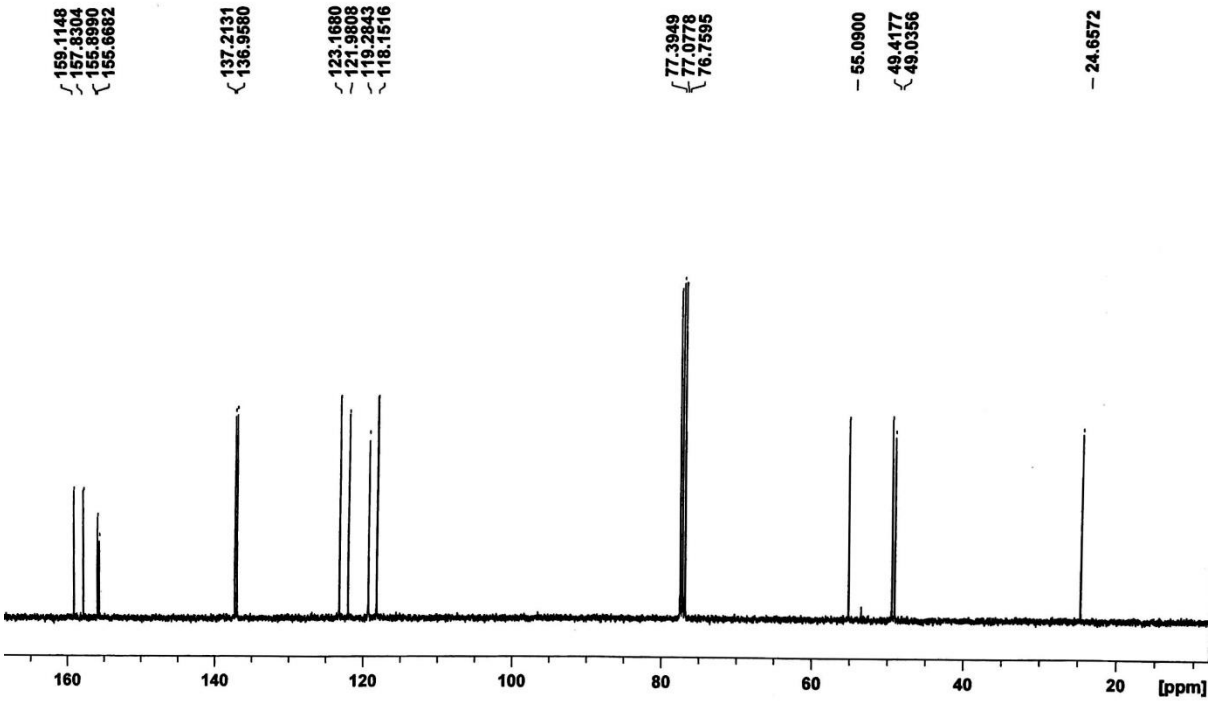

Figure 55: ^{13}C NMR spectrum of DMbmdet

In the mass spectrum of the ligand, two significant signals are observed at *m/z* 234.8 and *m/z* 468.4. The peak at *m/z* 468.4 can be assigned to singly protonated DMbmdet (Formula:

$C_{28}H_{34}N_7^+$, Molecular Mass: 468.618, Monoisotopic Mass: 468.288) and that at *m/z* 234.8 is consistent with the doubly protonated DMbmdet (Formula: $C_{28}H_{35}N_7^{2+}$, Molecular Mass: 469.625, Monoisotopic Mass: 469.295). The peak at *m/z* 490 corresponds to the sodiated DMbmdet (Formula: $[Na(C_{28}H_{33}N_7)]^+$, Molecular Mass: 490.599, Monoisotopic Mass: 490.270).

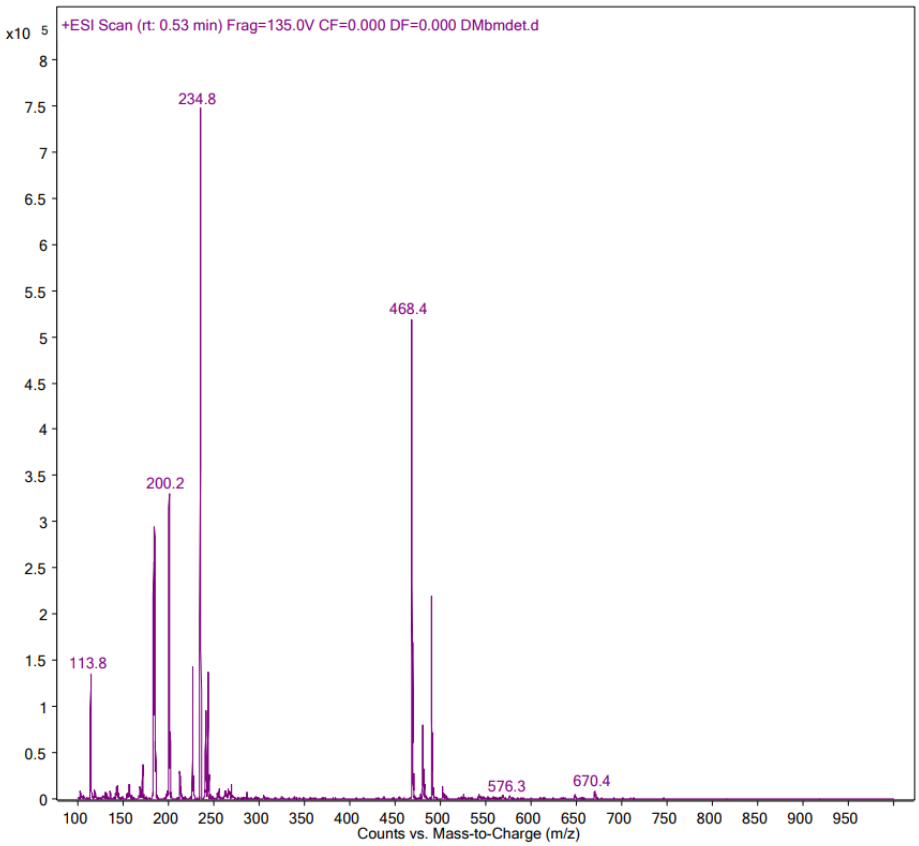

Figure 56: Mass spectrum of DMbmdet

After pure DMbmdet was successfully obtained, exploration of the complexes formed between DMbmdet and transition metal ions (the metal salts $Co(ClO_4)_2{\cdot}6H_2O$, $Cu(ClO_4)_2{\cdot}6H_2O$, $Fe(ClO_4)_2{\cdot}6H_2O$, $Ni(ClO_4)_2{\cdot}6H_2O$ and $Zn(ClO_4)_2{\cdot}6H_2O$ were used) was made using ESI-MS. These data are given and discussed below.

3.5.1 DMbmdet + $Co(ClO_4)_2{\cdot}6H_2O$

Figure 57 shows the mass spectra obtained from mixtures of DMbmdet and $Co(ClO_4)_2{\cdot}6H_2O$ in 1:1, 1:2 and 1:3 ratios. The base peak in all three spectra was observed at *m/z* 263.3 showing that the nature of the products is independent of the mole ratio used. This peak corresponds to the $[Co(DMbmdet)]^{2+}$ ion (Formula: $[Co(C_{28}H_{33}N_7)]^{2+}$, Molecular Mass:

526.543, Monoisotopic Mass: 526.213). The main differences in the three spectra are the decrease in intensity of the peak at *m/z* 525.3 and the increase in intensity of the peak at m/z 625.2 with increasing amounts of $Co(ClO_4)_2 \cdot 6H_2O$. The peak at *m/z* 525.3 can be attributed to the $[Co(DMbmdet\text{-}H)]^+$ ion (Formula: $[Co(C_{28}H_{32}N_7)]^+$, Molecular Mass: 525.535, Monoisotopic Mass: 525.205) and that at *m/z* 625.2 can be attributed to $[Co(DMbmdet)(ClO_4)]^+$ (Formula: $[Co(C_{28}H_{33}N_7)ClO_4]^+$, Molecular Mass: 625.993, Monoisotopic Mass: 625.161)

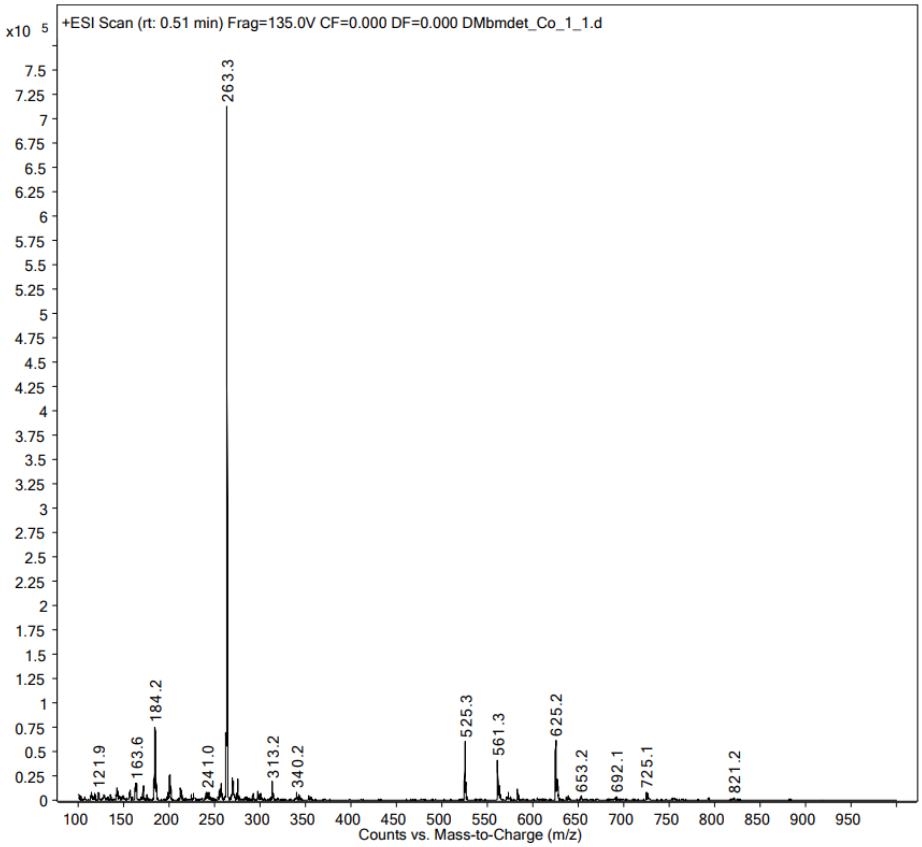

(A)

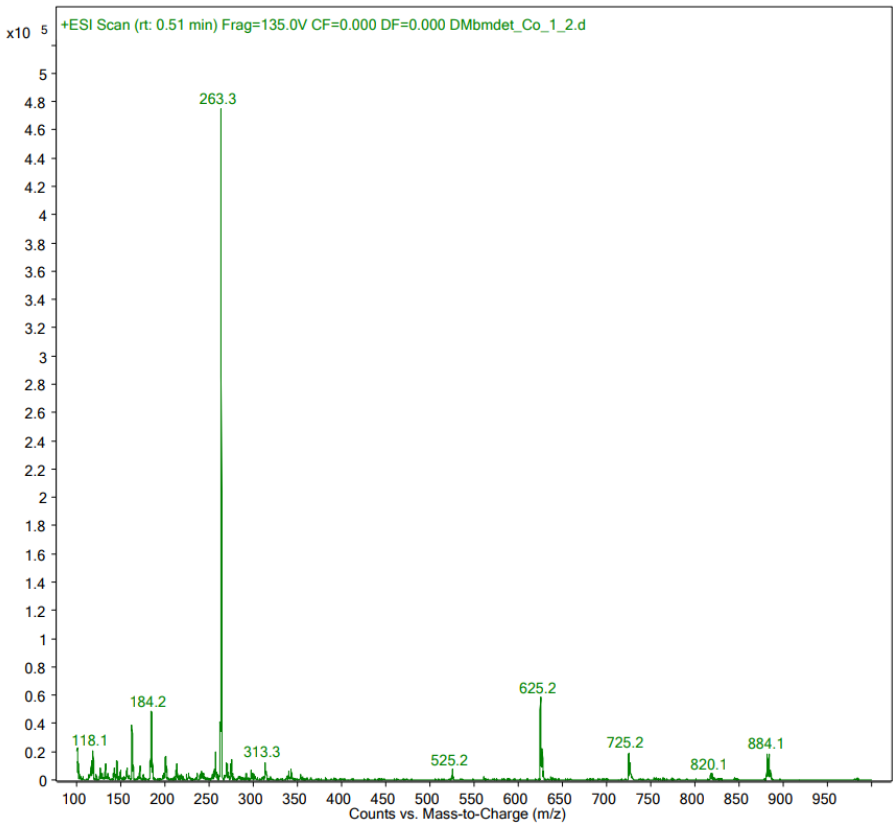

(B)

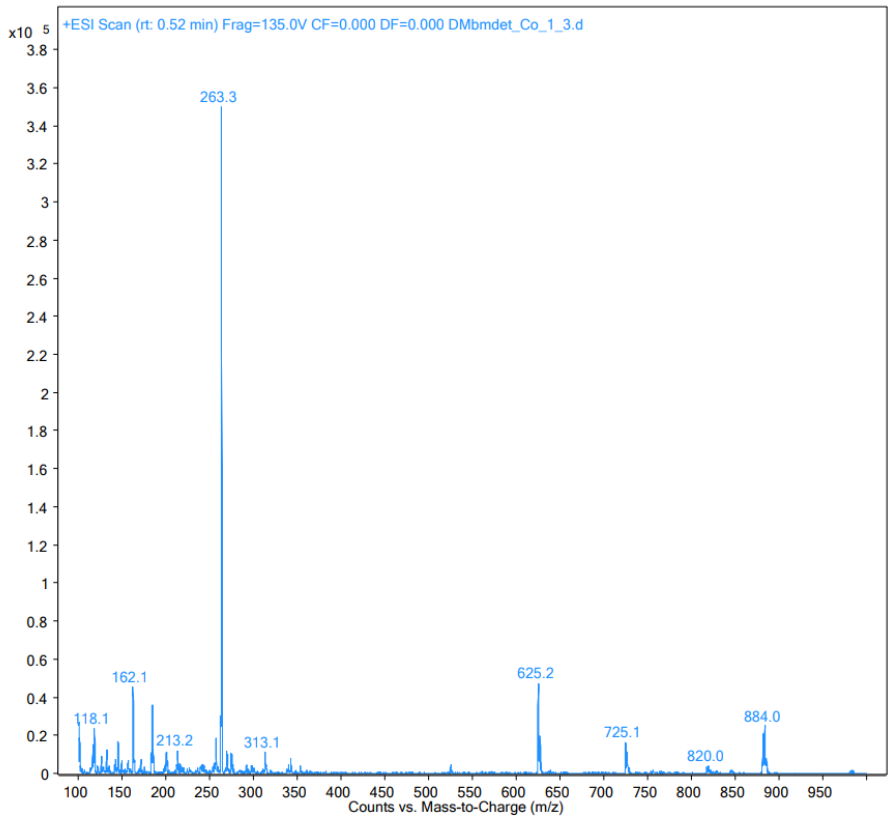

(C)

Figure 57: Mass spectra of DMbmdet/$Co(ClO_4)_2 \cdot 6H_2O$ (A). (1/1), (B). (1/2), (C). (1/3).

3.5.2 DMbmdet + $Cu(ClO_4)_2 \cdot 6H_2O$

Figure 58 shows the mass spectra obtained from mixtures of DMbmdet and $Cu(ClO_4)_2 \cdot 6H_2O$ in 1:1, 1:2 and 1:3 ratios. Base peaks at *m/z* 274.1 are present in all three spectra, and this is due to the $[Cu(DMbmdet)H_2O]^{2+}$ ion (Formula: $[Cu(C_{28}H_{33}N_7)H_2O]^{2+}$, Molecular Mass: 549.171, Monoisotopic Mass: 548.220). A peak with low intensity corresponding to the $[Cu(DMbmdet\text{-}H)]^+$ ion is observed only in the 1:1 spectrum at *m/z* 529.3 (Formula: $[Cu(C_{28}H_{32}N_7)]^+$, Molecular Mass: 530.148, Monoisotopic Mass: 529.202) and those corresponding to ion $[Cu(DMbmdet)ClO_4]^+$ can be observed in both 1:1 and 1:2 spectra at *m/z* 629.2 (Formula: $[Cu(C_{28}H_{33}N_7)ClO_4]^+$, Molecular Mass: 630.606, Monoisotopic Mass: 629.158) but not in the 1:3 spectrum. Similar to the bmdet and $Cu(ClO_4)_2 \cdot 6H_2O$ system, peaks consistent with the fragment of DMbmdet losing a 6-methyl-2,2'-bipyridin-6'-ylmethyl group and methylamine and the protonated fragment of DMbmdet losing 6-methyl-2,2'-bipyridine with a water molecule are observed in all three spectra at *m/z* 255.2 (Formula: $C_{15}H_{19}N_4$, Molecular Mass: 255.339, Monoisotopic Mass: 255.161) and *m/z* 317.2 (Formula: $[(C_{17}H_{25}N_5)H_2O]^+$, Molecular Mass: 317.430, Monoisotopic Mass: 317.222) respectively. A peak at *m/z* 246.1 is also present in all three spectra, and decreases in intensity as the amount of metal ion increases. This is due to the ion made of a 6-methyl-2,2'-bipyridin-6'-ylmethylene fragment and a Cu^{2+} ion (Formula: $[Cu(C_{12}H_{11}N_2)]^+$, Molecular Mass: 246.776, Monoisotopic Mass: 246.022).

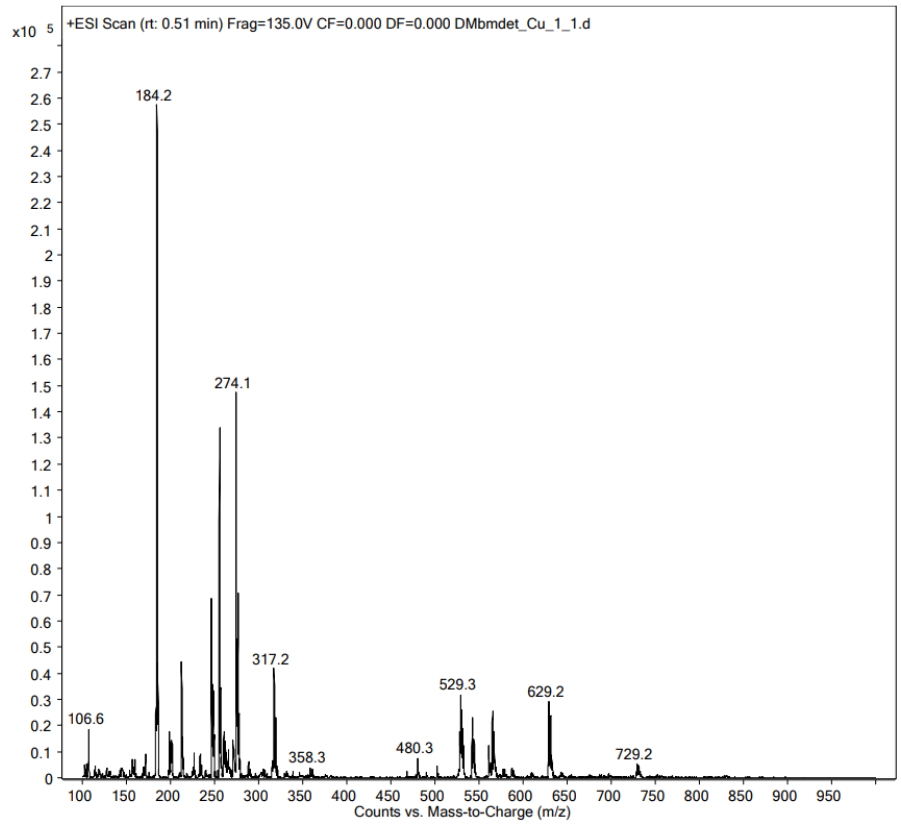
+ESI Scan (rt: 0.51 min) Frag=135.0V CF=0.000 DF=0.000 DMbmdet_Cu_1_1.d
x10 5
184.2
274.1
317.2
529.3
629.2
106.6
358.3
480.3
729.2
Counts vs. Mass-to-Charge (m/z)

(A)

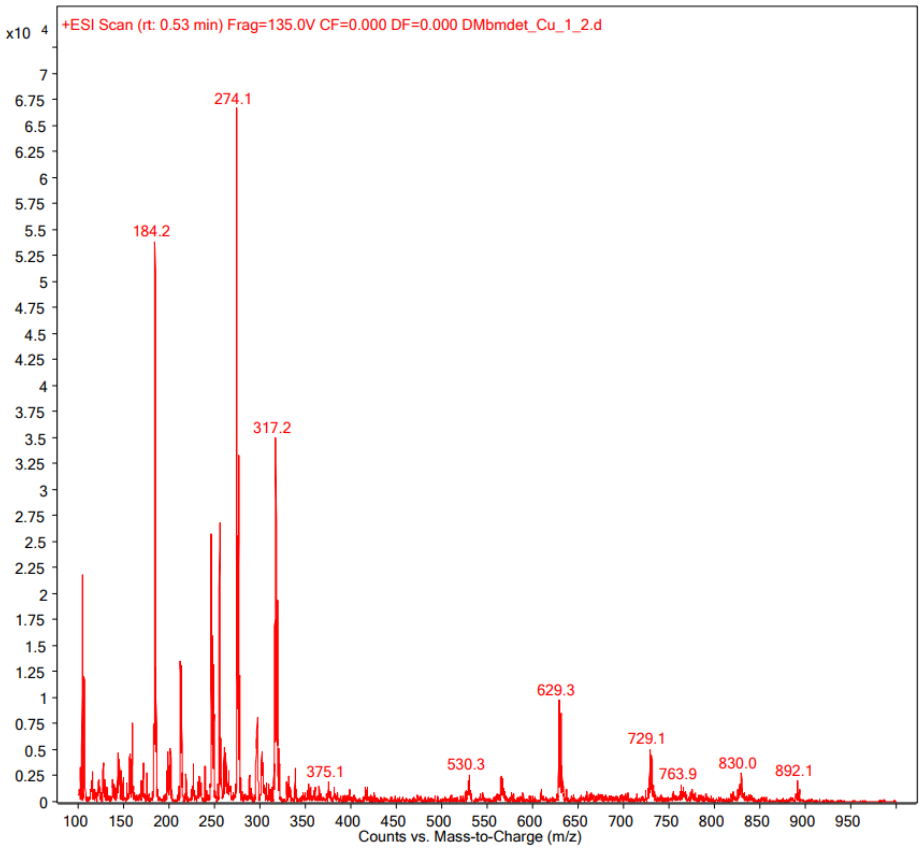
+ESI Scan (rt: 0.53 min) Frag=135.0V CF=0.000 DF=0.000 DMbmdet_Cu_1_2.d
x10 4
274.1
184.2
317.2
629.3
729.1
763.9
830.0
892.1
375.1
530.3
Counts vs. Mass-to-Charge (m/z)

(B)

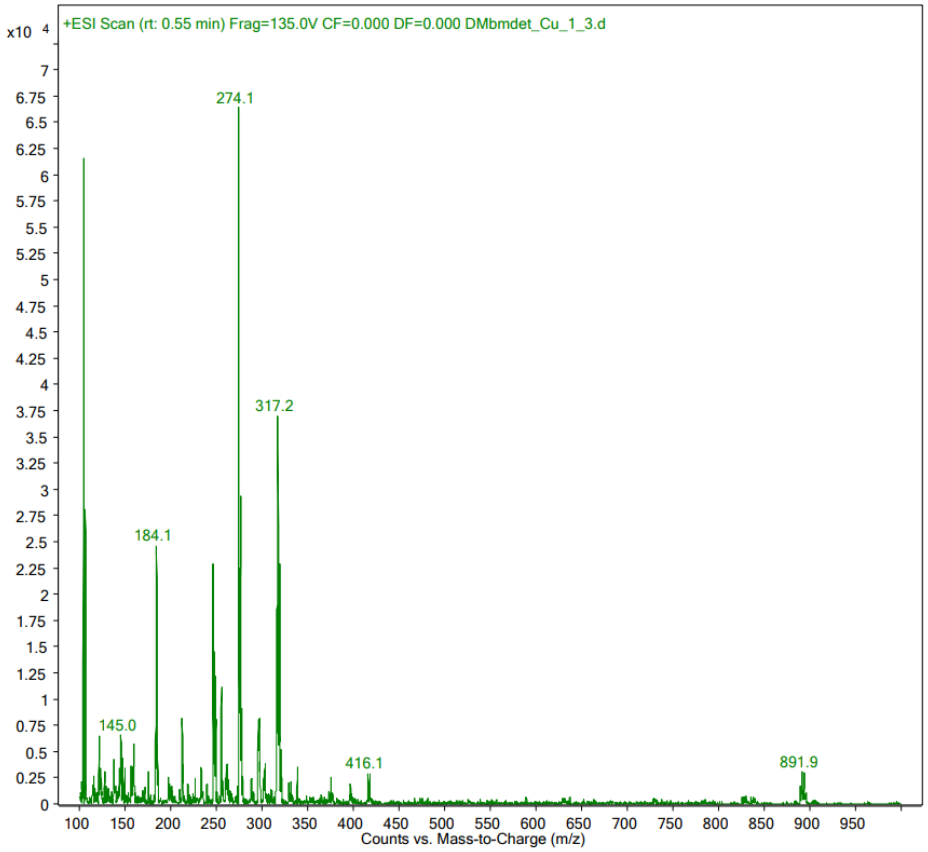

(C)

Figure 58: MS spectrum of DMbmdet/$Cu(ClO_4)_2 \cdot 6H_2O$ (A). (1/1), (B). (1/2), (C). (1/3).

3.5.3 DMbmdet + $Fe(ClO_4)_2 \cdot 6H_2O$

Figure 59 shows the mass spectra obtained from mixtures of DMbmdet and $Fe(ClO_4)_2 \cdot 6H_2O$ in 1:1, 1:2 and 1:3 ratios. The base peaks in all three spectra appear at *m/z* 261.7. This is consistent with the ion $[Fe(DMbmdet)]^{2+}$ (Formula: $[Fe(C_{28}H_{33}N_7)]^{2+}$, Molecular Mass: 523.455, Monoisotopic Mass: 523.215), and again shows the invariance of the products with mole ratio. A lower intensity peak at *m/z* 622.3 is also present in all three spectra, and is due to the $[Fe(DMbmdet)(ClO_4)]^{+}$ ion (Formula: $[Fe(C_{28}H_{33}N_7)ClO_4]^{+}$, Molecular Mass: 622.905, Monoisotopic Mass: 622.163). A peak at *m/z* 468.4 observed in the 1:1 and 1:2 spectra corresponds to protonated DMbmdet, suggesting that Fe does not bind strongly to the DMbmdet ligand.

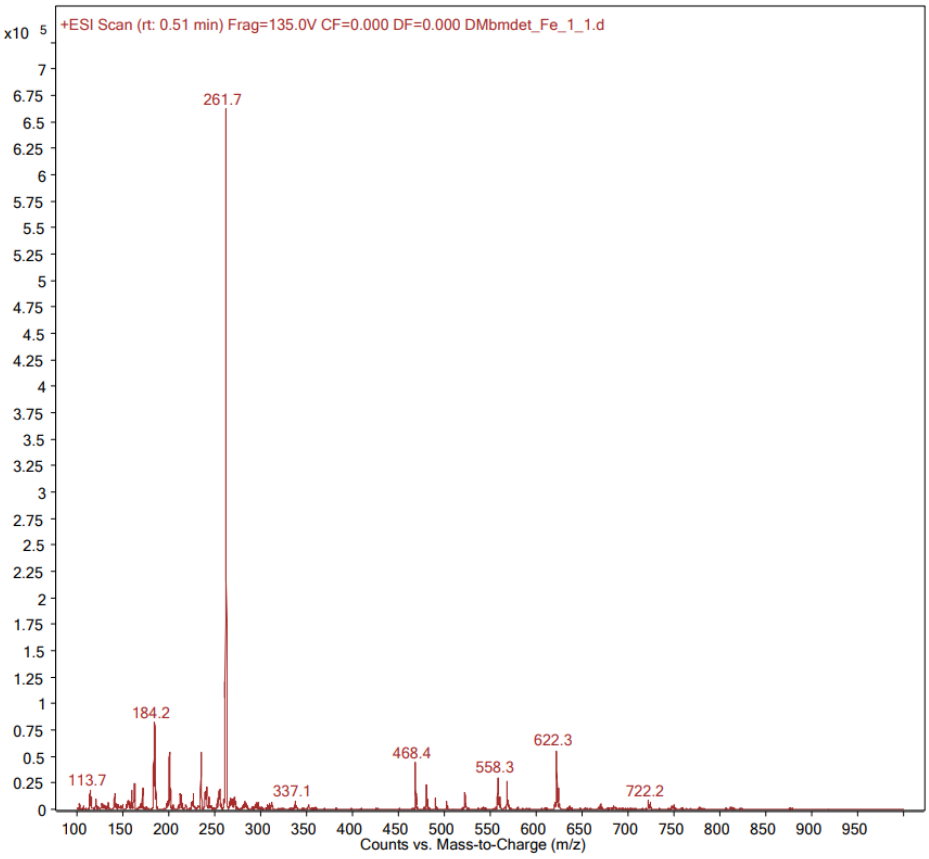
+ESI Scan (rt: 0.51 min) Frag=135.0V CF=0.000 DF=0.000 DMbmdet_Fe_1_1.d
x10 5
261.7
184.2
113.7
337.1
468.4
558.3
622.3
722.2
Counts vs. Mass-to-Charge (m/z)

(A)

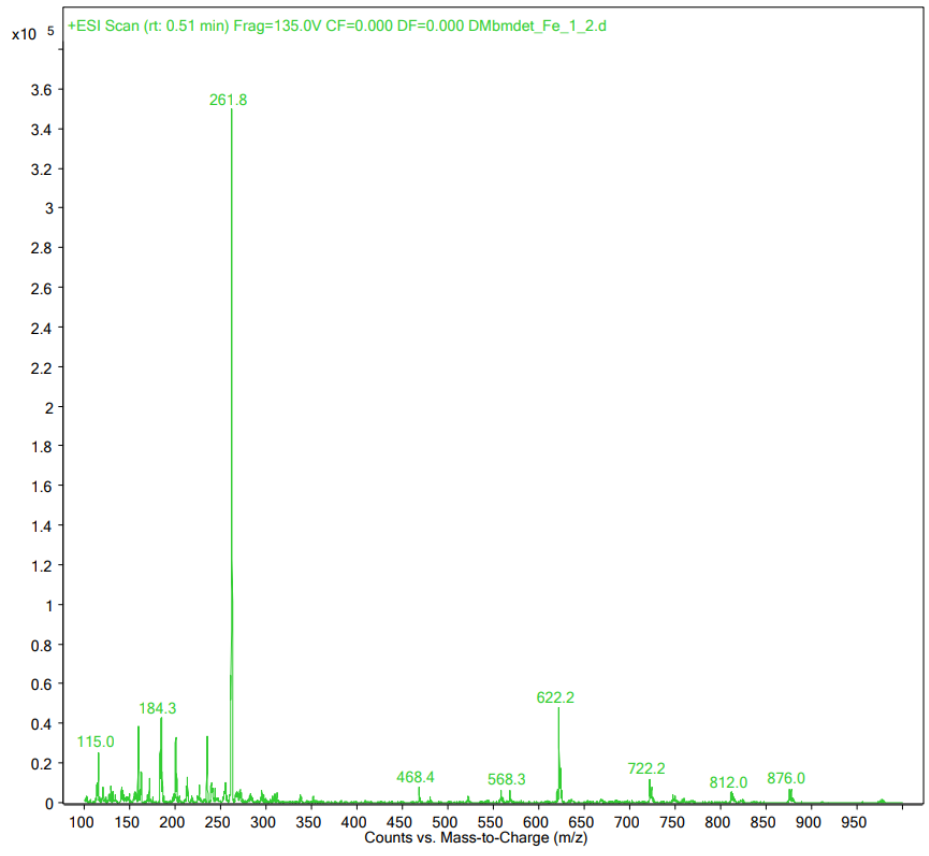
+ESI Scan (rt: 0.51 min) Frag=135.0V CF=0.000 DF=0.000 DMbmdet_Fe_1_2.d
x10 5
261.8
184.3
115.0
468.4
568.3
622.2
722.2
812.0
876.0
Counts vs. Mass-to-Charge (m/z)

(B)

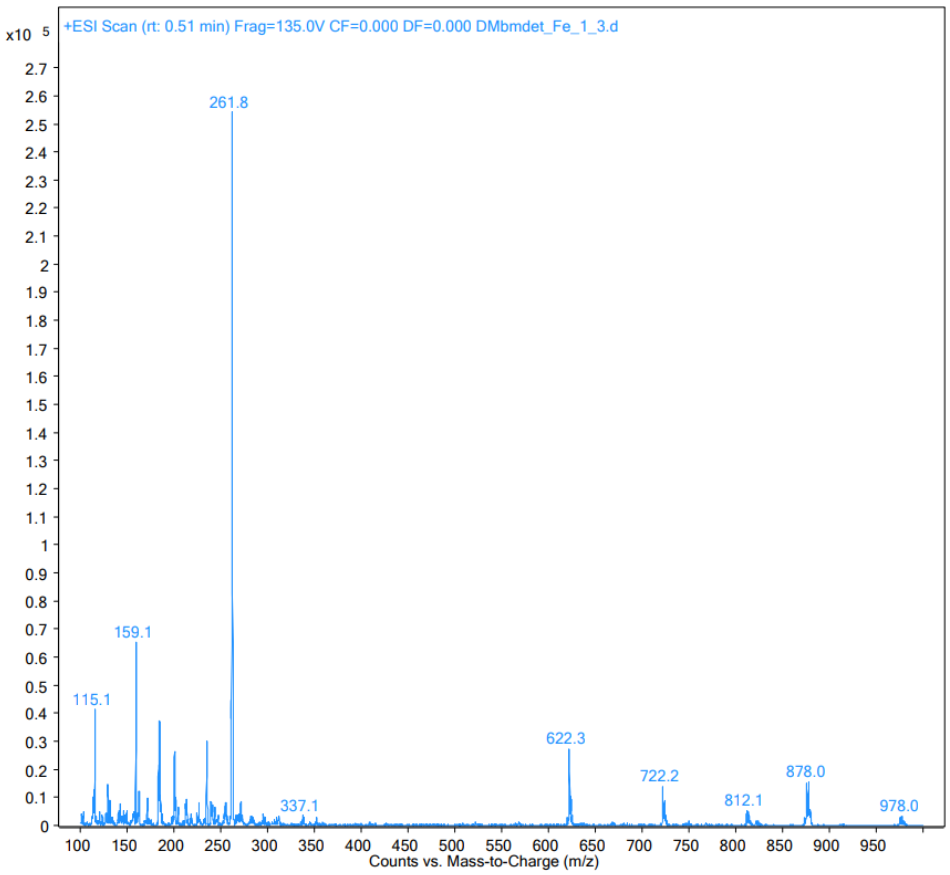

(C)

Figure 59: Mass spectra of DMbmdet/$Fe(ClO_4)_2 \cdot 6H_2O$ (A). (1/1), (B). (1/2), (C). (1/3).

3.5.4 DMbmdet + $Ni(ClO_4)_2 \cdot 6H_2O$

Figure 60 shows the mass spectra obtained from mixtures of DMbmdet and $Ni(ClO_4)_2 \cdot 6H_2O$ in 1:1, 1:2 and 1:3 ratios. All three spectra are very similar, with the base peak being at *m/z* 262.8 in all cases. This peak corresponds to the $[Ni(DMbmdet)]^{2+}$ ion (Formula: $[Ni(C_{28}H_{33}N_7)]^{2+}$, Molecular Mass: 526.303, Monoisotopic Mass: 525.215). This, like the other metal ions, shows that the products do not depend on the mole ratio used. The small signal at *m/z* 624.3 in all spectra corresponds to the $[Ni(DMbmdet)(ClO_4)]^+$ (Formula: $[Ni(C_{28}H_{33}N_7)ClO_4]^+$, Molecular Mass: 625.753, Monoisotopic Mass: 624.164). Interestingly, the intensity of the peak at *m/z* 882.0 can be observed gradually growing with the increase in amount of metal salt. This *m/z* value is consistent with a dimeric ion of formula $[Ni_2(DMbmdet)(ClO_4)_3]$ (Formula: $[Ni_2(C_{28}H_{33}N_7)(ClO_4)_3]^+$, Molecular Mass: 883.348, Monoisotopic Mass: 879.996).

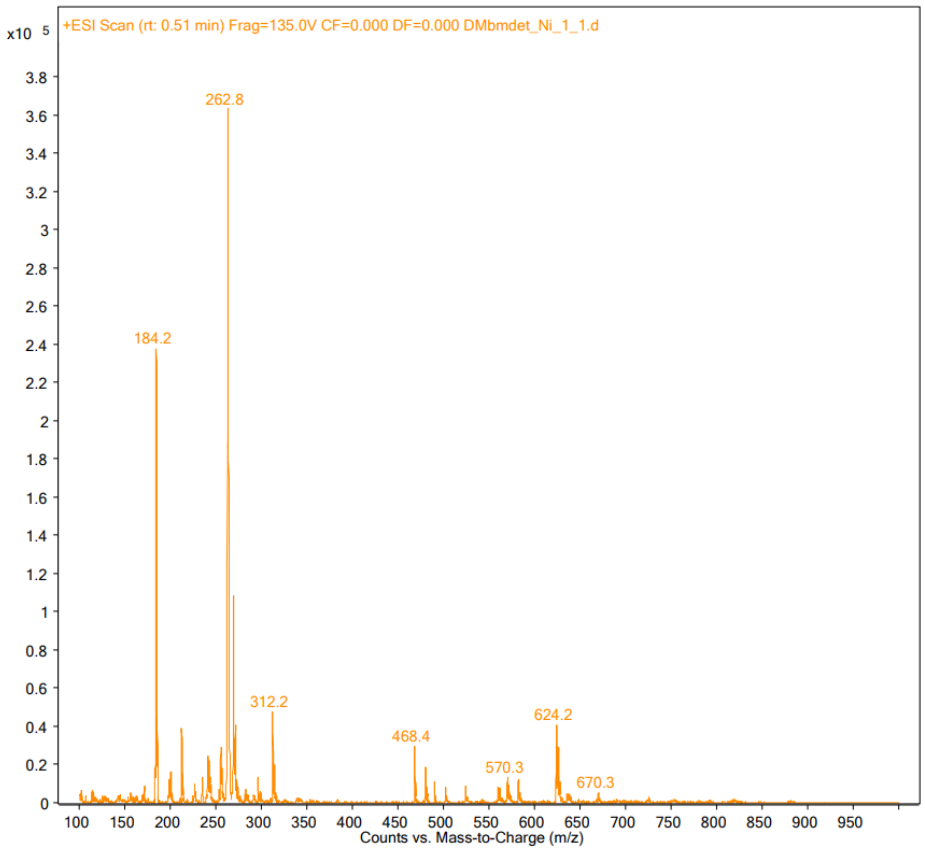
+ESI Scan (rt: 0.51 min) Frag=135.0V CF=0.000 DF=0.000 DMbmdet_Ni_1_1.d
x10 5
262.8
184.2
312.2
468.4
624.2
570.3
670.3
Counts vs. Mass-to-Charge (m/z)

(A)

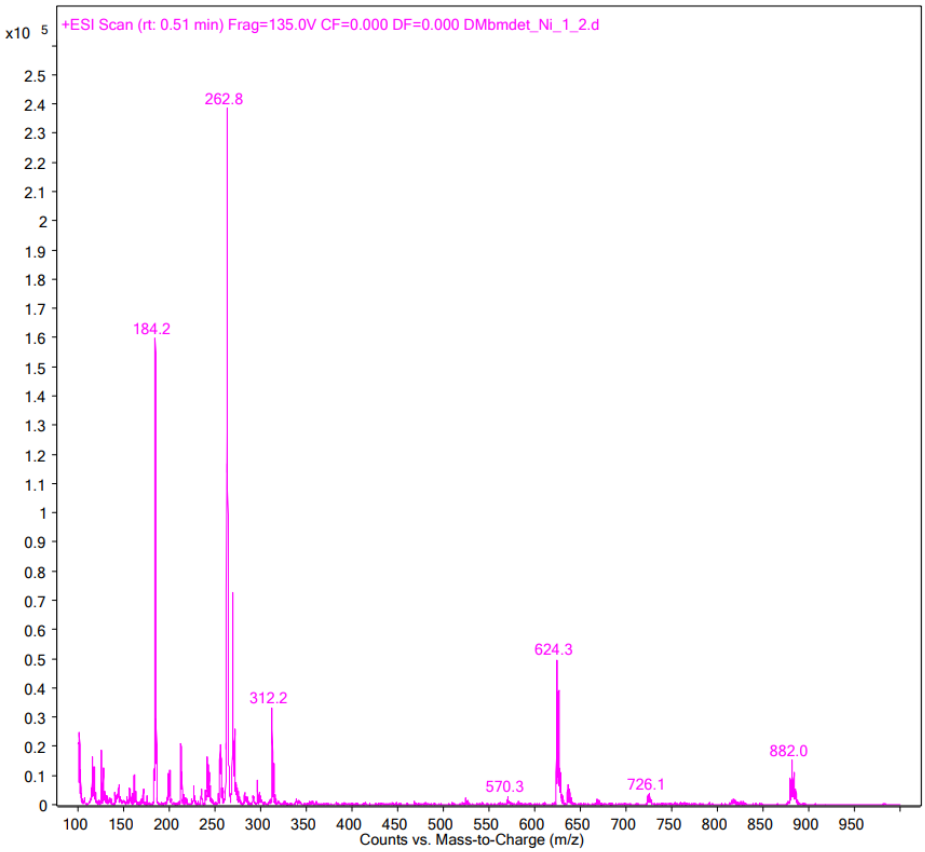
+ESI Scan (rt: 0.51 min) Frag=135.0V CF=0.000 DF=0.000 DMbmdet_Ni_1_2.d
x10 5
262.8
184.2
624.3
312.2
882.0
570.3
726.1
Counts vs. Mass-to-Charge (m/z)

(B)

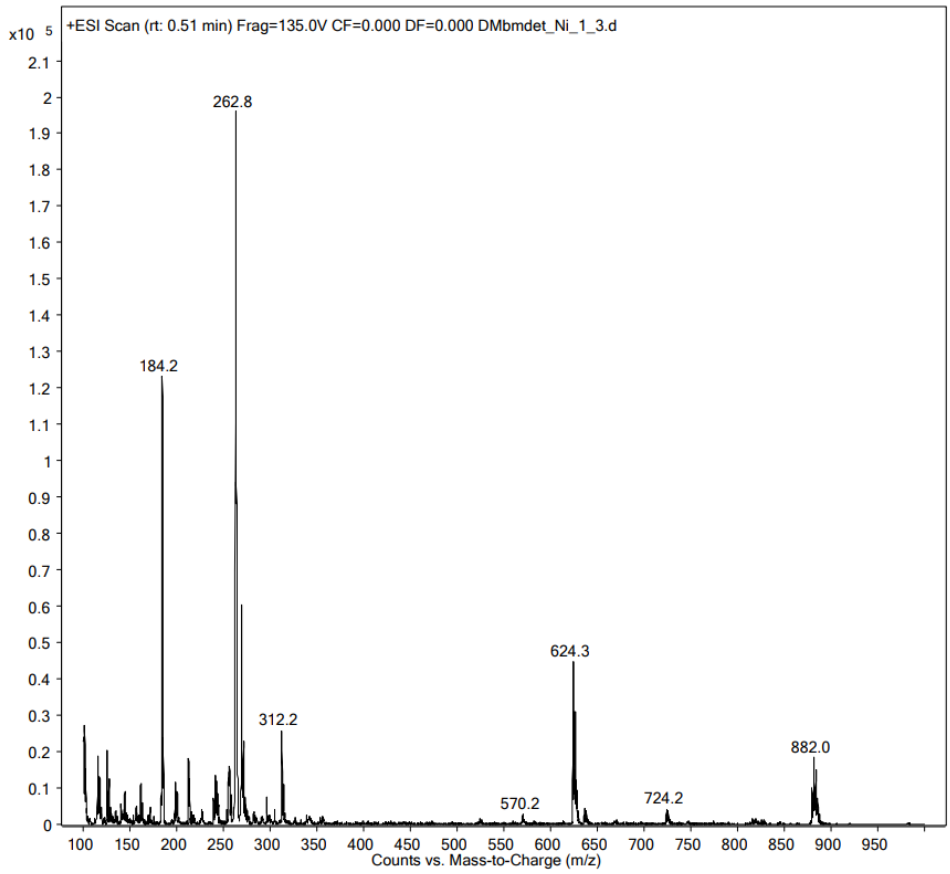

(C)

Figure 60: Mass spectra of DMbmdet/$Ni(ClO_4)_2 \cdot 6H_2O$ (A). (1/1), (B). (1/2), (C). (1/3).

3.5.5 DMbmdet + $Zn(ClO_4)_2 \cdot 6H_2O$

Figure 61 shows the mass spectra obtained from mixtures of DMbmdet and $Zn(ClO_4)_2 \cdot 6H_2O$ in 1:1, 1:2 and 1:3 ratios. The base peak can be observed in all three spectra at *m/z* 265.8, which corresponds to $[Zn(DMbmdet)]^{2+}$ (Formula: $[Zn(C_{28}H_{33}N_7)]^{2+}$, Molecular Mass: 532.987, Monoisotopic Mass: 531.209). Protonated DMbmdet is also found in the 1:1 sample (*m/z* 468.4). Signals corresponding to $[Zn(DMbmdet)(ClO_4)]^+$ can be seen in all three spectra though the peaks are small (m/z 630.2) (Formula: $[Zn(C_{28}H_{33}N_7)ClO_4]^+$, Molecular Mass: 632.438, Monoisotopic Mass: 630.157).

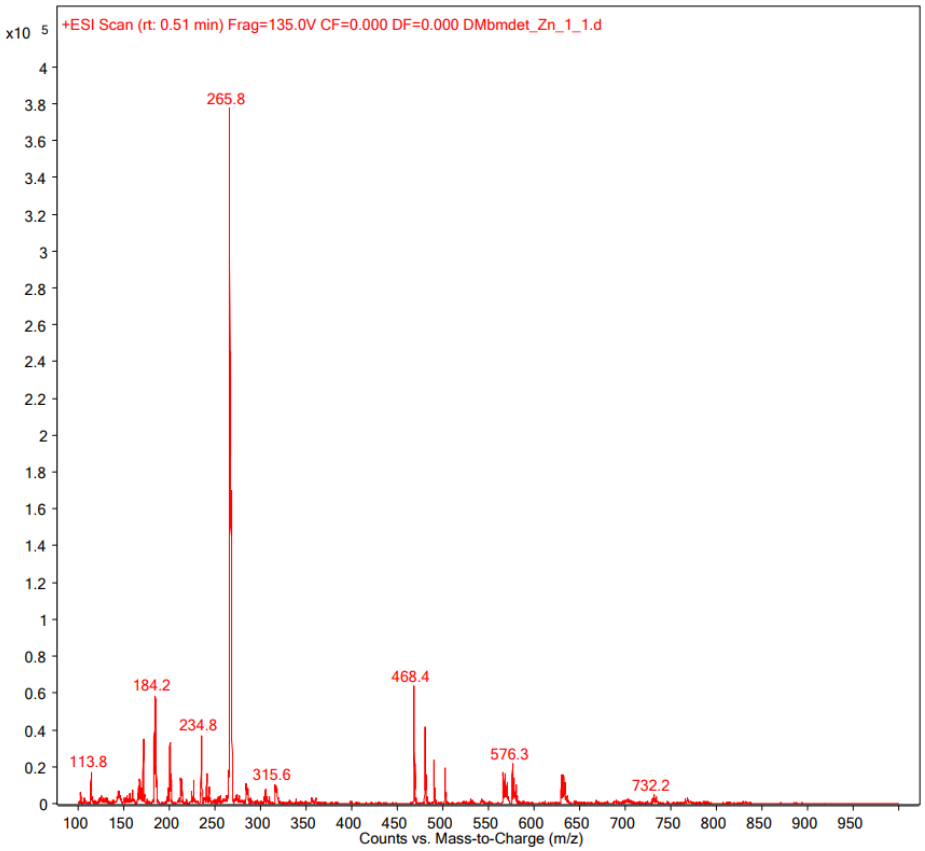
+ESI Scan (rt: 0.51 min) Frag=135.0V CF=0.000 DF=0.000 DMbmdet_Zn_1_1.d
x10 5
265.8
184.2
234.8
113.8
315.6
468.4
576.3
732.2
Counts vs. Mass-to-Charge (m/z)

(A)

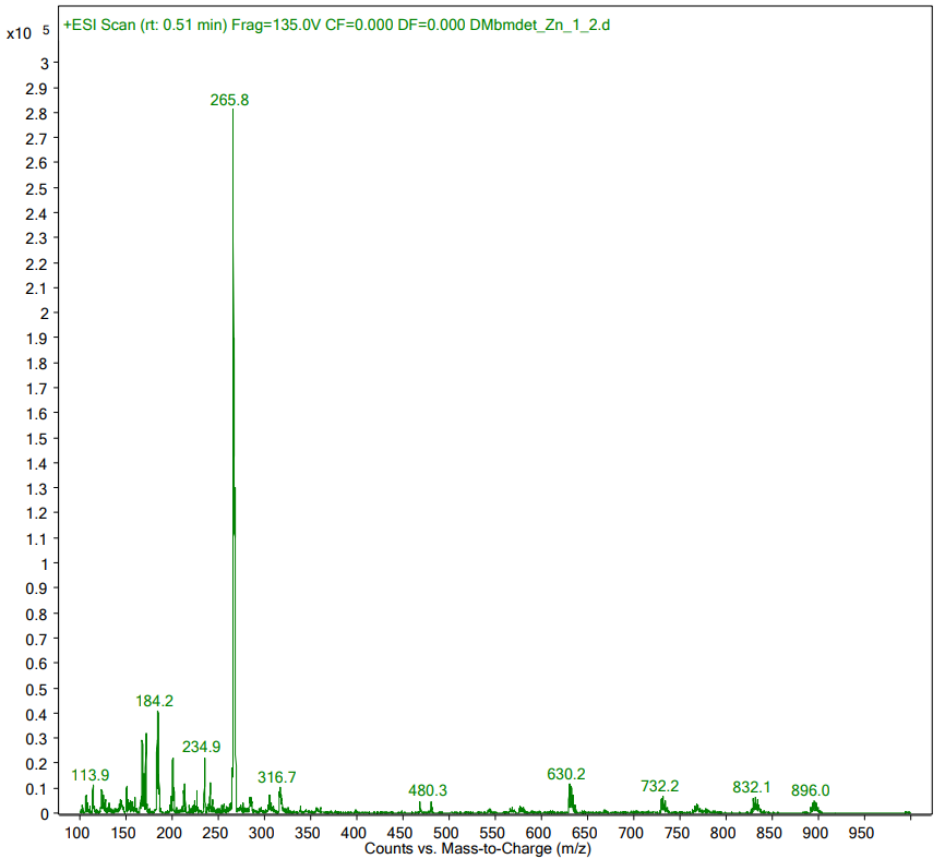
+ESI Scan (rt: 0.51 min) Frag=135.0V CF=0.000 DF=0.000 DMbmdet_Zn_1_2.d
x10 5
265.8
184.2
234.9
113.9
316.7
480.3
630.2
732.2
832.1
896.0
Counts vs. Mass-to-Charge (m/z)

(B)

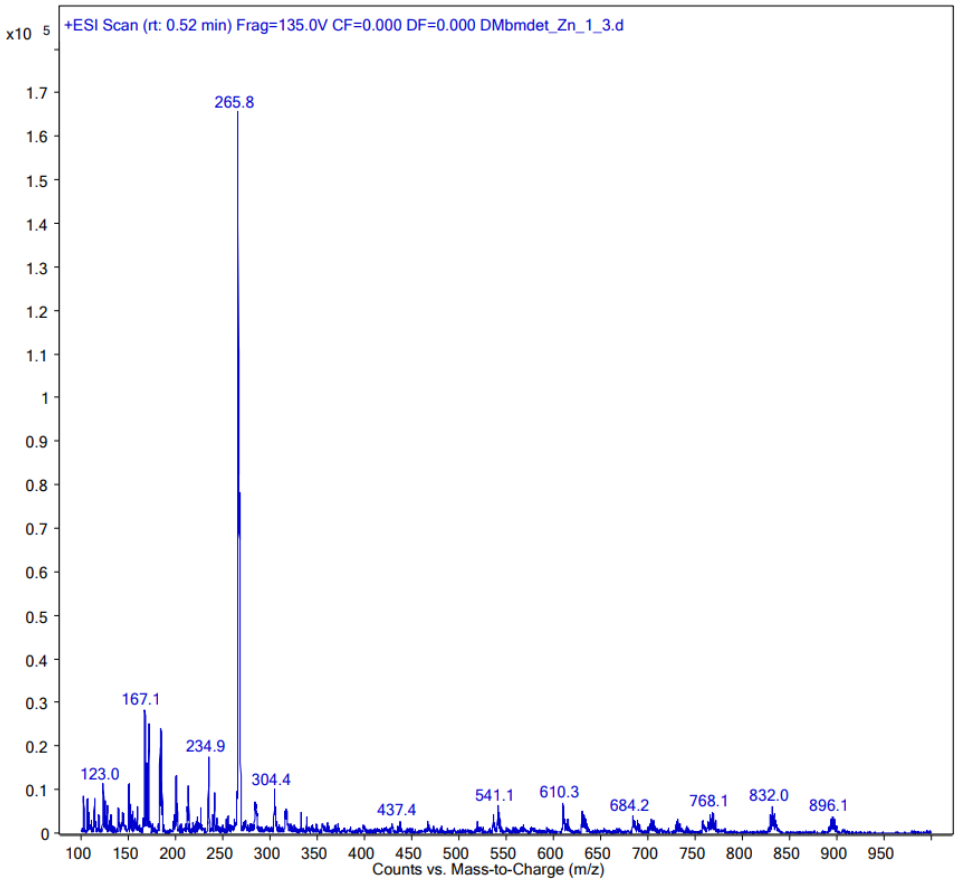

(C)

Figure 61: MS spectrum of DMbmdet/$Zn(ClO_4)_2 \cdot 6H_2O$ (A). (1/1), (B). (1/2), (C). (1/3).

3.6 Discussion

3.6.1 Heptadentate ligands

The new heptadentate ligand bmpy was successfully prepared from the reaction of 2,2'-bipyridine-6-carboxaldhyde with 2,6-diaminomethylpyridine, reduction of the resulting diimine with either $NaBH_4$ or $NaBH_3CN$, and purification by column chromatography. Interestingly, regardless of the reductant used and the mole ratio between this and the diimine, incomplete reduction was always observed, as shown by the mass spectrum of the product. The reason for this is not obvious; there do not appear to be any steric factors that would impede approach of the reducing agent, and there are no unusual electronic features of the molecule that would make the diimine difficult to reduce. After much experimentation it was finally found that the optimum method for purification of the ligand was column chromatography on silica.

Chromatographic methods were also developed for the purification of both bmdet and DMbmdet, with alumina being the solid phase of choice in these instances. In all cases, the ligands were characterised by ESI-MS, and ^{1}H and ^{13}C NMR spectrometry.

3.6.2 Transition metal complexes of bmpy

It was hoped that crystalline complexes suitable for X-ray structural determination would be obtained from reactions of the bmpy ligand with a variety of transition metal ions. Unfortunately, this did not occur. It was therefore necessary to rely on mass spectrometry to identify the complexes formed in solution.

The ligand (L) was reacted with $M(ClO_4)_2.6H_2O$ (M = Fe, Co, Ni, Cu, Zn) in 1:1, 1:2 and 1:3 (L:M) ratios, and the resulting reaction mixture was analysed by ESI-MS. In all cases except Zn^{2+}, complexation of the ligand by the metal ion was complete; with Zn^{2+}, a small peak attributable to free ligand was observed, indicating that binding to this metal ion was not as strong as observed for the others. For Co^{2+}, Fe^{2+}, Ni^{2+} and Zn^{2+}, formation of a mononuclear complex occurred essentially exclusively, and the base peak was due, somewhat surprisingly, to the 2+ ion in all cases. It might be expected that proton loss from the amine N atoms of the ligand to give the (presumably) lower energy 1+ species would be favoured but this appears not to be the case. Instead, ion-pairing with perchlorate to give the 1+ species $[M(L)(ClO_4)]^{+}$ was observed to occur, but the peaks corresponding to these species were always of much lower intensity than those for $[M(L)]^{2+}$. In the absence of X-ray crystallographic data, the geometries of these mononuclear complexes are uncertain; they may all be seven-coordinate, with all ligand N atoms bound, or six-coordinate, with a hypodentate ligand.

The Cu^{2+} system behaved very differently to the others, giving exclusive formation of the dimeric species $[Cu_2(L\text{-}2H)]^{2+}$ which comprises two metal ions and one doubly deprotonated ligand. The structure of this species would be of great interest, as there are apparently no other ligands (oxo, hydroxo, water, etc) involved. Again, in the absence of X-ray data, no definite conclusions can be made.

Of particular interest was the fact that, in all systems, the ratio of metal to ligand had no effect on the nature of the complexes formed. This does seem somewhat surprising, given the fact that the ligand has 7 possible donor atoms, which should allow for formation of mono-,

di- and trinuclear complexes in solution relatively easily, through formation of oxo and/or hydroxo bridges. However, it could be that such complexes are indeed formed, but break apart to mononuclear (or in the case of Cu^{2+}, dinuclear) species under the mass spectrometer conditions.

3.6.3 Transition metal complexes of bmdet and DMbmdet.

The ligands bmdet and DMbmdet have extremely similar structures, differing only in the presence of methyl groups at the 6 positions of the terminal pyridine rings in the latter. It was therefore of interest to see what, if any, effect these methyl groups had on the nature of the complexes formed.

As found for the complexes of bmpy, mononuclear complexes of both bmdet and DMbmdet are formed with the Fe^{2+}, Co^{2+}, Ni^{2+} and Zn^{2+} metal ions. In all cases, the base peak corresponds to the $[M(L)]^{2+}$ species, and the $[M(L)(ClO_4)]^{+}$ species are also formed in small amount. Some free ligand is also observed in the Fe system.

The behaviour of the Cu^{2+} system is different to both the other bmdet and DMbmdet systems, and also the bmpy system. In this case, Cu^{2+} predominantly forms a mononuclear $[Cu(L)(OH_2)]^{2+}$ ion with both bmdet and DMbmdet. The spectra in both systems are noticeably more complicated that those observed for all other systems studied. This may well be due to fragmentation processes, or may also be due to the fact that Cu^{2+}, unlike the other metal ions studied, is a mild oxidant, which may lead to decomposition of the ligands.

Chapter 4: Conclusion

A synthetic route to a new seven-nitrogen heptadentate ligand, N, N'-bis(2,2'-bipyridin-6-ylmethyl)pyridine-2,6-dimethylamine (bmpy), was developed, but the yield is low. Future work in this field should concentrate on the study of the reduction of the diimine, in order to improve the efficiency of this step. A chromatographic purification method was developed to separate the product from the incompletely reduced species. With the assistance of ESI-MS, Co^{2+}, Fe^{2+}, Ni^{2+} and Zn^{2+} were shown to form mononuclear complexes with the bmpy ligand, while Cu forms a dinuclear $[Cu_2(L\text{-}2H)]^{2+}$ species. All systems form the same complexes, independent of the ratio of metals and ligand used. Zn^{2+} ion is found to bind less strongly to the ligand, compared to other metal ions. Both crystallisation and recrystallisation from either water or acetonitrile of any solid materials obtained were unsuccessful. No crystal of X-ray quality was obtained.

Column chromatography conditions for purifying two seven-nitrogen heptadentate ligands, N, N'-bis(2,2'-bipyridin-6-ylmethyl)diethylamine-1,2-dimethylamine (bmdet) and N, N'-bis(6-methyl-2,2'-bipyridin-6'-ylmethyl)diethylamine-1,2-dimethylamine (DMbmdet), were successfully developed. All transition metal (Co^{2+}, Cu^{2+}, Fe^{2+}, Ni^{2+}, Zn^{2+}) complexes of bmdet are mononuclear according to the ESI-MS results and Ni^{2+} has weaker bonds to the bmdet compared to the other metals tested. All transition metals also form mononuclear complexes with DMbmdet, but Ni^{2+} slightly tends to form dimeric species with DMbmdet with the increasing amount of the Ni^{2+} ion. Both Ni^{2+} and Zn^{2+} are shown to bind less strongly to the ligand and Zn^{2+} binds even more weakly than Ni^{2+}.

Although transition metal complexes of all the ligands studied are shown to be formed (Co^{2+}, Cu^{2+}, Fe^{2+}, Ni^{2+}, Zn^{2+}), the coordination number of the metal ions and whether the ligand is acting as a heptadentate ligand cannot be stated with certainty due to the lack of crystal structure data. Further studies of these complexes should emphasise obtaining optimal conditions for crystallisation of the products.

References

1 E. C. Constable, *Chemistry*, 2019, **1**, 126–163.
2 The Nobel Prize in Chemistry 1913. NobelPrize.org. Nobel Prize Outreach AB 2023. Mon. 13 Feb 2023. <https://www.nobelprize.org/prizes/chemistry/1913/summary/>.
3 The Nobel Prize in Chemistry 1973. NobelPrize.org. Nobel Prize Outreach AB 2023. Mon. 13 Feb 2023. <https://www.nobelprize.org/prizes/chemistry/1973/summary/>.
4 MLA style: The Nobel Prize in Chemistry 1983. NobelPrize.org. Nobel Prize Outreach AB 2023. Mon. 13 Feb 2023. <https://www.nobelprize.org/prizes/chemistry/1983/summary/>.
5 The Nobel Prize in Chemistry 2005. NobelPrize.org. Nobel Prize Outreach AB 2023. Mon. 13 Feb 2023. <https://www.nobelprize.org/prizes/chemistry/2005/summary/>.
6 I. A. Popov, T. Jian, G. V. Lopez, A. I. Boldyrev and L.-S. Wang, *Nature Communications*, 2015, **6**, 8654.
7 K. Landskron, *Inorganic Coordination Chemistry*, LibreTexts, 2021, vol. Coordination Numbers and Structures.
8 E. L. Muetterties and R. A. Schunn, *Q. Rev. Chem. Soc.*, 1966, **20**, 245–299.
9 Roald. Hoffmann, B. F. Beier, E. L. Muetterties and A. R. Rossi, *Inorg. Chem.*, 1977, **16**, 511–522.
10 N. A. Hall, C. Duboc, M.-N. Collomb, A. Deronzier and A. G. Blackman, *Dalton Trans.*, 2011, **40**, 12075–12082.
11 Y. Mulyana, D. K. Weber, D. P. Buck, C. A. Motti, J. G. Collins and F. R. Keene, *Dalton Trans.*, 2011, **40**, 1510–1523.
12 A. K. Gorle, A. J. Ammit, L. Wallace, F. R. Keene and J. G. Collins, *New J. Chem.*, 2014, **38**, 4049–4059.
13 M. Hasegawa, H. Ohtsu, D. Kodama, T. Kasai, S. Sakurai, A. Ishii and K. Suzuki, *New J. Chem.*, 2014, **38**, 1225–1234.
14 O. Hamelin, S. Ménage, F. Charnay, M. Chavarot, J.-L. Pierre, J. Pécaut and M. Fontecave, *Inorg. Chem.*, 2008, **47**, 6413–6420.
15 T. Shimoda, T. Morishima, K. Kodama, T. Hirose, D. E. Polyansky, G. F. Manbeck, J. T. Muckerman and E. Fujita, *Inorg. Chem.*, 2018, **57**, 5486–5498.
16 L. Vaiana, M. Regueiro-Figueroa, M. Mato-Iglesias, C. Platas-Iglesias, D. Esteban-Gómez, A. de Blas and T. Rodríguez-Blas, *Inorg. Chem.*, 2007, **46**, 8271–8282.
17 R. L. Fanshawe and A. G. Blackman, *Inorg. Chem.*, 1995, **34**, 421–423.
18 A. J. Clarkson and A. G. Blackman, *Polyhedron*, 2006, **25**, 373–378.
19 R. F. Bogucki and A. E. Martell, *J. Am. Chem. Soc.*, 1958, **80**, 4170–4174.
20 J. L. Hoard, M. Lind and J. V. Silverton, *J. Am. Chem. Soc.*, 1961, **83**, 2770–2771.
21 S. Richards, B. Pedersen, J. V. Silverton and J. L. Hoard, *Inorg. Chem.*, 1964, **3**, 27–33.
22 M. D. Lind, M. J. Hamor, T. A. Hamor and J. L. Hoard, *Inorg. Chem.*, 1964, **3**, 34–43.
23 L. J. Wilson and N. J. Rose, *J. Am. Chem. Soc.*, 1968, **90**, 6041–6045.
24 M. G. B. Drew, J. Nelson and S. M. Nelson, *J. Chem. Soc., Dalton Trans.*, 1981, 1685–1690.
25 S. Salehzadeh, S. A. Javarsineh and H. Keypour, *Journal of Molecular Structure*, 2006, **785**, 54–62.
26 S. Salehzadeh, M. D. Ward and H. Adams, *Inorganic Chemistry Communications*, 2009, **12**, 433–435.
27 X.-H. Bu, W. Chen, Z.-H. Zhang, R.-H. Zhang, S.-M. Kuang and T. Clifford, *Inorganica Chimica Acta*, 2000, **310**, 110–114.

28 H. Khanmohammadi, S. Amani, M. H. Abnosi and H. R. Khavasi, *Spectrochimica Acta Part A: Molecular and Biomolecular Spectroscopy*, 2010, **77**, 342–347.
29 A. Hazell and H. Toftlund, *Acta Crystallographica Section E*, 2007, **63**, m328–m329.
30 A. Hazell and H. Toftlund, *Acta Crystallographica Section E*, 2007, **63**, m326–m327.
31 H. Keypour, A. A. Dehghani-Firouzabadi and H. R. Khavasi, *Transition Metal Chemistry*, 2011, **36**, 307–311.
32 C. Zhang, F. Zhou, Y. Li and Y. Zhang, *Suzhou Daxue Xuebao, Ziran Kexueban*, 2010, **26**, 73–76.
33 H. Keypour, H. Khanmohammadi, K. P. Wainwright and M. R. Taylor, *Inorg. Chim. Acta*, 2005, **358**, 247–256.
34 H. Keypour, H. Khanmohammadi, K. P. Wainwright and M. R. Taylor, *J. Iran. Chem. Soc.*, 2004, **1**, 53–64.
35 A. M. McDaniel, A. K. Rappe and M. P. Shores, *Inorg. Chem.*, 2012, **51**, 12493–12502.
36 S. Salehzadeh, R. Golbedaghi, J. Rakhtshah and H. Adams, *J. Mol. Struct.*, 2021, **1245**, 130982.
37 H. Khanmohammadi, S. Amani, H. Lang and T. Rueeffer, *Inorg. Chim. Acta*, 2007, **360**, 579–587.
38 M. Qian, S.-H. Gou, L. He, Y.-M. Zhou and C.-Y. Duan, *Acta Crystallogr., Sect. C: Cryst. Struct. Commun.*, 1999, **C55**, 742–744.
39 X.-H. Bu, W. Chen, L.-J. Mu, Z.-H. Zhang, R.-H. Zhang and T. Clifford, *Polyhedron*, 2000, **19**, 2095–2100.
40 Y. Mikata, A. Takekoshi, M. Kaneda, S. Yonemura, Y. Aono, A. Matsumoto, H. Konno and S. C. Burdette, *Eur. J. Inorg. Chem.*, 2021, **2021**, 1287–1296.
41 W. Park, M. H. Shin, J. H. Chung, J. Park, M. S. Lah and D. Lim, *Tetrahedron Lett.*, 2006, **47**, 8841–8845.
42 G. Yi, C. Zhang, W. Zhao, H. Cui, L. Chen, Z. Wang, X.-T. Chen, A. Yuan, Y.-Z. Liu and Z.-W. Ouyang, *Dalton Trans.*, 2020, **49**, 7620–7627.
43 A. Deroche, I. Morgenstern-Badarau, M. Cesario, J. Guilhem, B. Keita, L. Nadjo and C. Houee-Levin, *J. Am. Chem. Soc.*, 1996, **118**, 4567.
44 H. Keypour, H. Khanmohammadi, K. P. Wainwright and M. R. Taylor, *Inorg. Chim. Acta*, 2003, **355**, 286–291.
45 A. Bencini, A. Bianchi, P. Dapporto, E. Garcia-Espana, V. Marcelino, M. Micheloni, P. Paoletti and P. Paoli, *Inorg. Chem.*, 1990, **29**, 1716.
46 H. Keypour, S. Salehzadeh, R. G. Pritchard and R. V. Parish, *Polyhedron*, 2000, **19**, 1633–1637.
47 I. Morgenstern-Badarau, F. Lambert, J. Philippe Renault, M. Cesario, J.-D. Maréchal and F. Maseras, *Inorganica Chimica Acta*, 2000, **297**, 338–350.
48 A. J. Amoroso, P. G. Edwards, S. T. Howard, B. M. Kariuki, J. C. Knight, L. Ooi, K. M. A. Malik, L. Stratford and A.-R. H. Al-Sudani, *Dalton Trans.*, 2009, 8356–8362.
49 D. G. Lonnon, G. E. Ball, I. Taylor, D. C. Craig and S. B. Colbran, *Inorg. Chem.*, 2009, **48**, 4863–4872.
50 D. G. Lonnon, D. C. Craig and S. B. Colbran, *Inorg. Chem. Commun.*, 2002, **5**, 958–962.
51 G. Yi, H. Cui, C. Zhang, W. Zhao, L. Chen, Y.-Q. Zhang, X.-T. Chen, Y. Song and A. Yuan, *Dalton Trans.*, 2020, **49**, 2063–2067.
52 J. P. Joyce, R. I. Portillo, A. K. Rappe and M. P. Shores, *Inorg. Chem.*, 2022, **61**, 6376–6391.
53 A. G. Blackman, *C. R. Chim.*, 2005, **8**, 107–119.
54 A. Mustapha, G. Steel, J. Reglinski and A. R. Kennedy, *Polyhedron*, 2017, **129**, 222–228.
55 S. Salehzadeh, R. Golbedaghi and H. Adams, *Journal of Molecular Structure*, 2022, **1247**, 131359.

56 A. Mohamadou and C. Gérard, *J. Chem. Soc., Dalton Trans.*, 2001, 3320–3328.
57 I. Morgenstern-Badarau, F. Lambert, A. Deroche, M. Cesario, J. Guilhem, B. Keita and L. Nadjo, *Inorganica Chimica Acta*, 1998, **275–276**, 234–241.
58 T. K. Ronson, J. Nelson, G. B. Jameson, J. C. Jeffery and S. Brooker, *Eur. J. Inorg. Chem.*, 2004, 2570–2584.
59 G. De Martino Norante, M. Di Vaira, F. Mani, S. Mazzi and P. Stoppioni, *Inorg. Chem.*, 1990, **29**, 2822–2829.
60 M. Di Vaira, F. Mani and P. Stoppioni, *J. Chem. Soc., Dalton Trans.*, 1992, 1127–1130.
61 G. Brewer, C. Brewer, R. J. Butcher, G. T. Robichaux and C. Viragh, *Inorg. Chim. Acta*, 2014, **410**, 171–177.
62 C. Brewer, G. Brewer, R. J. Butcher, E. E. Carpenter, L. Cuenca, A. M. Schmiedekamp and C. Viragh, *Dalton Trans.*, 2005, 3617–3619.
63 G. Brewer, M. J. Olida, A. M. Schmiedekamp, C. Viragh and P. Y. Zavalij, *Dalton Trans.*, 2006, 5617–5629.
64 C. Brewer, G. Brewer, R. J. Butcher, E. E. Carpenter, L. Cuenca, B. C. Noll, W. R. Scheidt, C. Viragh, P. Y. Zavalij and D. Zielaski, *Dalton Trans.*, 2006, 1009–1019.
65 T. Nagano, T. Hirano and M. Hirobe, *Journal of Biological Chemistry*, 1989, **264**, 9243–9249.
66 E. Kimura, A. Yatsunami, A. Watanabe, R. Machida, T. Koike, H. Fujioka, Y. Kuramoto, M. Sumomogi, K. Kunimitsu and A. Yamashita, *Biochimica et Biophysica Acta (BBA) - Protein Structure and Molecular Enzymology*, 1983, **745**, 37–43.
67 E. Kimura, A. Sakonaka and M. Nakamoto, *Biochimica et Biophysica Acta (BBA) - General Subjects*, 1981, **678**, 172–179.
68 A. J. D. Magenau, N. C. Strandwitz, A. Gennaro and K. Matyjaszewski, *Science*, 2011, **332**, 81–84.
69 X. Xu, C. Bao, M. Hong, D. Li and Q. Zhang, *Polym. Chem.*, 2020, **11**, 6356–6364.
70 T. Gunnlaugsson, A. J. Harte, J. P. Leonard and M. Nieuwenhuyzen, *Chem. Commun.*, 2002, 2134–2135.
71 P. Antal, B. Drahoš, R. Herchel and Z. Trávníček, *Inorg. Chem.*, 2016, **55**, 5957–5972.
72 B. Drahoš, I. Císařová, O. Laguta, V. T. Santana, P. Neugebauer and R. Herchel, *Dalton Trans.*, 2020, **49**, 4425–4440.
73 S. K. Gill, MSc Thesis, Auckland University of Technology, 2021.
74 C. Liu, H. Lei, Z. Zhang, F. Chen and R. Cao, *Chem. Commun.*, 2017, **53**, 3189–3192.
75 K. J. Schmalzl and L. A. Summers, *Aust. J. Chem.*, 1977, **30**, 657.
76 L.-Y. Liao, X.-R. Kong and X.-F. Duan, *J. Org. Chem.*, 2014, **79**, 777–782.
77 F. R. Heirtzler, M. Neuburger, M. Zehnder and E. C. Constable, *Liebigs Ann./Recl.*, 1997, 297–301.
78 L. J. Baird, C. A. Black and A. G. Blackman, *Polyhedron*, 2007, **26**, 378–384.
79 M. Walther, K. Wermann, M. Lutsche, W. Guenther, H. Goerls and E. Anders, *J. Org. Chem.*, 2006, **71**, 1399–1406.
80 F. Schrumpf, personal communication.
81 M. X. Zhou, MSc Thesis, Emporia State University, 1992.